STRENGTH ENVELOPES FOR FLORIDA ROCK AND INTERMEDIATE GEOMATERIALS

By

THAI NGUYEN

A DISSERTATION PRESENTED TO THE GRADUATE SCHOOL OF THE UNIVERSITY OF FLORIDA IN PARTIAL FULFILLMENT OF THE REQUIREMENTS FOR THE DEGREE OF DOCTOR OF PHILOSOPHY

UNIVERSITY OF FLORIDA

2018

ACKNOWLEDGEMENTS

I would like to acknowledge and thank the following important people who have supported me throughout my Ph.D. program.

First and foremost, to Dr. Michael McVay, who provided me with great guidance in this research effort. In all of Dr. McVay's classes, he always packs in a lot of material so that students have to swim fast to avoid losing track. Following him, I packed a lot of material in some of my conference presentations, but I have yet been able to talk fast and keep all the audience awake.

Special thanks go to Dr. Scott Wasman, Dr. Xiaoyu Song, and Dr. Timothy Townsend for their guidance and support.

I am blessed with the tremendous help from numerous people involved with the research project: David Horhota, Rodrigo Herrera, Juan Castellanos, Larry Jones, Jose Hernando, Dino Jameson, Glenn Johnston, Chen Weng, Beth Machosky, William Greenwood, Dan Pitocchi, Brian Strode, Barbara Beatty, Awilda Merced, Jon Sinnreich, Richard Booze, Wing-Kong Cha, Wei Meng, Zaid Ajlani, Austin Smith, Ashton Huff, Kaiqi Wang, and Kunyu Yang.

I am thankful for my friends here in and outside the University of Florida for their encouragement and support.

I am deeply grateful for my dad, my in-laws, my brother's family, and all my extended families for cheering me up from half a world away in my home country – Vietnam.

Finally, I wish to thank my wife, my son, and my daughter for their love and supporting me emotionally during my stay at school.

TABLE OF CONTENTS

page

LIST OF TABLES

LIST OF FIGURES

Abstract of Dissertation Presented to the Graduate School
of the University of Florida in Partial Fulfillment of the
Requirements for the Degree of Doctor of Philosophy

STRENGTH ENVELOPES FOR FLORIDA ROCK
AND INTERMEDIATE GEOMATERIALS

By

Thai Nguyen

December 2018

Chairman: Michael McVay
Major: Civil Engineering

For shallow foundation bearing capacity, a strength envelope is required. For soils, the well-known Mohr-Coulomb linear envelope with two parameters: cohesion, c, and internal friction, φ, is used universally. For rocks with brittle stress-strain behavior, either the Mohr-Coulomb or the Hoek-Brown envelope is applicable. However, rocks with ductile stress-strain behavior within the range of shallow foundation confining stress have never been explored for bearing capacity analyses. Therefore, for Florida carbonate-rocks, there are two concerns: i) what are strength envelopes for Florida carbonate-rocks? Are they following envelopes for brittle rocks or ductile rocks? ii) Florida rock cores often do not have enough specimens that are long enough to satisfy the strength test standard, thus there is a need to correlate rock index parameters to basic strength parameters.

In this study, two large data sets containing rocks all over the state of Florida were studied. Data set #1 contains more than 8,000 results of the unconfined compression test (q_u), Brazilian splitting tension test (BST), and bulk dry unit weight (γ_{dt}). Data set #2 contains approximately 570 data points with q_u, BST, γ_{dt}, rock formation identification, carbonate content, and porosity components (vug and inner porosities). The study indicates that Florida carbonate-rocks are

porous to very porous, with porosity up to 60% and a median porosity of 37%. Due to high porosity, recent deposition (many rock formations deposited within the last 2 million years, which actually is a very short time for rocks to deposit), and low carbonate content, Florida rocks have low strengths, with median BST of 0.6 MPa (90 psi) and median q_u of 3 MPa (435 psi). The study has established strong correlations to estimate BST and q_u from bulk dry unit weight, formation identification, and carbonate content.

Most importantly, a rock triaxial system with a modified volume change measurement device has been setup to analyze Florida carbonate-rocks' stress-strain and volumetric responses. Based on more than 200 triaxial test results, it is concluded that most Florida rocks are in the ductile range when subjected to confining stresses typical for shallow foundation loadings. Based on the test results, a threshold for rocks to change from brittle to ductile behavior has been summarized. Finally, strength envelopes for the rocks in the study have been developed from triaxial test results. These envelopes show significant downward slope, at much steeper rate than the envelopes for brittle rocks. Additionally, guidelines to establish the strength envelope for other rocks in Florida is also recommended in the appendix.

CHAPTER 1
INTRODUCTION

Most of the Florida Department of Transportation (FDOT) bridges are founded on deep foundations (drilled shafts, driven piles, and a minority of projects on other types of piles). Many of these deep foundation elements derive their bearing capacities from the Florida carbonate-rocks and intermediate geomaterials (IGM). In some areas where shallow rock formations exist (i.e., rocks encountered at a starting depth of less than 5-m or 15-ft), designers have proposed the use of shallow foundations (i.e., spread footings) for support of bridge piers or bents. Required for design is the assessment of the rocks' bearing capacity which requires strength envelopes for the rock material, as well as identifying the stress-strain response to assess the failure modes (general, local, and punching). One option is to modify and use existing strength envelope models. One such model is the well-known Hoek and Brown criterion (Hoek and Brown 1980, 1988, and 2018), originally developed for underground excavation (tunnel) in hard rock. Another model is the Johnston (1985) criterion, which is very similar to Hoek - Brown criterion.

However, the rocks tested by Hoek and Brown (1980, 1988, and 2018) and Johnston (1985) typically had high strengths, with brittle rupture failure response. The problem with the adoption of these strength criteria is that Florida carbonate-rock is generally weaker than rock formations in other areas of the world, probably due to its fairly recent deposition as the Florida peninsula underwent varying degrees of submersion prior to its current layout. Florida materials, especially at shallow depths, are porous to very porous and their stress-strain responses are not necessarily brittle. Given the differences, the recommended parameters suggested in the literature for use in Hoek-Brown or Johnston criteria has been brought into question when applied to Florida rocks.

Additionally, due to the highly heterogenous nature of Florida carbonate-rocks, the rock core recovery, REC = (sum of lengths of all recovered core pieces) / (total length of the core run), as well as rock quality designation, RQD = (sum of lengths of pieces that are longer than 4 inches) / (total length of the core run), are typically less than 100%, and frequently less than 50%. At the same time, specimens for unconfined compression or triaxial strength tests are required to have a length / diameter ratio of 2.0 (i.e., the core pieces need to be longer than 5 or 8 inches for 2.5-in or 4.0-in core barrels, respectively). Therefore, often there are not enough long pieces for strength tests. Thus, the first two objectives of this research are to:

1. Investigate the Florida rock index properties.
2. Establish correlations from rock index properties to conventional strength results (Brazilian splitting tension – BST and unconfined compression – q_u) to enable rock strength estimates from index testing of available core pieces from the core runs.

Then, the research aims to:

1. Develop strength envelopes for both compression (underneath the footing) and extension (outside the footing) loading of Florida carbonate-rocks.
2. Develop stress-strain and volumetric strain models for Florida carbonate-rocks.

To cover the above objectives, the following chapters are presented, with Tables and Figures placed at the end of each chapter:

- Chapter 2: Overview of Rock Identification and Geological Setting. This chapter presents a literature review into rock descriptions, with a focus on the shallow formations found in Florida.
- Chapter 3: Overview of Laboratory Tests. This chapter presents a literature review into the procedures of laboratory tests commonly performed on rock in Florida.
- Chapter 4: Properties of Carbonate-Rocks and IGMs. Shown in this chapter are the results characterizing the index properties from two data sets of Florida carbonate-rocks.
- Chapter 5: Splitting Tension and Unconfined Compression Strengths of Florida Carbonate-Rocks and IGMs.

- Chapter 6: Strength Envelopes of Florida Carbonate-Rocks and IGMs. The chapter has three main parts:

    a) Review of conventional strength envelopes (Mohr – Coulomb, Hoek-Brown, and Johnston)

    b) Description of the triaxial system and its modification to perform tests on Florida carbonate-rocks

    c) Test results and strength envelope construction for Florida carbonate-rocks.

The study presented in this dissertation has several significances: i) different components of porosities ; porous and vuggy scales are also recommended as there is no consistent grading scale that is available; ii) Basic strength parameters are correlated to index rock parameters based on equations provided in Chapter 5, which are helpful in situation when the recovered rock specimens are too short for strength tests; iii) Florida carbonate-rocks were found to have a predominantly ductile stress-strain response when the unconfined compression strength, q_u, is less than 9 MPa (1,300 psi), making strength envelopes for brittle rock unsuitable and necessitated the development of a strength envelope model for the different Florida formations that can be applied in evaluating shallow foundation bearing capacity on Florida carbonate-rocks.

CHAPTER 2
FLORIDA SURFACE ROCK GEOLOGY AND GENERAL TERMINOLOGIES

2.1 Geology of Florida Surface Rocks

Florida carbonate-rocks are chemical and/or biochemical sedimentary rocks. Chemical/biochemical sedimentary rocks are composed of minerals precipitated mainly from ocean or lake water by inorganic (chemical) and/or organic (biogenic) processes. The sediment and the cementation processes were governed by many factors, including the changes in water level. During the Holocene Epoch, the sea water level apparently fluctuated as much as 120 m (400 ft) (Chappell, 2009). As a result, the shallow soils and rocks have high spatial variability, or heterogeneity. This heterogeneous feature of Florida materials is depicted in Figure 2-1, which shows the stratigraphy of shallow materials within two pits in Lee county (Missimer and Scott 2001).

According to Figure 2-2, the Florida carbonate-rocks are very young. The oldest rock in the state only dates back to the Eocene Epoch, which is only approximately 1% of the maximum time scale of 4.6 billion years presented in Figure 2-2. As the Florida carbonate-rocks are very young, many believe that some Florida carbonate-rocks are still in the process of "forming", which may take millions or hundreds of millions of years. Therefore, while still in the forming process, some of our rocks have already been exposed to the weathering process, which weaken the rock strengths.

The Florida carbonate-rocks can be divided into: (i) limestone, (ii) dolostone, (iii) and marls. Limestones are composed mainly of the mineral calcium carbonate $CaCO_3$. The same chemical composition $CaCO_3$ can exist in different crystalline structures: (1) Rhombohedral for Calcite, and (2) Orthorhombic for Aragonite. Per Boggs (2006), the modern shallow-water carbonate

sediments are composed mainly of aragonite. Aragonite is metastable at the low pressures near the Earth's surface and is thus commonly replaced by calcite in fossils. As such, most limestones in Florida are calcite while some mollusk shells and calcareous coral endoskeletons are aragonite. Aragonite has specific gravity (GS) from 2.85 to 2.94, which is higher than that for calcite (GS = 2.70 to 2.72) per Hester & Schmoker (1985). Using measured specific gravity results, Hester & Schmoker (1985) estimated that the aragonite content is substantially high (91% to 99%) for the Bahamian Oolites (Holocene epoch). However, for the older Pleistocene Miami limestones, aragonite had been replaced by calcite, thus the aragonite content reduces to typically between 30% and 5%. Apart from pure calcite, limestones can also contain several percent of magnesium in their content, for example, their chemical composition can be described as $Mg_{0.06}Ca_{0.94}CO_3$ with an informal name of mgcalcite.

Dolostones are composed mainly of the mineral dolomite $MgCa(CO_3)_2$. Dolomitization is a process by which limestone is altered into dolomite; when limestone comes into contact with magnesium-rich water, the mineral dolomite, $MgCa(CO_3)_2$, replaces the calcite, $CaCO_3$, in the rock, volume for volume. Dolomitization involves recrystallization on a large scale. The dolomite mineral grains often show distinct faces, are of more or less uniform size throughout, and are larger than the calcite crystals in the limestone. When the recrystallization is not complete, the dolomite crystals are scattered throughout a calcite matrix. Sometimes rocks are formed that show zones of dolomite mottling the limestone where the magnesium-rich waters are thought to have filtered through the rock. In the process of dolomitization the dolomite crystals cut across original calcite grains, fossils, and oölites (spherical modules of calcite) and sometimes include quartz grains within their boundaries. Dolomites do not preserve the textures of the original limestone nor the fossils therein. Fossils are uncommon in dolomites but

sometimes remain as faint shadows outlining the original shape without showing internal detail or as molds with poor detail and filled with tiny dolomite crystals.

Marl or marlstone is a calcium carbonate or lime-rich mud or mudstone which contains variable amounts of clays and silt. The dominant carbonate mineral in most marls is calcite, but other carbonate minerals such as aragonite, dolomite, and siderite may be present. Marl was originally an older term loosely applied to a variety of materials, most of which occur as loose, earthy deposits consisting chiefly of an intimate mixture of clay and calcium carbonate, formed under freshwater conditions; specifically, an earthy substance containing 35–65% clay, silt, or sand and 65–35% carbonate. Marl specimens subjected to prolong air-dry condition gain significant strength. In the opposite direction, marl specimens subjected to prolong moisture condition in moisture room would lose their strengths and will not retain their own cylindrical shapes. Therefore, it is critical to preserve the natural moisture content of the cores and test the specimens right away. Once the marl specimens have been subjected to air-dry condition, their strengths have been naturally altered and should not be evaluated.

Most carbonate-rocks have micro-crystallite structure, i.e., the rock grain contains small crystals visible only through microscopic examination. Rocks with very large grain size – when the grains are visible under human vision – are calcarenite and coquina (for example Anastasia formation). Calcarenite is a clastic (cementation of sand and/or mud by calcite) sedimentary rock that is made up predominantly of recycled carbonate particles of sand size while coquina is composed of either wholly or almost entirely of the transported, abraded, and mechanically-sorted fragments of shells.

Quartz (sand) is also a major component of Florida rocks, with contents of up to 50% by weight. The higher the quartz content, the lower the cementation of the rocks. Apart from four

major minerals of calcite, aragonite, dolomite, and quartz, Boggs (2006) stated that minor amount of feldspars and clay minerals are present in most carbonate-rocks, with minor to trace elements of Al, K, Mn, Na, Fe, Zn, B, Be, Ba, Sr, Br, Cl, Co, Cr, Cu, Ga, Ge, and Li. Many organisms concentrate and incorporate trace elements into their skeletal structures.

In urban or suburban areas of Florida where bridges are constructed, the following carbonate-rock formations are typically encountered at shallow depths:

Qm: Miami formation consists of two facies, an oolitic facies and a bryozoan facies. The oolitic facies is poorly to moderately indurated. The bryozoan facies is poorly to well indurated and tends to have more concentrations of fossils (Scott 2001).

Qk: Key Largo formation is moderately to well indurated fossiliferous, coralline limestone composed of coral heads encased in a calcarenitic matrix (Scott 2001).

Qa: Anastasia formation is composed of interbedded sands and coquinoid limestones. It is unindurated to moderately indurated, coquina of whole and fragmented mollusk shells in a matrix of sand often cemented by sparry, i.e., coarse-grained, calcite (Scott 2001).

Tqsu: Shelly sediments of Plio-Pleistocene age (informal name as Okeechobee shelly sediments), formerly known as Caloosahatchee/Bermont/Fort Thompson formations (Scott 2001). They are sands to limestone mixtures. The Fort Thompson formation is typically found around Hendry county and may extend toward Palm Beach and Broward counties. Caloosahatchee formation is typically found in Lee county. Bermont is typically found in Charlotte and/or Glades counties and it overlies the Caloosahatchee formation and underlies the Fort Thompson formation.

To: Ocala limestone: the lower Ocala Limestone is poorly to moderately indurated, very fossiliferous limestone. Where present, dolomite content increases with depth in the Ocala

Limestone, especially in the southwestern part where the base of the unit is often dolomitized (Arthur et al. 2008). These dolostones can be either (1) friable, light to medium brown, sucrosic (i.e., coarsely recrystallized), or (2) indurated, dark gray to dark brown, dense, crystalline. The upper part of the Ocala Limestone is poorly to well indurated, very fossiliferous limestone. It tends to be more mud-supported (i.e., mudstone to wackestone) and chalky. Mineralogy of the Ocala Limestone unit is predominantly calcite, and to a lesser extent, dolomite. Siliciclastics are rare; however, chert occurs throughout the formation and is generally more common where the unit occurs at or near land surface.

Hawthorn formation: The Hawthorn formation can be divided into many subgroups (Scott 2001) and is typically encountered at depths deeper than 30 feet. Two following subgroups are evaluated in this research:

i) Marl: carbonate contents can be as high as 80% or as low as 20%. Core specimens subjected to prolong air-dry condition would gain significant strength. At low carbonate contents (such as below 50%), core specimens subjected to prolong moisture condition in moisture room would lose their strengths and could not retain their own cylindrical shapes. Therefore, it is critical to preserve the natural moisture content of the cores and test the specimen right away. Once the core specimens have been subjected to air-dry condition, their strengths have been naturally altered and should not be evaluated.

ii) Hawthorn limestone/dolostone: this subgroup contains a mixture of calcite and dolomite, as well as quartz sand.

2.2 Example Pictures of Florida Rocks

Some example pictures of the Florida carbonate-rocks are presented in Figure 2-3 through Figure 2-6, which highlight the heterogeneity of Florida rocks. Therefore, it is expected that all test results should display considerable scatter and the coefficient of determination R^2 is expected to be low when correlating rock strength parameters. Additionally, despite having

abundant holes (vugs) or scales (such as of coral heads), no distinctive rock joint or joint face could be identified in Florida carbonate-rocks (Truzman 2016).

2.3 General Carbonate-Rock Terminologies

This section presents some common terminologies commonly used for rocks:

REC: Recovery - length of recovered rock divided by the total length of the core run.

RQD: Rock Quality Designation - a core recovery percentage that is intended to be an indicator of the number of fractures and the amount of softening in the rock mass that is observed from the drill cores. Only the intact pieces with a length greater than 100 mm (4 in.) are summed and divided by the total length of the core run.

GSI: Geological Strength Index - an engineering judgement index, based on rock mass evaluation of the rock blocks and joints (Hoek and Brown 1980, 1988, and 2018). For Florida rocks and IGMs, the materials appear as having no joints, thus making it very difficult to judge the GSI value.

RMR: Rock Mass Rating - also an engineering judgement index, which is based on six parameters: strength, RQD, joint spacing, joint condition, and joint orientation. Similar to the GSI, the RMR is not commonly used in Florida due to the jointless appearance of Florida rocks.

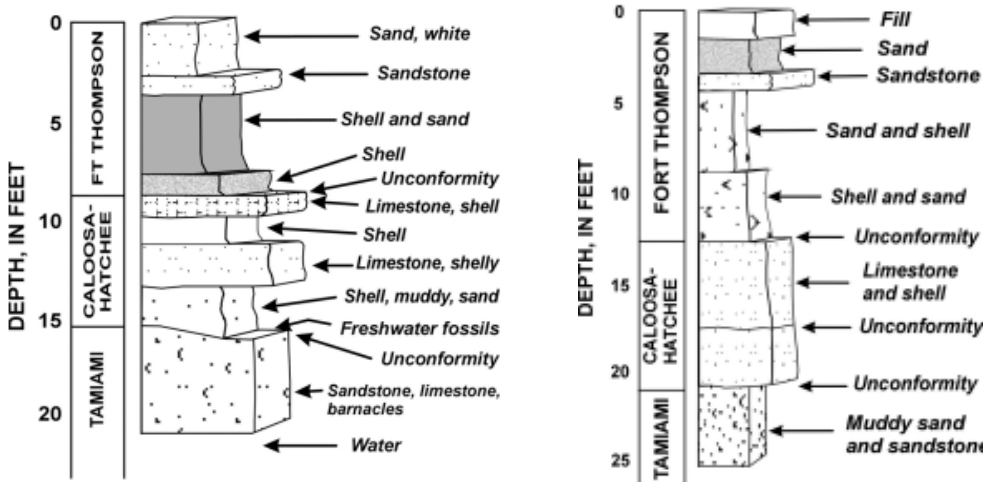

Figure 2-1. Stratigraphy of the Burnt Store Road and Nelson Road Pits in Lee County, Florida (Missimer and Scott 2001; FGS Public Report)

ADAPTED FROM OPEN-FILE REPORT 80 - GEOLOGIC MAP OF FLORIDA

Eon	Era	Period	Epoch	Comments	Subsurface	Millions Years
Phanerozoic	Cenozoic	Quaternary	Recent or Holocene	ice age ends	Soils (Qh)	
					Soils (Qal Qbd Qtr Qu)	0.01
			Pleistocene	ice age begins	**Anastasia/ Key Largo/ Miami** Soils (TQu, TQd, TQuc); S/**LS** mix (**Tqsu**) TQsu	1.6
		Tertiary – Neogene	Pliocene	earliest humans	**Tic: Intracoastal LS**; Soils (Tt, Tjb, Tci, Tmc, Tc) Soils (Thcc, Thp, Thpb)	5.3
			Miocene		**Chatahoochee DS; St Marks LS; Torreya** (Soils/**LS**); Other soils (Trm, Tab, Th, Thc, Ths) **Arcadia formation (Tha, That)**	23.7
		Tertiary – Paleogene	Oligocene		**Suwannee LS; Some dolostone (Ts, Tsm)**	36.6
			Eocene		**Ocala LS/ Avon Park (To, Tap)**	57.8
			Paleoenece			66
	Mesozoic	Cretaceous				144
		Jurassic				208
		Triassic				245
	Paleozoic	Permian				
		Carboniferous	Pennsylvanian			
			Mississippian	First reptiles		
		Devonian		First amphibians		
		Silurian				
		Ordovician		First land plants		
		Cambrian		First fish		545
Precambrian					Note: LS - Limestone	4600

Figure 2-2. Geologic units of Florida geology (Scott et al. 2001; FGS Public Report)

Figure 2-3. Newberry quarry excavation (Paul Bullock 2004; FDOT Public Report)

a)

b)

c)

Figure 2-4. Heterogenous rock specimens: a) Half vuggy limestone, half coralline specimen, b) "Scaled" coralline limestone specimen, c) Two different limestones within one specimen. (Photo courtesy: Thai Nguyen)

d) 

e) 

f) 

g) 

Figure 2-4. Continued: d) Half solid, half porous specimen, e) Solid rock with vug, f) Vuggy and porous limestone specimens, g) Fresh roots living in the vugs of limestone specimens

Figure 2-5. Weak poorly cemented silt, sand, limestone mixture in a core run (Photo courtesy: Thai Nguyen)

Figure 2-6. Examples of core runs with low RQD (Photo courtesy: Thai Nguyen)

CHAPTER 3
OVERVIEW OF CONVENTIONAL LABORATORY TESTS FOR CARBONATE-ROCKS

3.1 Porosity and Unit Weight Tests

For saturated soil, there are two volumes of interest: (1) Volume of solids, V_s, and (2) Volume of water, V_w, which is assumed to be unbound (free to move). In the case of saturated rock, there are actually four volumes of interest with diagram shown in Figure 3-1: (1) Solid, V_s, (2) Inner impermeable void (bound water in occluded pores), V_i, (3) Inner permeable (i.e. unbound) void, V_p, and (4) Vug, V_v respectively. In unsaturated medium, both soil or rock materials will have one more volume, air. To account for all four volumes in describing Florida carbonate-rocks, all related parameters are defined below.

γ_w = water unit weight = 9.81 kN/m^3 (62.43 pcf).

SSD = Saturated Surface Dry condition, this is the condition where the inner porous volume of the sample is saturated, but the surface is damp-dry for laboratory test per American Association of State Highway and Transportation Officials (AASHTO) method T-85 or American Society for Testing and Materials (ASTM) method D6473.

$V = (\pi L D^2/4)$ = Total (true) cylindrical volume of the core specimen.

V_s = Solid volume, this is the volume of the rock particles which is difficult to evaluate. Hester & Schmoker (1985) described a porosimeter used in the Petroleum industry to measure V_s based on the volume of sample not occupied by helium at 0.7 MPa (100 psi) in a carefully calibrated chamber that accommodates 1-in diameter samples. The porosimeter is expensive ($15,000 in 2016) and has a sample diameter limitation of 2.5-cm (1-in), which is much smaller than the most common diameters of 6-cm to 10-cm (2.4-in to 4-in) for rock cores in Florida

practice. Therefore, the specific gravity method for soil, the AASHTO method T-100 or ASTM method D-854 (Specific Gravity by Water Pycnometer for soils passing #4 sieve), was improvised so that it can be applied to Florida rocks. All rock specimens were pulverized to powder (100% passing through #40 sieve and 80% passing through #200 sieve), satisfying the sieve requirement to be tested per AASHTO T-100 or ASTM D-854. Furthermore, the powder can also be used for Powder X-ray Diffraction (XRD) test – see Section 3.3

V_{sa} = Apparent solid volume, to include the impermeable pore volume V_i that water is unable to enter into under submerged condition (Figure 3-1).

V_{ta} = Apparent total volume. This is the total displaced volume when the SSD sample is submerged under water (Figure 3-1).

V_v = Volume of vugs, which are holes significantly larger than the rock particle size (Sowers 1996). As rock cores are sufficiently small in diameter compared to the rock mass size, vugs are typically exposed on the outer face of the core. Therefore, in the laboratory testing condition, the vugs will not be able to retain free-standing water and the rock volume will be different than the cylindrical volume of the rock core specimen. As such, conventional test methods (ASTM D6473) will not yield meaningful moisture contents because the water will immediately drain from the free-standing core.

V_p = Volume of permeable voids, which are connected inner voids and can retain saturated water under laboratory testing condition so that saturated surface-dry (SSD) test condition per ASTM D6473 can be obtained. The mass of saturated water occupying V_p volume is Q_w (Figure 3-1).

V_i = Impermeable voids, which are occluded voids and the pore water can be evaporated in the drying oven. However, during the laboratory water submersion time (typically 24 ± 4 hours),

they are essentially water proof. The size of impermeable voids is very small. However, many well-distributed voids throughout the rock could sum up to a considerable volume, such as the case for Key Largo formation. In fact, when tested according to the ASTM D6473 method, some Key Largo rock pieces initially float in water before sinking very slowly to the bottom. The impermeable porosity is part of the coherent rock structure and is not as detrimental to their unconfined strengths (as opposed to the case of n_v and n_p); thus, the existence of the impermeable porosity makes the rocks light weight, but still they retain their unconfined strengths.

A = Dry mass in air (the notations A, B, and C below are used by ASTM D6473 method).

B = SSD mass in air; $B = Q_w + A = V_p \gamma_w + A$.

C = Buoyant mass of submerged specimen in water; however, as there may be internal pores, V_i, that is not permeable, the water does not come in all the pores; $C = A - V_{sa}\gamma_w$

$(B-C)/\gamma_w$ is supposed to present the total specimen volume. However, $(B-C)/\gamma_w = V_p + V_{sa}$ actually presents the apparent total specimen volume as vugs do not retain water, thus are not part of the SSD mass B, Figure 3-1.

The A, B, and C notations are also used in the AASHTO T-85 for specific gravity of rock and coarse aggregate. In the following equations, the ones denoted with an asterisk (i.e., Eqs. 3-3 and 3-5) are derived from A, B, and C per AASHTO T-85/ ASTM D6473.

$$C = A - V_{sa}*62.43 = B - V_{ta}*62.43 \quad (3\text{-}1)$$

Dry bulk (true) dry unit weight $\gamma_{dt} = A / V$ (3-2)

Dry apparent dry unit weight (*) $\gamma_{da} = A / V_{ta} = \gamma_w A / (B-C)$ (3-3)

Solid true unit weight $\gamma_{st} = GS\ \gamma_w$ (3-4)

Solid apparent unit weight (*) $\gamma_{sa} = A / V_{sa} = \gamma_w A / (A-C)$ (3-5)

In Eq. 3-4, GS value is obtained from AASHTO T-100/ ASTM D-854. This is the true solid specific gravity, which is in fact a weighted average value of the mineral specific gravities, depending on the percentage of each mineral in the rock specimen. Mineral specific gravities cited in literature are presented in Table 3-1.

It should be noted that most index parameter tests are performed on the same specimens that are tested for strength (i.e. q_u or BST), after the specimen have been fractured. Thus, extreme care needs to be taken to collect every single broken piece to obtain the total oven-dried weight of the specimen. In addition to the traditional bulk porosity parameter in Eq. 3-6 below, additional porosity components are evaluated in Eqs. 3-7 through 3-9:

Bulk porosity is defined as $n = V_{v+p+i} / V = 1 - \gamma_{dt}/\gamma_{st} = n_i + n_p + n_v$ (3-6)

Impermeable porosity: $n_i = V_i/V = \gamma_{dt}(1/\gamma_{sa} - 1/\gamma_{st}) = \frac{A}{V}(\frac{V_{sa}}{A} - \frac{V_s}{A})$ (3-7)

Permeable porosity: $n_p = V_p/V = \gamma_{dt}(1/\gamma_{da} - 1/\gamma_{sa}) = \frac{A}{V}(\frac{V_{ta}}{A} - \frac{V_{sa}}{A})$ (3-8)

Vug porosity: $n_v = V_v/V = 1 - \gamma_{dt}/\gamma_{da} = 1 - \frac{V_{ta}}{V}$ (3-9)

where n_v is termed as "wash content" by Hester & Schmoker (1985), as there might be insitu soft materials in the vugs before being washed away during the rock coring process.

Limestones in literature, such as those listed by Goodman (1989), are very dense with corresponding low bulk porosity: Solenhofen limestone, n = 5%; Great Britain limestone, n = 6%; Salem/ Bedford limestone, n = 12% to 13%. Therefore, the perception of "porous" rocks is very different to that of Florida rocks. For instance, Fereidooni and Khajevand (2018) indicated that travertine samples with n of 7% were porous; Schwartz (1964) considered the Pottsville

sandstone and Indiana limestone as porous rocks, with porosities of n = 14% to 20%, respectively. Gowd and Rummel (1980) considered n = 15% as porous. In Mogi (1966), rocks with n = 1% to 10% were grouped as porous, and n > 10% as very porous, with a highest porosity cited as n = 22%. In comparison, 90% of Florida limestone has porosity n ≥ 20% and only 10% of Florida limestone has porosity between 5% and 20%, i.e., the rocks that are typically considered porous in literature are considered "dense" and "outlier" data for Florida in general. Due to the fact that there is no consistent grading scale in literature to identify a rock as vuggy or porous, Tables 3-2 and 3-3 are proposed to describe the rocks based on magnitudes of different porosities.

3.2 Carbonate Content Test

Florida method FM 5-514 details a procedure to obtain total carbonate contents (which can be CaCO3, MgCO3, and $CaMg(CO_3)_2$, etc.). A summary of FM 5-514 for short method is itemized below.

For aggregates:

- Obtain a 50-lb gross sample at air dried condition.
- Quarter (split) the sample to 3 to 5-lb fractions. Then oven dry the fraction at 230^0F for 12-hr.
- Continue per steps below.

For rock cores and quartered aggregates:

- Crush the carbonate-rock to fragments of sand size. Then quarter (split) the sample to ¼ to 1-lb sample.
- Pass one fraction through a finer grinder so that 100% material passes through #10 sieve and 90% material passes #40 sieve (which is the fine sand size). In reality, the finer the material, the easier it takes to do the carbonate content tests. Therefore, most of the Florida rocks were

actually pulverized to much finer than the requirement, with 100% passing #40 sieve (fine sand size), and approximately 40% to 80% passing #200 sieve (silt size).

- Stir sample with spatula.
- Weight w= 1-gram specimen using a scale with accuracy of 0.0001 gram. Transfer the specimen to a 300-mL beaker by brushing.
- Add 20 mL of 1:5 hydrochloric acid HCl to the beaker slowly, the following reaction occurs:

$$CaCO_3 + 2HCl = CaCl_2 + CO_2 + H_2O \quad (3\text{-}10)$$

$$CaMg(CO_3)_2 + 4HCL = CaCl_2 + MgCl_2 + 2CO_2 + 2H_2O \quad (3\text{-}11)$$

- To aid the above chemical reaction, momentarily boil the beaker over a Bunsen flame or hot plate. Stand until the last gas has evolved.
- Drop three drops phenolphthalein $C_{20}H_{14}O_4$ - this is a weak acid.
- Neutralize to faint pink using 1:5 ammonium hydroxide NH_4OH (this is a weak base) (phenolphthalein turns pink in bases).
- Momentary boil the solution, then allow it to cool until the precipitate has settled enough for rapid filtration. Filter the solution through No. 41 paper, and transfer all the precipitate to the filter paper by washing with water. Wash the paper five times, allowing paper to drain between washings.
- Ignite the content wrapped in the filter paper in a porcelain crucible at 1550 to 1750°F until all carbon is destroyed (30 minutes or longer). The filter paper will burn out without any ash as No. 41 paper is an ashless filter paper.
- Then cool the crucible with remaining ash down; weight the crucible content in gram. This content is insoluble residue (R), which contains non-carbon portions of the rocks, such as quartz and metals such as Al, Fe, etc.
- Carbonate content then is (w - R)/w x 100%.

3.3 Powder X-ray Diffraction (XRD)

Powder X-ray Diffraction (XRD) is one of the primary techniques used by mineralogists and solid-state chemists to examine the physical-chemical make-up of unknown materials. The XRD technique takes a powdered sample in a holder, then the sample is illuminated with x-rays of a

fixed wave-length and the intensity of the reflected radiation is recorded using a goniometer. This data is then analyzed for the reflection angle to calculate the inter-atomic spacing (D value in Angstrom units or 10^{-8} cm). The intensity (λ) is measured to discriminate the various D spacings. The results are plotted as reflected angle, 2θ, versus intensity, where $2\theta = 2\{\text{acsin}(\lambda/(2D))\}$. Figure 3-2 presents the XRD patterns for typical minerals Dolomite, Aragonite, Calcite, and Quartz. Figure 3-3 presents the XRD results for actual specimens. Rietveld refinement technique - a signal matching analysis between simulation and measured intensity graphs - is then performed to estimate the percentage of each mineral within the specimen. For example, specimens 4434/ 5246 in Figure 3-3 are estimated by the Rietveld refinement signal-matching program to have 94% and 99% calcite, respectively. It is evident that the signals of these two specimens resemble the calcite intensity peaks shown in Figure 3-2. Specimen 4337 in Figure 3-3 has intensity peaks that resemble both calcite and aragonite in Figure 3-2. The Rietveld refinement signal-matching program estimates that this specimen has 63% calcite and 36% aragonite.

3.4 Brazilian Splitting Test

The Brazilian Splitting Test (or Brazilian Strength Test – BST) is used indirectly to evaluate the tension strength of rocks. In this test, the compressive loads are line loads applied parallel to the core's axis by steel bearing plates between which the specimen is placed horizontally. Loading is applied continuously at a constant rate of deformation – typically 0.015 to 0.03 in/min – such that failure occurs within one to ten minutes so that the specimens are reasonably free from rapid loading effects. The splitting tensile strength of the specimen is calculated as $2P/(\pi LD)$, where P is the applied load, L is the length, and D is the diameter of the

specimen. Tests shall be performed in accordance with ASTM D-3967 except that the minimum t/D (length-to-diameter) ratio shall be much longer than ASTM D-3967 method – approximately t/D = 1 due to the nature of Florida carbonate-rocks (FDOT 2018). The splitting tension strength is historically denoted as q_t, however in this research it is denoted as BST to make it clear that it is not the same as direct tension strength.

Per Perras and Diederichs (2014), the q_t/BST ratio of the test results of the two methods (direct tension strength versus BST) for sedimentary rock ranges from 0.4 to 1.2, with a mean value of 0.7, as shown in Figure 3-4. For concrete, the scatter of the q_t/BST spread is less, and thus Hannant et al. (1973) suggests a factor of q_t/BST = 0.9 for concrete.

Impacting the strength results are the orientations and distributions of the vugs within the specimens relative to the loading line. Figure 3-5 to Figure 3-9 illustrate different splitting behavior of Florida carbonate-rocks. If the rocks are relatively uniform without vugs, the specimens likely exhibit center splitting. However, when the rocks are not uniform or contain vugs, the BST strengths are likely to be low due to the failures through the weakest path as well as off center. Figure 3-7 to Figure 3-9 presents some examples where the BST results would expect to be low, as those specimens did not split through the center as expected. Thus, the splitting tension strength through the center of these specimens could be higher, but the specimens already failed elsewhere before the center splitting happened. Figure 3-10 presents an example where an uneven diameter specimen could introduce local stress concentration from the steel platen of the BST test, thus the BST result could be lower than expected.

3.5 Unconfined Compression Test

Unconfined compression tests are performed in accordance with ASTM D-7012 (formerly D-2938) method. The specimen is placed in the testing machine and loaded axially at an approximately constant rate such that failure occurs within 2 to 15 minutes. The axial compression pressure at failure is the unconfined compression strength, q_u. This is the most popular parameter to describe rock strengths. Some carbonate-rocks q_u values in literature are presented in Table 3-4, which indicate high strength values. In contrast, Florida carbonate-rocks, with high porosities (from 10% to 60%) and of younger formations, typically have much lower strengths than those shown in Table 3-4 and their strengths will be discussed in detail in Chapter 5.

Table 3-1. Mineral specific gravities from literature

Mineral	Jumikis (1983)	Goodman (1989)	Lambe & Whitman (1969)	Hester & Schmoker (1985)
Calcite	2.71 - 3.72	2.7	2.72	2.71
Aragonite				2.91-2.94
Dolomite	2.80 - 3.00	2.8-3.1	2.85	
Quartz		2.65	2.65	2.65

Table 3-2. Proposed vug descriptions

n_v	0 to 5%	5 to 10%	10 to 15%	15 to 20%	>20%
Vug porosity	No vug, relatively smooth rock	Slightly vuggy	Vuggy to Very vuggy	Very vuggy	Extremely vuggy

Table 3-3. Proposed porosity descriptions

n	0 to 15%	15 to 30%	30 to 45%	>45%
Bulk porosity	Dense	Slightly porous	Porous	Very porous

Table 3-4. Typical carbonate-rock strengths

Source	q_u (ksi)	q_u (MPa)
Solenhofen Limestone (Jaeger and Cook 1969; Goodman 1989)	32 to 36	220 to 250
Bedford Limestone (Goodman 1989)	7 to 8	48 to 55
Tarvernalle Limestone (Goodman 1989)	14	100
Malaysian Limestone (Zazir et al. 2013)	8 to 16	55 to 110
Virginia Limestone (Jaeger and Cook 1969)	48	330
Australian Limestone and Dolostone (Johnston 1985)	6 to 75	38 to 520
Limestone (Hoek and Brown 1980)	6.4 to 29	44 to 200
Dolostone (Hoek and Brown 1980)	21 to 73	150 to 500

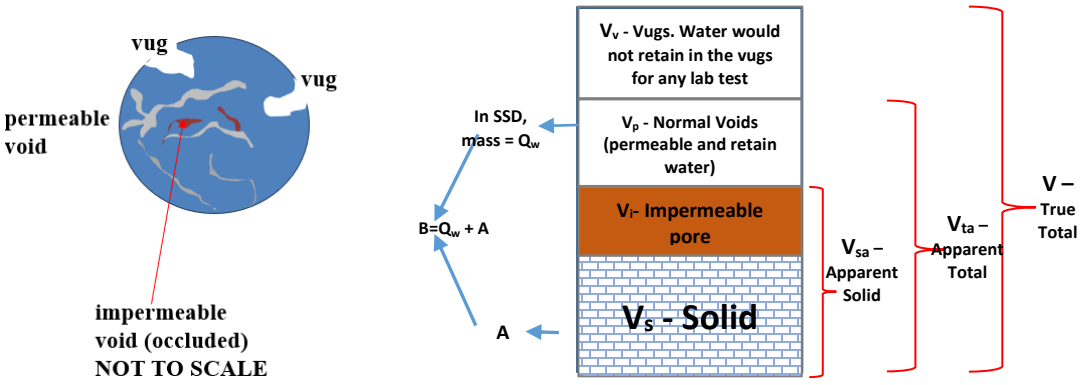

Figure 3-1. Rock phase diagram

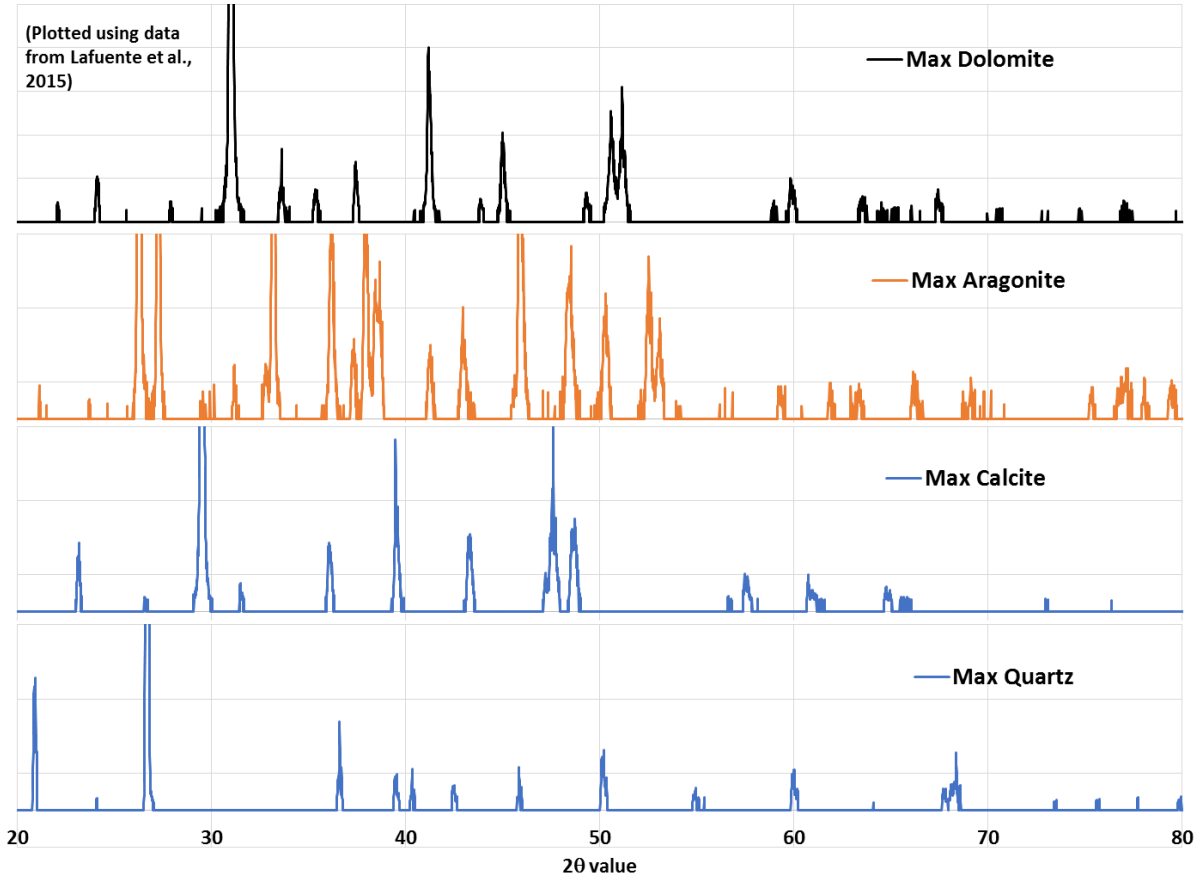

Figure 3-2. XRD major 2θ peaks for typical minerals

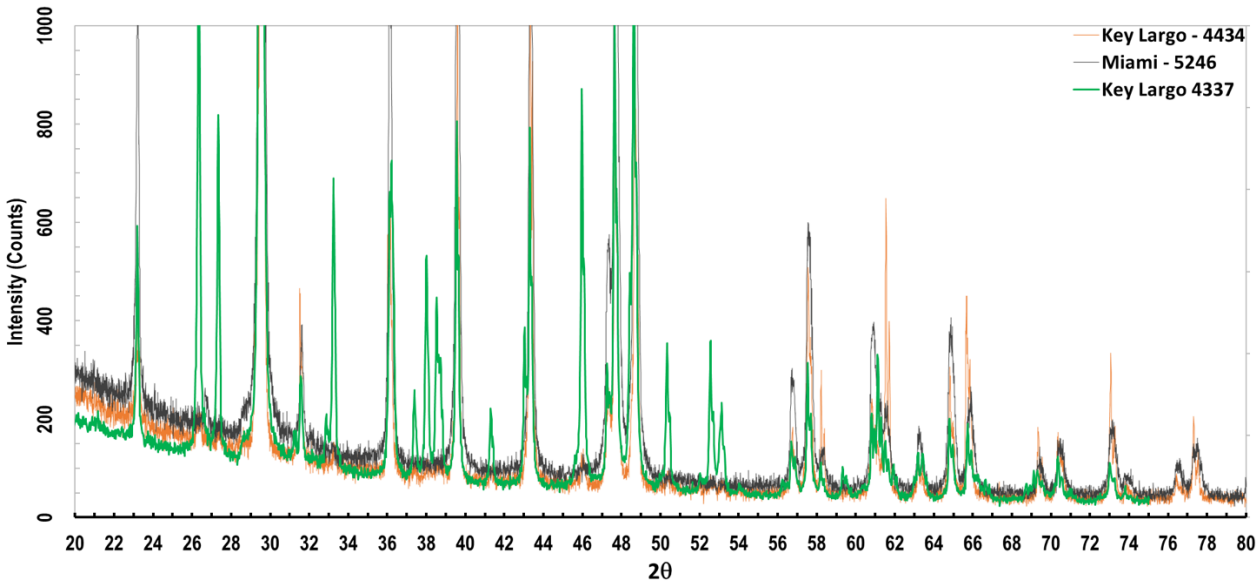

Figure 3-3. Example XRD patterns of Miami and Key Largo limestone specimens

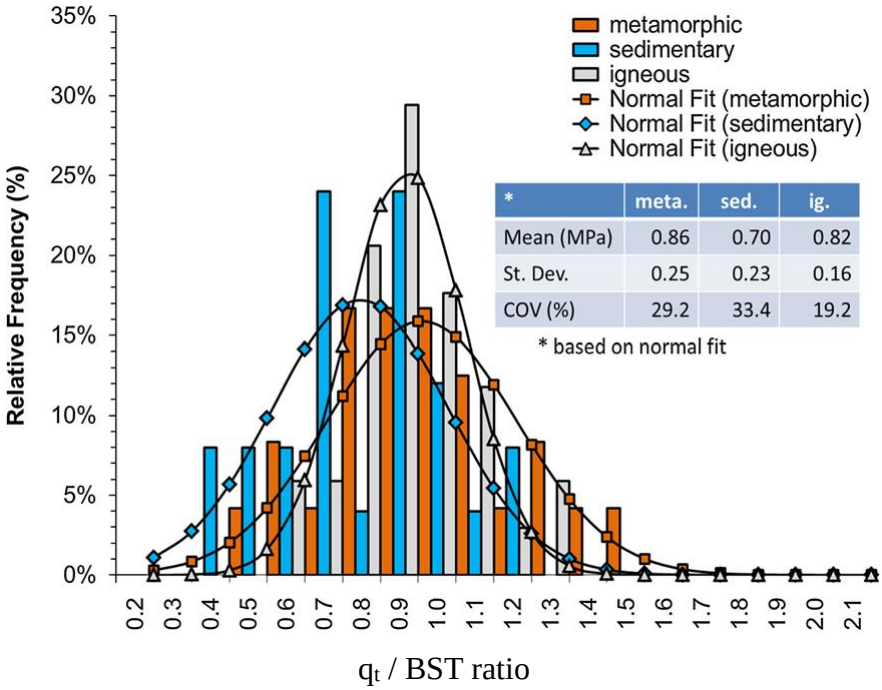

Figure 3-4. BST versus DTS relationship

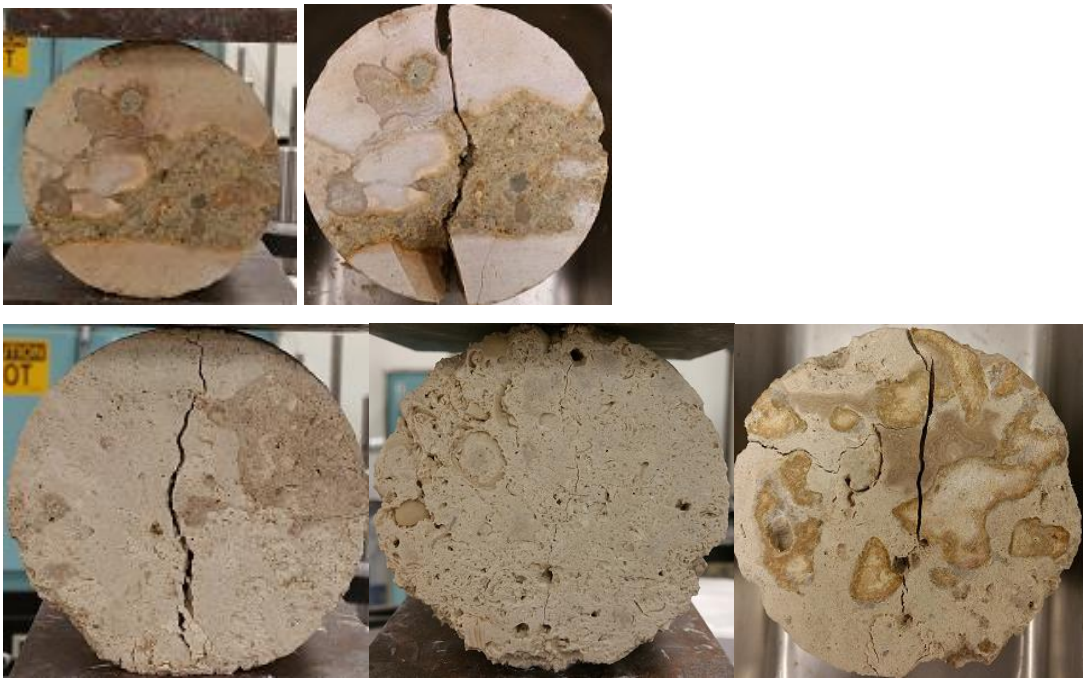

Figure 3-5. Examples of BST center splitting (Photo courtesy of Thai Nguyen)

a) b)

Figure 3-6. BST test on sample 543-1: a) Splitting on center on one face b) Splitting off-center on the other face. (Photo courtesy of Thai Nguyen)

Figure 3-7. Non-center splitting - BST tests on samples 534-1 and 541-6 (Photo courtesy of Thai Nguyen)

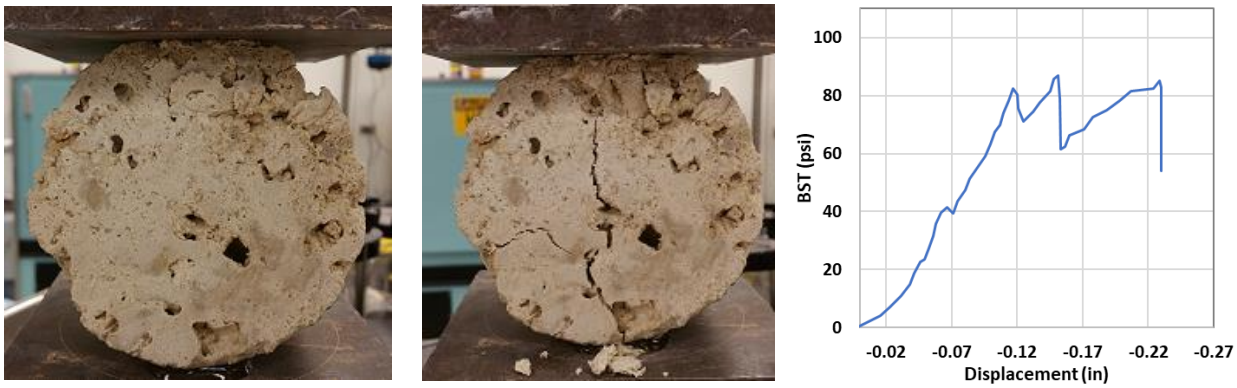

a) b) c)

Figure 3-8. BST test on sample 545-2: a) compression crushing occurred at contact between the steel platen and specimen, b) splitting occurred after significant crushing c) splitting stress versus displacement. (Photo courtesy of Thai Nguyen)

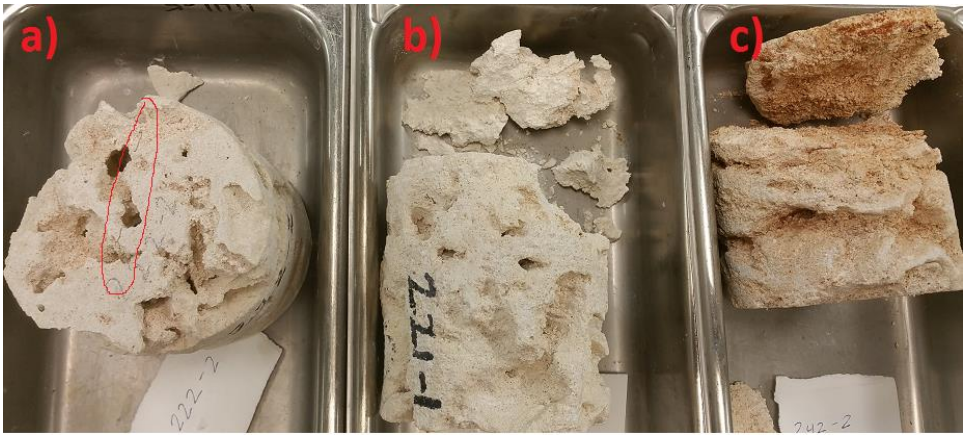

Figure 3-9. BST tests on vuggy porous limestones
a) splitting, b) crushing thorough soft end, c) crushing through weak zone
(Photo courtesy of Thai Nguyen)

Figure 3-10. BST on sample 624-3 with uneven diameter
(Photo courtesy of Thai Nguyen)

CHAPTER 4
PROPERTIES OF CARBONATE-ROCKS AND IGMS

4.1 Florida Data

Two sets of data for carbonate-rocks and Intermediate Geo-Materials (IGM) throughout the state of Florida were utilized in this study with results presented in the subsequent sections:

Data set #1 contains over 8,000 historical data points, which were collected by the Florida Department of Transportation (FDOT) for projects from 1990 to 2017, listed in Table 4-1. Data set #1 includes the following three parameters: 1) Unconfined compression strength results – q_u, 2) Brazilian splitting tension strength results – BST, and 3) bulk dry unit weight results – γ_{dt}. Data set #1 includes a subset #1a of 98 points of data, where rock formation identifications were available.

Data set #2 consists of approximately 573 data points (270 BST, 80 q_u, and 223 triaxial test results) performed specifically for this study. The data comes from 8 different sites across Florida, as shown in Table 4-2. For data set #2, in addition to the three parameters referenced above, the following rock index parameters were obtained: 4) rock formation identification, 5) carbonate content, and 6) vug and inner porosity. The rock core descriptions for data set #2 and photographs of the cores are presented in Appendices A and B, respectively.

4.2 Florida Carbonate-Rock Porosity and Unit Weight Results

Moist unit weights (γ) are presented along with bulk dry unit weights (γ_{dt}) in Figure 4-1. This figure indicates that the tested rock specimens were at different degrees of saturation. For example, when γ_{dt} = 70 pcf, γ could vary from approximately 70 pcf (i.e., specimen was dry) to

110 pcf (i.e., specimen was fully saturated). In the field, most of the rocks are fully saturated due to the depth of the rocks and the relative shallow ground-water table depths in Florida. However, it is impossible to retain the water from running out of the vugs in laboratory. Therefore in Chapter 5, rock strengths are not being correlated to laboratory moisture content, rather they are being correlated to the bulk dry unit weight or porosity.

From data set #1, most (80%) of the specimens have dry unit weights (γ_{dt}) between 80 and 130 pcf (Figure 4-2). Specimens having γ_{dt} of less than 80 pcf are typically very porous, vuggy, and of low strengths – thus, not typically suitable to be utilized to support foundation structures. Specimens having γ_{dt} higher than 130 pcf are typically not encountered consistently or in substantial lengths (i.e., rock layers are typically only a few inches or a foot thick). Therefore, outlier rocks with γ_{dt} more than 130 pcf should be conservatively treated as rocks with the same strengths as those with γ_{dt} = 130 pcf. Also, from Figures 4-2 and 4-3, the median bulk dry unit weight and median bulk porosity for Florida carbonate-rocks are approximately 105 pcf and 37%, respectively, which indicate that Florida carbonate-rocks are much more porous than other rocks in literature (Section 3.1).

Figure 4-4.a presents the bulk porosity versus vug porosity of the FDOT carbonate-rock specimens. These results agree with data collected by Hester & Schmoker (1985), plotted by Thai Nguyen in Figure 4-4.b. Evident from Figure 4-4, they have a wide range of bulk porosity, n, from approximate 5% (relatively dense rock) to 60% (very porous rock) and the vug porosity, n_v, from 0% (no vugs) to 35% (extremely vuggy). Figure 4-5 highlights different proportions of porosities, namely vug (n_v) and permeable (n_p) within the bulk porosities (n) of multiple Florida rock formations.

4.3 Florida Carbonate-Rock Minerals

The key component of the carbonate-rocks is carbonate content. To quantify the mineral components of Florida rocks, carbonate contents per Florida method FM 5-514 (FDOT 2015) and Powder X-ray Diffraction (XRD) tests have been conducted in this study. The carbonate contents are presented in Figure 4-6 and are described below:

Ft Thompson of the Shelly sediments of Plio-Pleistocene age (Tqsu): Typically, this formation is a calcite limestone and quartz. Ft. Thompson formation has a low carbonate content compared to other Florida rock formations - it ranges from 65% to 80%.

Anastasia (Qa): Anastasia formation has a wider range of carbonate content, typically from 65% to 95%, and the remaining component is quartz. The carbonate is typically calcite, with a minor percentage of aragonite.

Miami (Qm): This formation is also a calcite, with a minor percentage of aragonite, and quartz. Depending on the location of the Miami formation, which can be the oolitic facies (Atlantic Coastal Ridge) or the bryozoan facies (toward the Everglades) and depending on degree of induration, the carbonate content of Miami formation can range from 80% at one location to 98% at another location, also as shown in Figure 4-6 for three different Miami sites.

Key Largo (Qk) formation has the highest carbonate contents (near 100%), which consist of mainly calcite, averaging at about 80%, and a minor amount of aragonite averaging 20%.

Undifferentiated Hawthorn group (Th): Among this group, there are two subgroups of carbonate-rocks that were tested in this study:

i) Hawthorn dolostone/limestone: in this subgroup, the carbonate contents typically range from 65% to 95%, with feldspar/ quartz as the remaining mineral component. The carbonates are mixtures of dolomite and calcite.

ii) Hawthorn marl: the marl has the same main minerals as the other Hawthorn rocks: dolomite, calcite, and an earthy mineral (quartz). However, the carbonate content is much lower in marl. For marl, the natural moisture contents of the specimens control the strengths of the material. If the specimens lose their moisture content, their dry strengths (i.e., unconfined compression or splitting tension) are typically much higher than their true strengths. However, if the specimens are subject to unnatural moisture (such as in a moisture room, without the natural overburden confining pressure), the material will disintegrate (lose strength). In Figure 4-6, marl specimens typically have carbonate contents less than 65%. However, many marl specimens had the same properties (same dry unit weights, same carbonate contents of between 65% and 85%) as the Hawthorn dolostone. Due to exposure issues (quartz located at surface of the cores), it was decided to classify them as Hawthorn marl, whereas for cores that the marl was not exposed (i.e., dolostone is on the cover of the cores, and marl lens is buried inside), the specimens with carbonate content exceeding 65% are categorized as dolostone for strength purpose. The reason is that when marl is exposed at the surface of the cores, when tested for strength tests (BST or q_u), the marl on the surface of the core would collapse or chip away, leading the loading frame to stop the test due to excessive deformation.

Arcadia formation of Hawthorn group (Tha): This formation is somewhat similar to the subgroup a) of the undifferentiated Hawthorn group: Arcadia formation is also a dolostone, with carbonate content typically from 70% to 90%.

The XRD tests were performed on a limited number of specimens and the mineral components of the rocks are calculated using Rietveld Refinement analyses in columns 5 through 11 of Table 4-3. The sum of columns 6 through 11 is the total carbonate content, which is presented in column 4. These results in column 4 agree well with total carbonate content results performed by FM 5-514 method in column 3. From Table 4-3, it can be seen that each formation contains three main minerals: For the youngest formations (approximately less than 2 million years old), the three minerals are calcite, aragonite, and quartz. For older formations, aragonite typically does not exist as it is replaced by calcite (refer to Section 2.1), at the same time, some dolomitization occurred due to the flow of magnesium-rich water. Thus, the three main minerals for older formations are calcite, dolomite, and quartz.

For example, the specific gravity of specimen #4337, performed per ASTM D854 method, is GS = 2.77. XRD result indicates that specimen #4337 has 63.5% calcite with $GS_{calcite}$ = 2.70, 36.3% aragonite with $GS_{aragonite}$ = 2.91, and 0.2% quartz with GS_{quartz} = 2.65. Therefore, the specimen's specific gravity is 63.5% * 2.70 + 36.3% * 2.91 + 0.2% * 2.65 = 2.77, which confirms the GS value performed by ASTM D854 method. For specimens having no XRD results, the aragonite (for young formations of less than 2 million years old) or dolomite (for older formations) content can be back calculated from GS and carbonate test results. For example, specimen #3221 (Anastasia formation, Quaternary period, young formation) has 91.6% carbonate (FM 5-514 test result), 8.4% quartz, and GS = 2.73 (ASTM D854 test result), the aragonite content, C_a, is back calculated as: (91.6% - C_a) * 2.7 + C_a * 2.91 + 8.4% * 2.65 = 2.73, thus C_a = 17%. From these back calculations of the aragonite or dolomite contents, Table 4-4 presents a summary of the calculated mineral contents of various Florida formations.

4.4 Subsurface Spatial Variability

With the exception of some isolated areas of Florida where a few carbonate-rocks are dense with low porosity, many Florida carbonate-rocks – as shown in Section 2.2 – are nonuniform, porous, and often times vuggy to the extent that plant roots are able to grow through a connected vug structure. The rock recovery (REC) and rock quality designation (RQD) are generally poor when at least one of the following conditions is encountered: poor cementation (poor induration – generally low strength rocks), or brittle rocks, and/or interbedded rock/soil types, and/or extreme vugs/voids. An example of the graphical coring logs are presented in Figure 4-7 where each curve represents one borehole within each project site. In the figure, the recovery was poor to decent (typically 40% to 80%) and RQD was very poor to decent (typically 0% to 60%). All

parameters (REC, RQD, and coring time) in the figure would indicate subsurface spatial variability. Furthermore, when presenting the bulk dry unit weight, γ_{dt}, with depth (Figure 4-8), the subsurface spatial variability really stands out. For each site, within a very short vertical distance, γ_{dt} can vary up to 8 kN/m^3 (50 pcf) indicating a very wide range of rock densities, from very porous (γ_{dt} = 12.5 kN/m^3 or 80 pcf) to dense (γ_{dt} = 20.5 kN/m^3 or 130 pcf). This reflects the extreme heterogenous nature of Florida carbonate-rocks.

4.5 Summary

Florida carbonate-rocks and IGMs are young and thus their crystal bonding strengths may influence their unique geotechnical properties. They are generally very porous, with porosity up to 60%. The carbonate, such as $CaCO_3$ or $CaMg(CO_3)_2$, acts as binder for the cementation of the material. However, some formations have very low carbonate contents of only 80% down to even 65%. Below 65% carbonate content, the IGMs are typically not testable for unconfined compression nor splitting tension strengths as specimens can easily disintegrate during handling for strength testing.

Based on the results of carbonate content tests, X-ray diffraction (XRD) tests, as well as rock porosities of many Florida formations – different strength correlations may exist among the formations and the strengths are a function of the material characteristics, such as dry unit weight (porosity), carbonate content, and crystalline structure. These correlations are investigated and presented in Chapter 5.

Table 4-1. List of projects in data set #1

Name	ID	District	Location
I-75 over Manatee River	1	1	27°31'26.50"N 82°30'21.21"W
I-75 over Golden Gate Canal	2	1	26°10'06.6"N 81°43'50.0"W
Edison Farm	3	1	Not provided
I275 over Yukon St	14	7	28°01'45.1"N 82°27'18.6"W
SR-20 @ Lochloosa Creek, Alachua Co.	4	2	29.600716, -82.144517
SR-25 @ Santa Fe River	5	2	29°51'11.18"N 82°36'30.74"W
SR-10 @ CSX RR (Beaver St. Viaduct), Duval Co.	6	2	30.334805, -81.685905
SR-9 (I-95) Overland	7	2	30.31361, -81.65231
I 95 (Fuller Warren Bridge) over St. Johns River	8	2	30°18'53.7"N 81°40'10.7"W
CR-326 @ Waccasa River	9	2	29°13'17.40"N 82°45'29.03"W
I-295 Dames Point Bridge	10	2	30°23'8.09"N 81°33'26.24"W
I-295 Buckman Bridge over St Johns River	11	2	30.1901°N 81.6665°W
I-95 @ I-295 Cloverleaf	12	2	30°10'00.4"N 81°33'16.9"W
Acosta Bridge Research (Modulus)	13	2	30°19'18.6"N 81°39'52.2"W
US-98 / SR-30 @ Wakulla River	15	3	30°10'32.8"N 84°14'43.6"W
Bridge #530022 US 98 over Wakulla	16	3	Not provided
Rob Forehand Road Over Little Creek	17	3	30°53'53.6"N 85°43'06.5"W
Lost Creek Bridge #590048	18	3	30°09'38.4"N 84°22'53.2"W
I 10, SR 8 over Ochlockonee River (#550089EB, #550050WB)	19	3	30°29'06.5"N 84°23'50.9"W
SR 63, US 27 Ochlockonee Relief Bridge	20	3	30°33'14.2"N 84°23'03.1"W
SR 8 over Choctawhatchee River	21	3	30.7557092, -85.8298427
I 10, SR 8 Over Apalachicola River (#500087)	22	3	30.6335607, -84.9045483
I 10, SR 8 over Chipola River (#530052)	23	3	30.7245131, -85.1997390
SR-20 over Chipola River	24	3	30.4310665, -85.1718566
SR 166 over Chipola River	25	3	30.7928089, -85.2217664
I 10, SR 8 Over CSX, Little River	26	3	Not provided
US 90 over Little River	27	3	30°28'48.2"N 83°32'49.1"W
Sr 267 over Rocky Comfort Creek (#500027, 28)	28	3	30°29'33.3"N 84°36'49.2"W
Dry Creek SR 73 (#530089) (actually Chipola River)	29	3	30°41'22.1"N 85°14'10.3"W
SR30/US98 @ Aucilla River	30	3	30°08'47.2"N 83°58'24.5"W
SR-2 Bridge over Choctawhatchee River	31	3	30.9500870, -85.8431570
SR-10 (US90) Bridge over Choctawhatchee River	32	3	30°46'31.84"N, 85°49'37.56"W
Merritts Mill Pond US-90 SR-10	33	3	30°45'12.8"N 85°11'36.3"W
SR-166 Rock Slope Design	34	3	30.78819, -85.18632
Fisher Creek Bridge CR 2203	35	3	30°18'52.4"N 84°23'57.2"W
CR 166 Alligator Creek Bridge	36	3	30°47'30" N, 85°33'47" W
SR-8 (I-10) @ CR-286 High Mast	37	3	30°38'11.0"N 84°56'41.0"W
Holmes Creek - Cr 166 Bridge	38	3	30°47'58.3"N 85°36'08.9"W
CR 12A (Kemp Road Bridge)	39	3	30°37'38.4"N 84°22'06.3"W
Natural Bridge over St. Marks River	40	3	30°17'02.7"N 84°09'02.8"W
SR 71 over Rocky Creek	42	3	30°39'26.5"N 85°09'44.8"W
SR-20 @ Blountstown (Apalachicola river)	43	3	30°26'13.6"N 85°00'03.6"W
US-90 Victory Bridge	44	3	30°42'05.6"N 84°51'32.3"W
SR-2 Cowarts Creek	45	3	30°56'50.6"N 85°15'30.4"W
SR-2 Marshall Creek Jackson Co.	46	3	30°56'10.9"N 85°17'47.6"W
SR-2 Spring Branch Jackson Co.	47	3	30°56'14.4"N 85°19'26.0"W

Table 4-1. Continued

Name	ID	District	Location
SR-261 Capital Circle	48	3	30°27'13.9"N 84°13'35.1"W
US-98 / SR-30 @ St. Marks river	49	3	30°11'56.6"N 84°10'41.0"W
I-10 Tower site @ Snead's weigh station	50	3	30°38'23.5"N 84°58'58.3"W
SR A1A Flagler Memorial Bridge	51	4	26.718431, -80.047041
SR A1A over Sebastian Inlet	52	4/5	27.860028, -80.448415
US 1 over Dania Cutoff Canal	64	4	26.059517, -80.143883
SR 858 (Hallandale Beach Bridge) over Intercoastal	65	4	25.986404, -80.121659
SR 600 (Broadway Bridge) over Halifax River	66	5	29.216332, -81.015482
SR40 WB over Tomoka River 1991	67	5	29.254847, -81.123547
NW 36th Street Bridge Replacement	53	6	25°48'30.4"N 80°15'42.7"W
NW 12th Ave (SR 933) Miami River Bridge	54	6	25°46'58.83"N 80°12'53.34"W
MIC- People Mover Project	55	6	Not provided
Verona Ave Bridge over Grand Canal	56	6	25°57'36.8"N 80°07'18.6"W
HEFT / SR 874 PD&E	57	6	25°39'00.8"N 80°23'05.0"W
Wall @ Service Rd. South of Snake Creek	58	6	24.95092, -80.59129
17th St. Causeway, Miami	59	6	26°06'02.4"N 80°07'06.8"W
96th St. & Indian Creek (Pump Station @ Bal Harbour)	60	6	25°53'12.7"N 80°07'41.6"W
Jewfish Creek	61	6	25°11'04.2"N 80°23'17.2"W
NW 5th Street Bridge over Miami River	62	6	25°46'41.8"N 80°12'24.9"W
Radio Tower Everglades Academy (Florida City) Pump Station	63	6	Not provided

Table 4-2. List of projects in data set #2

Site	Address	Area	Notes	Geology	Triaxial tests
1	I-75/ I-595	Davie (Broward)	Interchange; 75-ft from a wet retention pond	Qm overlays Tqsu; Specimens below 8-ft, identified as Tqsu (Ft Thompson)	Yes
2	SW 13th St	Miami	Underpass; no near-by body of water	Qm (Miami); 0.5 miles from the ocean	Yes
3	SR80 Bingham Island	West Palm	Bridge end bent; 35-ft from sea water	Qa (Anastasia)	Yes
4	SR 5-Marvin Adams Way	Key Largo	Bridge end bent; 25-ft from sea water	Qk (Key Largo)	Yes
5	SR 836 Ext - NW 12 St-MDX	Miami	Underpass; closest fresh water is 500-ft away	Qm (Miami), poor induration	Yes
6	SR 997-Krome Avenue		Existing culvert (no bridge) over a small canal	Qm (Miami), poor to moderate induration	Yes
7	S Tamiami Trail over Catfish creek	Sarasota	Small bridge. Limited specimens for q_u and BST tests only	Tha (Arcadia formation)	No
8	Fuller-Warren bridge	Jackson-ville	This is a deep foundation project. Data was collected for rock characterization.	Th (undifferentiated Hawthorn group)	Yes

Table 4-3. Carbonate content versus XRD interpreted results

Formations	Number of XRD specimens	% Carbonate content (FM5-514)	% of mineral by XRD results							
			Carbonate Content	Quartz	limestone			dolostone (dolomite)	portlandite $Ca(OH)_2$	periclase MgO
					Calcite	Mgcalcite	Aragonite			
①	②	③	④	⑤	⑥	⑦	⑧	⑨	⑩	⑪
Ft. Thompson	4	64 - 77	68 - 79	18 - 32	66 - 76	0 - 0.5	0 - 5.5	0	0	0.5 - 1
Anastasia	6	67 - 98	66 - 99	1 - 34	62 - 90	0 - 5	2 - 9	0	0	0 - 2
Key Largo	6	99 - 100	99 - 100	0 - 1	26 - 98	0 - 5	1 - 72	0 - 1	0	0
Poor indurated Miami	3	77 - 89	82 - 91	9 - 18	70 - 80	0 - 1.5	0 - 20	0 - 1	0 - 3	0
Medium indurated Miami	3	89 - 98	89 - 100	0 - 11	82 - 98	0 - 4	0 - 3	0	0	0 - 1
Medium to well-indurated Miami	4	88 - 99	88 - 100	0 - 11	78 - 98	0 - 5	0 - 6	0 - 1	0	0 - 1
Arcadia dolostone	5	64 - 96	64 - 100	0 - 36	0 - 2	0	0	63 - 100	0 - 1	0 - 1
Hawthorn dolostone	7	67 - 93	66 - 93	7 - 34	0 - 2	0	0	60 - 92	0	0 – 3
Hawthorn marl	6	23 - 65	24 - 65	35 - 76	0 - 0.5	0	0	23 - 64	0	0 – 2
Hawthorn limestone	2	76 - 88	71 - 88	12 - 29	68 - 77	0 - 1	0 - 1	9 - 10	0 - 1	0

Table 4-4. Estimated mineral components from carbonate content and specific gravity results

Formations	Number of specimens	% carbonate		% calcite		% aragonite		% dolomite		% quartz	
		range	average	range	average	range	average	range	average	range	average
Ft. Thompson	14	64-80	72	55-78	67	0-15	5			20-36	28
Anastasia	40	66-98	90	50-98	84	0-47	6			2-34	10
Key Largo	39	99-100	99.5	39-95	79	5-61	20			0-1	0.5
poor indurated Miami	12	77-90	84	52-82	70	0-34	14			10-23	16
medium indurated Miami	34	89-98	95	74-97	91	0-22	4			2-11	5
medium to well indurated Miami	14	88-99	96	76-99	91	0-21	5			1-12	4
Arcadia dolostone	26	64-96	84	0-18	2			49-94	82	4-36	16
Hawthorn marl	22	23-77	64	0-40	12			12-73	51	23-77	36
Hawthorn dolostone	49	67-93	81	0-38	12			38-87	69	7-33	19
Hawthorn limestone	7	77-89	84	62-83	76			0-16	8	11-23	16

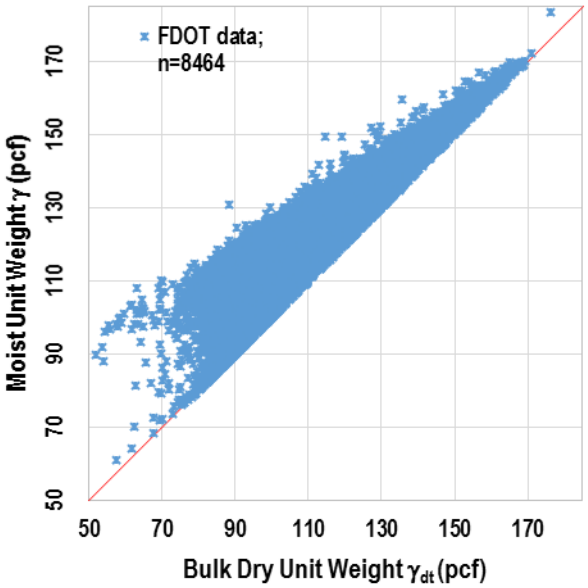

Figure 4-1. Data set #1 – Range of unit weights

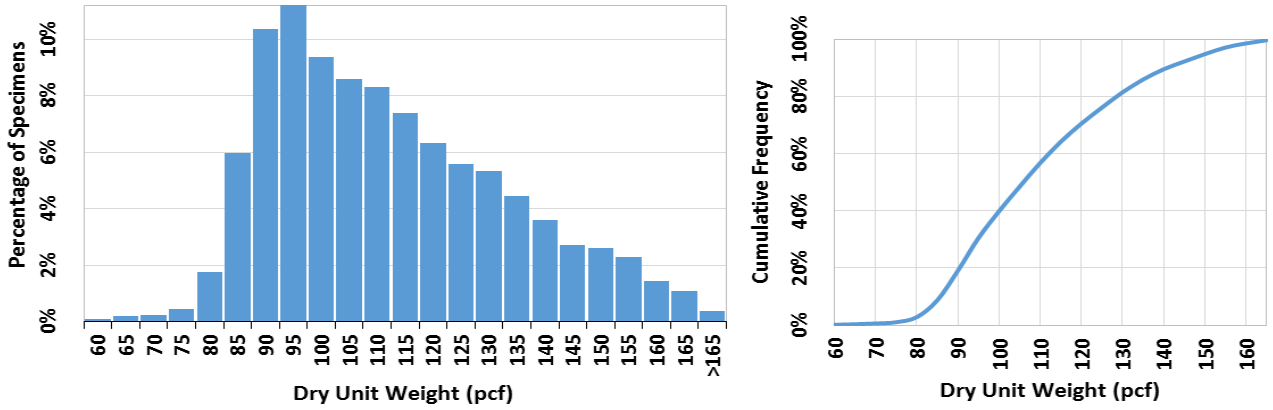

Figure 4-2. Data set #1 – Dry unit weight histogram

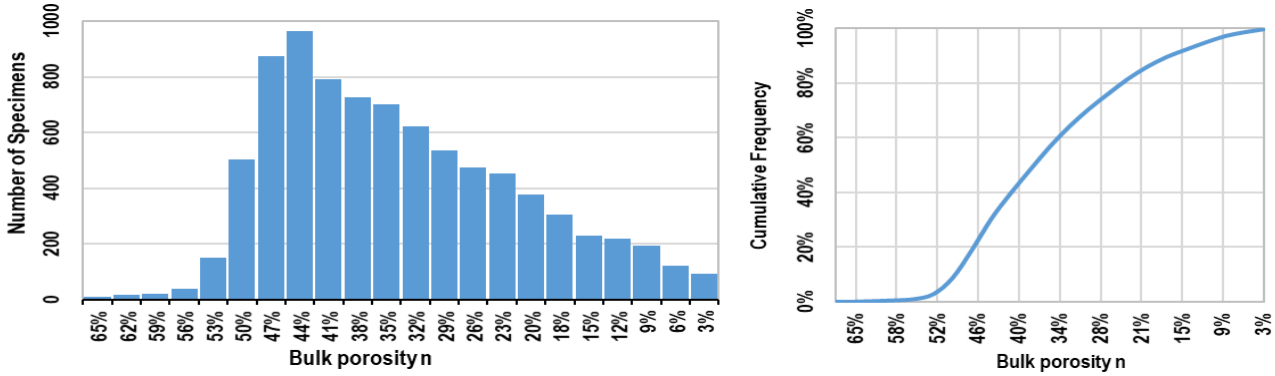

Figure 4-3. Data set #1 – Porosity histogram

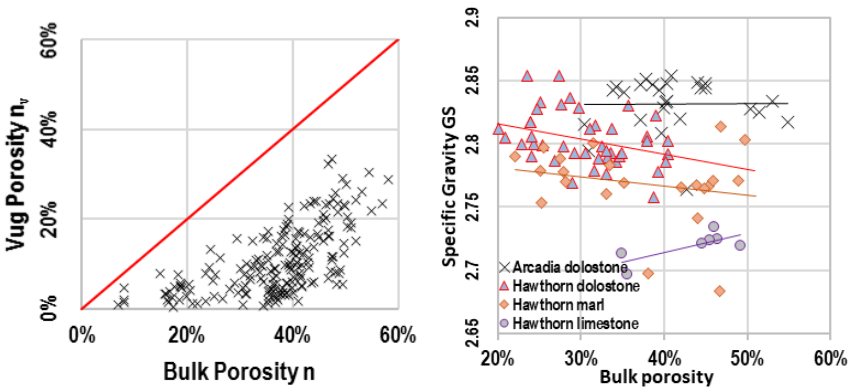

a)

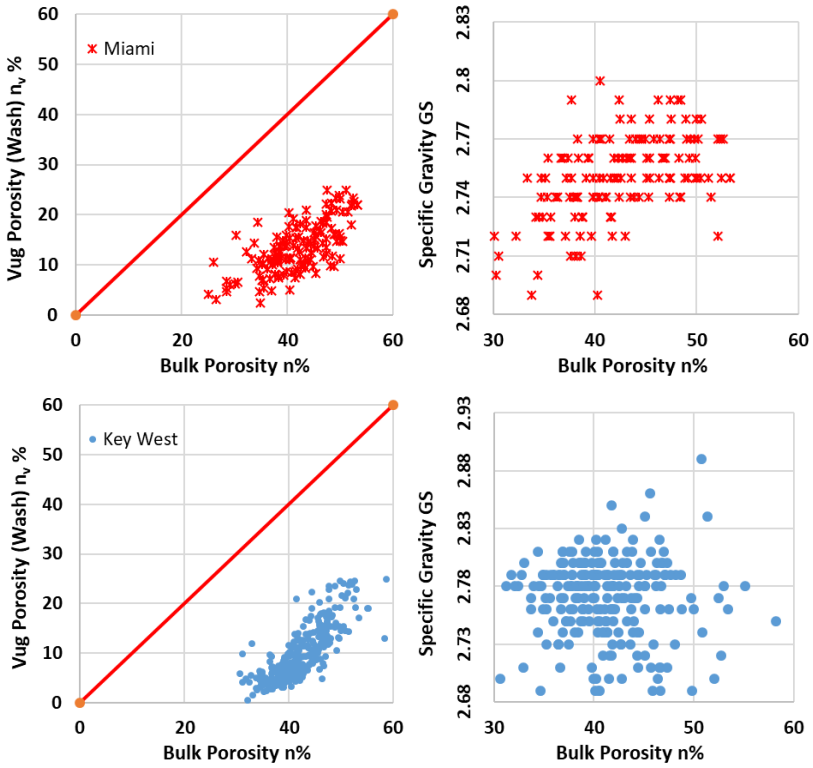

b)

Figure 4-4. Vug porosity versus bulk porosity: a) Plotted using data from this study, b) Plotted using text data from Hester & Schmoker (1985)

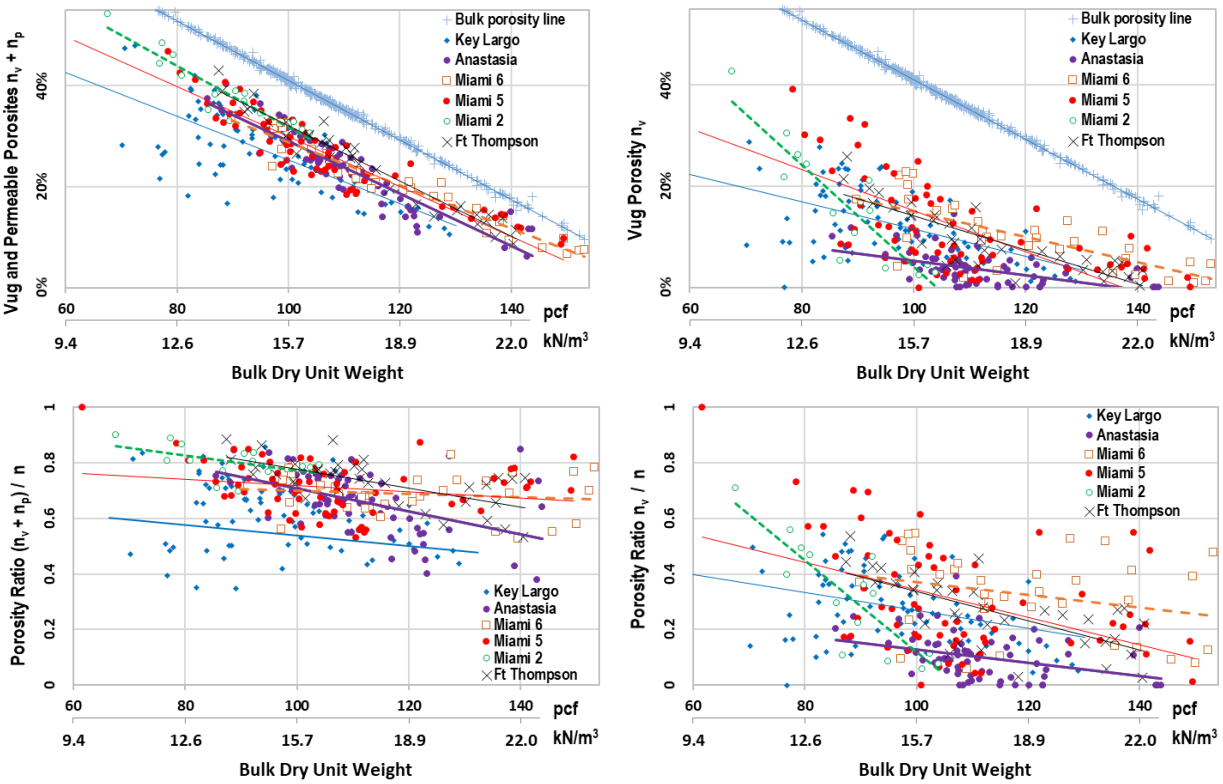

Figure 4-5. Porosities of Florida carbonate-rocks: a) Vug and permeable porosities, b) Vug porosity only

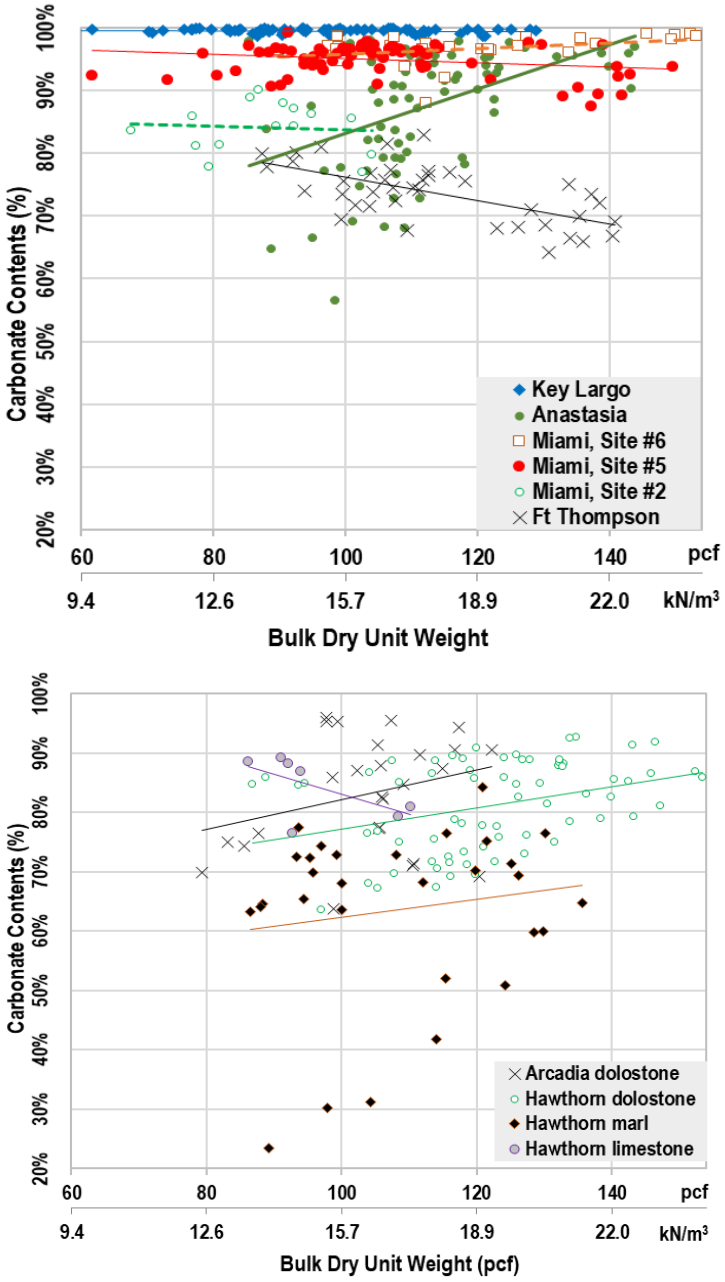

Figure 4-6. Carbonate content versus bulk dry unit weight γ_{dt}

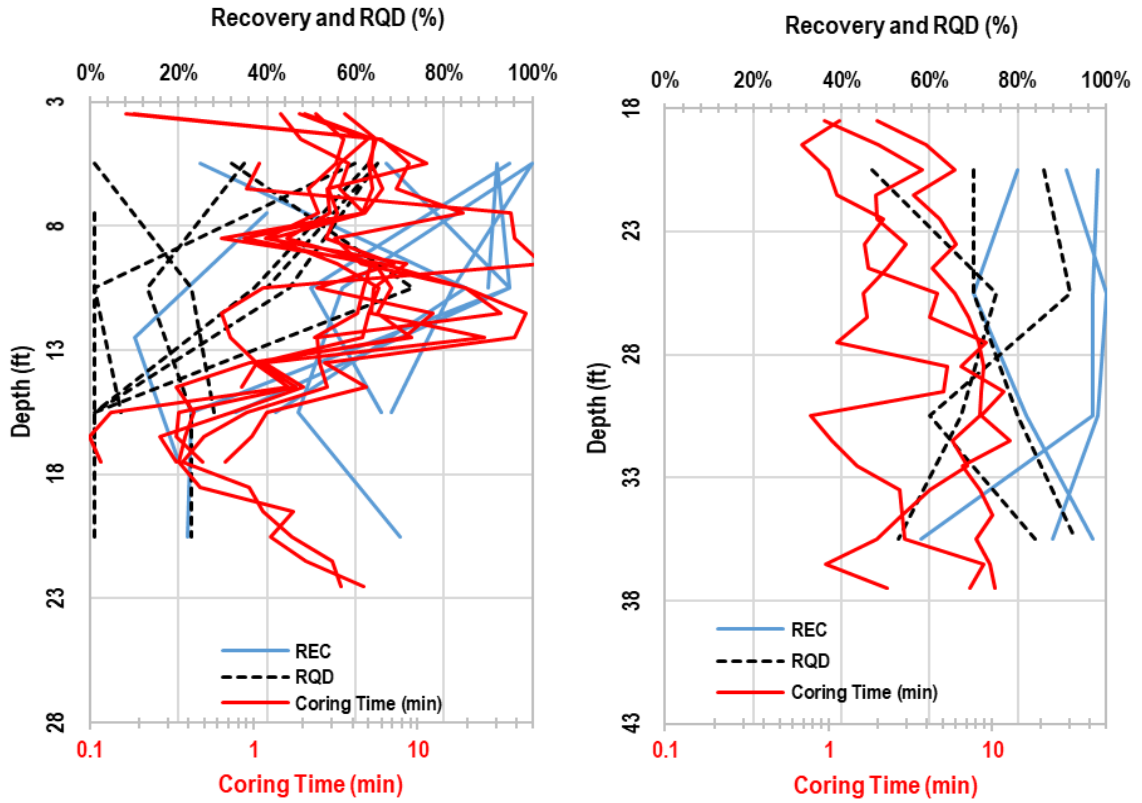

Figure 4-7. Examples of rock core records: a) Ft. Thompson site, b) Anastasia site

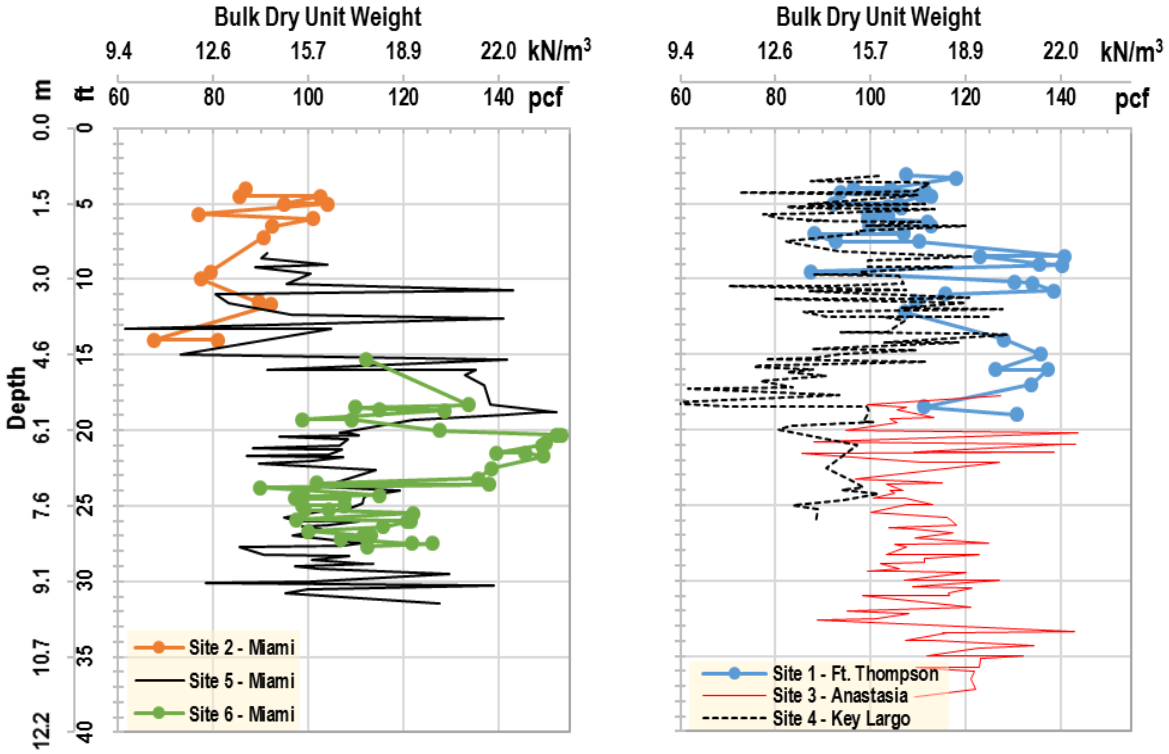

Figure 4-8. Bulk dry unit weight γ_{dt} with depth

CHAPTER 5
SPLITTING TENSION AND UNCONFINED COMPRESSION STRENGTHS OF FLORIDA CARBONATE-ROCKS AND IGMS

5.1 Necessity for Florida Rock Strength Correlation

To describe rock strengths, the two most popular rock strength parameters are unconfined compression strength (q_u) and Brazilian splitting tension strength (BST), which are obtained via laboratory tests (American Society for Testing and Materials methods ASTM D7012 and ASTM D3967, respectively) on rock core specimens. In a difficult terrain or deep exploration (e.g., for petroleum engineering projects), it is expensive to retrieve rock cores for laboratory tests. As result, many authors have published correlations to obtain rock strengths from the rock physical, index, and mechanical parameters. However, a number of publications contain a very limited number of specimens per rock formation, sometimes only three specimens per rock formation. Fereidooni and Khajevand (2018), based on database of 12 rock specimens of 4 different rock formations with porosity (n) between 0.04 to 0.10 (4% to 10%), presented correlations to estimate q_u and BST based on a single input parameter – the input parameter can be Schmidt rebound hardness, point load index, block punch index, or cylindrical punch index. Chang et al. (2006) gathered the results from 12 different authors from 1971 to 2001, used rocks all over the world, and tabulated 31 different empirical equations to estimate q_u and BST, typically from a single input parameter, such as porosity, modulus, or shear wave velocity. The carbonate-rocks (limestone and dolostone) examined to have typical porosity of 0 to 20%. Chang et al. (2006) noted that many correlations do a poor job in fitting measured data because they were originally proposed to fit a subset of data only. All the mentioned rocks, especially carbonate-rocks (limestone or dolostone), have much lower porosity than Florida carbonate-rocks, and subsequently have much higher strengths than Florida ones.

What stands out is that Florida carbonate-rocks have low strength, high porosity, and high variability. As such, the perception of "porous" rocks is very different between Florida rocks and those cited in literature. Fereidooni and Khajevand (2018) indicated travertine samples with n of 0.07 as porous. In Schwartz (1964), the Pottsville sandstone and Indiana limestone were considered as typical porous rocks, and their porosities are n = 0.14 and 0.20, respectively. Gowd and Rummel (1980) considered n=0.15 as porous. In Mogi (1966), rocks with n = 0.01 to 0.10 were grouped as porous, and n > 0.10 as very porous. In comparison, Figure 4-3 in previous chapter shows that 90% of Florida limestone has porosity n ≥ 0.20 and only 10% of Florida limestone has porosity between 0.05 and 0.20, i.e., the limestone or dolostone that are typically considered porous in literature are considered "dense" and "outlier" data in Florida. In addition, Section 4.4 indicates that within short vertical distances (cm or inches) of one another, one Florida rock specimen may have a bulk dry unit weight (γ_{dt}) of 20.5 kN/m^3 (130 pcf) and the adjoining rock specimen may have γ_{dt} of 12.5 kN/m^3 (80 pcf), indicating extreme differences in rock porosities. As results, the Rock Designation Quality (RQD) values are often times low as seen in Figure 2-6, with specimens having insufficient lengths for strength testing, but of sufficient size for rock index testing. In this case, it would be beneficial to be able to estimate the unconfined strengths from the index parameters, and save the long specimens for triaxial tests, if available.

The following sections present the correlations developed between BST and rock's index parameters, q_u and rock's index parameters, and finally the correlation between BST and q_u for different Florida formations.

5.2 Brazilian Splitting Tension Strength Test (BST)

Shown in Figure 5-1, the majority of Brazilian splitting tension strength (BST) results in data set #1 are less than 1.7 MPa (250 psi), with a median BST = 0.6 MPa (90 psi). Figures 5-2 and 5-3 show the relationship between BST and bulk porosity n. It should be noted that bulk porosity n and bulk dry unit weight γ_{dt} have a direct relationship of $n = 1 - \gamma_{dt}/(GS*\gamma_w)$, where GS is the sample specific gravity and γ_w is water unit weight. Because GS is generally a constant in Florida rocks (i.e., it varies within a narrow band depending on the percentage of calcite, quartz, dolomite, or aragonite within the carbonate-rocks), for a given bulk dry unit weight, the porosity, n, fluctuates within a typical margin of 3% depending on value of GS. For example, γ_{dt} = 15.7 kN/m^3 = 100 pcf, then n could vary from 0.405 to 0.418, or 40.5% to 41.8% when GS = 2.69 to 2.75. Rock's GS is difficult to measure while γ_{dt} is very easy to obtain – simply oven-dried weight divided by the cylindrical volume. Therefore, the key parameter to correlate the Florida rock strength is its bulk dry unit weight γ_{dt}. Figure 5-4 presents the BST results versus bulk dry unit weight for data set #1 with a general correlation between the predicted BST and dry unit weight as:

$$BST\ (\text{kPa}) = 26.64 \exp(0.191 \gamma_{dt} B) \quad (5\text{-}1a)$$

$$BST\ (\text{psi}) = 3.864 \exp(0.03 \gamma_{dt} B) \quad (5\text{-}1b)$$

where,

γ_{dt} - the bulk dry unit weight (kN/m^3 or pcf)

$B = 1$ if $\gamma_{dt} < \gamma_{dt0}$

$B = \sqrt{\gamma_{dt}/\gamma_{dt0}}$ if $\gamma_{dt} \geq \gamma_{dt0}$

γ_{dt0} = 22 kN/m^3 (140 pcf)

The very large data set (5,116 data points) has a coefficient of determination of $R^2 = 0.63$. It still can clearly be seen that there exists a large scatter in the data in Figure 5-4. For the data set #2 in Figure 5-5, the coefficient of determination, R^2, for the same correlation was 0.47. This lower value may be attributed to the difference in sample properties of each formation. As stated earlier, in addition to bulk dry unit weight, other index parameters are available for data set #2. One of the most important additional parameters is the rock formation identification, which relates to the mineral structure (i.e., calcite, aragonite, dolomite, etc.), as well as weathering state (i.e., carbonate content and porosities). As shown in Figure 5-6, each formation has a distinctive trendline with regard to the bulk dry unit weight. To discern the formation factor, the bias ratio ($Bias_1$) between measured values (BST_m) and predicted values using Eq. 5-1 ($Bias_1 = BST_m$/ Eq. 5-1) is then plotted for each project site (Figure 5-7): Sites 2, 5, and 6 in Miami formation[1], Site 1 in shallow Ft. Thompson formation[2], Site 3 in Anastasia formation, site 4 in Key Largo formation, site 7 in Arcadia dolostone, and site 8 in Hawthorn formation. The average $Bias_1$ ratio value presented in Figure 5-7 is the splitting tension formation factor, F_t. F_t is then generalized as in Figure 5-8 and Table 5-1.

Based on Figure 5-8, for Florida carbonate-rocks having different index properties than the rocks presented in this study, F_t can be approximately estimated as:

$$F_t = 1.6C_{ave} - 0.43 + P_n \quad (5\text{-}2)$$

C_{ave} - the average carbonate content for the formation;

[1] Per Scott (2001), the Miami formation forms the Atlantic Coastal Ridge

[2] Shallow Ft. Thompson formation exists near the ground surface to the west and north-west of the Atlantic Coastal Ridge. In the Atlantic Coastal Ridge, the deeper Ft. Thompson formation is overlaid by the Miami formation. In data set #2, only shallow Ft. Thompson formation samples were recovered and analyzed.

P_n - porosity structure factor with suggested value varying from approximately -0.2 to +0.3 as:

If porosity ratio $n_v / n < 0.1$ or $(n_v + n_p)/ n < 0.6$, then $P_n = +0.3$

If porosity ratio $n_v / n > 0.2$ and $(n_v + n_p)/ n > 0.7$, then $P_n = -0.2$

P_n is a judgment factor, as presented below based on the quantitative estimates of vug porosity or the sum of vug and permeable porosities. To examine the formation factor (F_t) or its related porosity structure factor (P_n), let us refer to Figure 5-9.c: Both of them have the same bulk dry unit weight $\gamma_{dt} = 15.7$ kN/m^3 (100 pcf), thus both of them have approximately the same bulk porosity n. However, the red specimen (A) has higher vug porosity and smaller impermeable porosity. Therefore, the failure surface would more likely go through the weakest path connecting the vugs and the permeable porosity in the red specimen. Thus, the blue specimen (B) would likely have higher unconfined strength. This is the same reason for the Key Largo and Anastasia to have higher trend of splitting tension formation factors, F_t, while other formations would have lower trend of F_t values (corresponding to a given carbonate content) in Figure 5-8:

For Anastasia formation, there are two factors that help the formation factor, F_t:

a) The detrimental porosities $(n_v + n_p)$, despite being more than that of Key Largo formation, is still lower than other formations (Figure 4-5.a);

b) The vug porosity (n_v) is most importantly the lowest for Anastasia formation (Figure 4-5.b).

For Key Largo formation, detrimental porosities $(n_v + n_p)$ are the lowest among the tested formations (Figure 4-5.a). The lower the detrimental porosity, the higher the porosity structure factor P_n. For example, a P_n factor of +0.3 can be used for Key Largo, while a P_n factor is much less for most other formations.

The $Bias_1$ ratio is then correlated against carbonate content (C) and formation factor (F_t) as follows:

$$Bias_1 = 0.64\ F_t \exp(0.4214C) \quad (5\text{-}3)$$

Multiplying Eq. 5-3 into 5-1, a revised predicted BST value based on γ_{dt}, C, and F_t is presented as Eq. 5-4:

$$BST\ (\text{kPa}) = 17.05 * F_t \exp(0.191\gamma_{dt}\ B) \exp(0.4214C) \quad (5\text{-}4a)$$

$$BST\ (\text{psi}) = 2.47 * F_t \exp(0.03\gamma_{dt}\ B) \exp(0.4214C) \quad (5\text{-}4b)$$

This correlation yields an improved coefficient of determination of 0.66. The power parameter 0.4214 for carbonate content, C, was simplified to a simpler value of 0.5 and it was found that the coefficient of determination stays the same as $R^2 = 0.66$ (Figure 5-10):

$$Bias_1 = 0.639\ F_t \exp(0.5C) \quad (5\text{-}5)$$

And multiplying Eq. 5-5 into 5-1:

$$BST\ (\text{kPa}) = 17\ F_t \exp(0.191\gamma_{dt}\ B) \exp(0.5C) \quad (5\text{-}6a)$$

$$BST\ (\text{psi}) = 2.468\ F_t \exp(0.03\gamma_{dt}\ B) \exp(0.5C) \quad (5\text{-}6b)$$

It is noted that this is the same population of n=270 for data set #2, but the R^2 has improved significantly from 0.47 when the correlation is to one parameter (Figure 5-5) versus 0.66 when the correlation employs three index parameters (Figure 5-10), namely γ_{dt}, F_t (Table 5-1), and C.

For Miami formation, the Florida Geological Survey (Scott 2001) describes it as having two distinct facies -- an eastern oolitic facies that forms the Atlantic Coastal Ridge, and the bryozoan facies to the west toward the Everglades. In some areas, the two facies may intermix each other. The oolitic facies can be further divided into a cross-bedded and a bioturbated facies. Collected for shallow foundation projects, rocks from 3 Miami sites show completely different magnitude

of indurations. Therefore, it may be logical to use separate formation factors for Miami formation depending on degrees of indurations - as shown in Table 5-1. If the degree of induration is uncertain, a single formation factor of 0.9, also shown in Table 5-1, can be used. Figure 5-11 indicates that both methods would yield good coefficient of determination R^2.

Next, a new bias ratio between measured and predicted values ($Bias_2 = BST_m$/ Eq. 5-6) was plotted versus the vug porosity (n_v) to see if strength correlations could be improved using numerical values of these porosity properties. As seen in Figure 5-12, no clear relationship was found to exist. As discussed earlier, impacting the strength results are the orientations and distributions of the vugs within the specimens relative to the loading line. If the vugs are aligned with the loading line, then the failure loads and the associated interpreted strengths are lower than the rocks with the same vug porosity n_v but with different orientation of the vugs. In short, vugs play very significant role in scattering the interpreted strengths without any clear numerical correlations.

5.3 Unconfined Compression Strength q_u

As result of the geological history described in Chapter 2 and the carbonate contents, dry unit weights, and porosities as reported in Chapter 4, Florida carbonate-rocks' strengths are generally low, as seen in Figure 5-13 where the majority (80%) of the rocks have unconfined compression strength q_u less than 9 MPa (1,300 psi), with a median q_u = 3 MPa (435 psi). Figure 5-14 presents q_u versus bulk dry unit weights from data set #1. In this figure, the coefficient of determination of $R^2 = 0.69$ does show, despite the scatter, that there is a good correlation between unconfined compression strength, q_u, and the single index parameter of bulk dry unit weight, γ_{dt}. The equation is presented below, which is quite similar to BST Eq. 5-1:

$$q_u \text{ (kPa)} = 40.3 \exp(0.255 \gamma_{dt} B) \quad (5\text{-}7a)$$

$$q_u \text{ (psi)} = 5.89 \exp(0.04 \gamma_{dt} B) \quad (5\text{-}7b)$$

The population for q_u results in data set #2, n = 80, is significantly less than the population for BST results (n = 270). Furthermore, 71 of these 80 q_u results belong to only one formation (Anastasia) while other three formations have only 2 to 5 q_u data points. The reason is that most of the available long specimens were used for triaxial tests with results presented in Chapter 6. Due to the small population of q_u result in data set #2, especially when only 2 to 5 data points were available per formation, a different approach was employed to establish a correlation between q_u and the index parameters of γ_{dt}, C, and compression formation factor - F_u. The approach, utilizing a combination of data set #2 and subset #1a with a total population of 178 (Figure 5-15), is described below.

First, by comparing Eq. 5-7 to 5-1, a general relationship between q_u and BST was first established:

$$q_u \text{ (kPa)} = 0.51 * BST^{4/3} \quad (5\text{-}8a)$$

$$q_u \text{ (psi)} = 0.97 * BST^{4/3} \quad (5\text{-}8b)$$

The inversion of this relationship is:

$$BST \text{ (kPa)} = 1.96 * q_u^{3/4} \quad (5\text{-}9a)$$

$$BST \text{ (psi)} = 1.03 * q_u^{3/4} \quad (5\text{-}9b)$$

Relationships for BST/q_u have been proposed by many authors for many materials. For example, a comparison of BST with q_u for concrete is quite simple because it is easy to pair a BST specimen to another q_u specimen that have the same index properties. Arioglu et al. (2006) developed the following equation for concrete:

$$BST \text{ (MPa)} = 0.387 q_u^{0.63} \quad (5\text{-}10a)$$

$$BST \text{ (psi)} = 2.44039 * q_u^{0.63} \quad (5\text{-}10b)$$

For carbonate-rocks, it is much more difficult and sometimes impossible to find a pair of q_u and BST specimens that have similar index properties (i.e., same mineral components, porosities, dry weights, etc.). As identified in Section 4.4 , within short vertical distances (cm or inches) of one another, one Florida rock specimen may have γ_{dt} of 20.5 kN/m^3 (130 pcf) and the adjoining rock specimen may have γ_{dt} of 12.5 kN/m^3 (80 pcf). Thus, pairing these two specimens is not recommended despite being at almost the same depth. Johnston (1985) - based on Australian rock database - paired triaxial test and direct tension test results versus q_u results by selecting only measured q_u values that fall within 50% of the estimated q_u value best-fitting the strength envelope connecting the tension test result and the triaxial test result. Johnston (1985) then recommended the following equation for carbonate-rocks, which exhibit q_u in the range of 38 to 520 MPa (5,500 to 75,400 psi) in his database:

$$q_t \text{ (kPa)} / q_u \text{ (kPa)} = (1\text{-}0.0172\log^2 q_u) / (2.065+0.170 \log^2 q_u) \quad (5\text{-}11)$$

For mudstones (different crystal or cleavage structure than carbonate-rocks), Johnston (1985) suggested a lower q_t/q_u ratio of:

$$q_t \text{ (kPa)} / q_u \text{ (kPa)} = (1\text{-}0.0172\log^2 q_u) / (2.065+0.231 \log^2 q_u) \quad (5\text{-}12)$$

It is noted that Eqs. 5-11 and 5-12 are for the direct tension test result, q_t. Per Perras and Diederichs (2014), the q_t/BST ratio for sedimentary rocks ranges between 0.4 to 1.2, with a mean value of 0.7. For concrete, Arioglu et al. (2006) used a ratio of 0.9 for q_t/BST.

Bullock (2004) tabulated BST versus q_u by pairing specimen at similar depths and similar densities (reproduced in Figure 5-16) and yielded the following relationship:

$$BST \text{ (psi)} = 6.73\ q_u^{0.5} \quad (5\text{-}13)$$

This relationship is almost identical to the American Concrete Institute (ACI 2014) relationship for concrete:

$$BST\ (kPa) = 17.59\ q_u^{0.5} \quad (5\text{-}14a)$$

$$BST\ (psi) = 6.7\ q_u^{0.5} \quad (5\text{-}14b)$$

Rodgers (2016) established the following relationship based on data from Little River (Gadsden County, Florida) carbonate-rocks:

$$BST\ (kPa) = 0.765\ q_u^{0.825} \quad (5\text{-}15a)$$

$$BST\ (psi) = 0.545\ q_u^{0.825} \quad (5\text{-}15b)$$

For the Little River project, Rodgers (2016) converts BST to q_t by a factor of 0.8 and arrived at the following equation:

$$q_t\ (kPa) = 0.612\ q_u^{0.825} \quad (5\text{-}16a)$$

$$q_t\ (psi) = 0.436\ q_u^{0.825} \quad (5\text{-}16b)$$

Finally, these different BST versus q_u relationships are plotted together in Figure 5-17, where the proposed relationship is described earlier in Eq. 5-8 or 5-9. Evident from the figure, the proposed relationship is in good agreement to other relationships, especially when plotted within typical Florida rock strengths (Figure 5-17.a). For rocks that are outside of typical Florida strengths (Figure 5-17.b), the relationships still agree with each other, with exception that concrete shows different trend than the carbonate-rock relationships.

Plugging Eq. 5-6 into Eq. 5-8, the following equation can be used to estimate q_u based on dry unit weight γ_{dt}, compression formation factor F_u, and carbonate content C:

$$q_u\ (kPa) = 22.34\ F_u\ e^{2C/3} * e^{0.255\ \gamma_{dt}\ B} \quad (5\text{-}17a)$$

$$q_u\ (psi) = 3.24\ F_u\ e^{2C/3} * e^{0.04\ \gamma_{dt}\ B} \quad (5\text{-}17b)$$

The compression formation factor, F_u, is derived as follows:

- Measured q_u results, only for specimens with known rock formation identifications, are tabulated (Figure 5-15). The majority of the data in Figure 5-15 comes from data subset #1a.
- As the carbonate contents were not recorded for this set of data, the average carbonate content values obtained from data set #2, tabulated in Table 5-2, were used in Eq. 5-17.
- F_{ui} is then calculated for each q_u data point by solving Eq. 5-17:
- $F_{ui} = q_{u\ measured} / (22.34\ e^{2C/3} * e^{0.255\ \gamma_{dt}\ B})$
- The average F_u for each formation is then presented in Table 5-3. It is noted that the F_u factor is different than the F_t factor due to the differing boundary conditions of the two different test methods and differing loading line orientation.

Statistical results using Eq. 5-7 are presented in a) b) Figure 5-18.a, whereas the results using Eq. 5-17, plugging in the F_u value from Table 5-3, are presented in a) b) Figure 5-18.b. It can be seen that the correlation has improved when using three index parameters versus one parameter. Due to limited population in data set #2 and the assumption that carbonate content for each formation in subset #1a equals to the average carbonate content from data set #2, it is recommended that the compression factor F_u be calibrated for available local data when it becomes available.

5.4 Unconfined Strengths of Marls

A limited quantities of marl specimens from Hawthorn formation were provided from Site #8 (Fuller Warren bridge) and unconfined strength tests were performed on these specimens. No specimens were available for triaxial tests. Unfortunately, the rock cores' natural moistures had not been preserved. When the cores arrived at the laboratory, they had already been air-dried. The unconfined strengths of these air-dried specimens are presented in Figure 5-19 and Figure 5-20 for BST and q_u, respectively. Some other marl specimens were placed in the moisture room.

However, depending on the locations of the specimens in the moisture room, many of them disintegrated and became of slumps of mushy cones and were not testable. The remaining were tested as "moist" specimens and are also presented in Figures 5-19 and 5-20. It is evident from these figures that the air-dried specimens have significantly higher unconfined strengths than the moist specimens. In summary, the marl strength is highly sensitive to the specimen moistures, and it is critical to test the specimens at their natural moisture contents, otherwise their strengths would alter and are not reliable.

5.5 Stress – Strain Behavior

A relationship that should also be identified in addition to peak strengths (splitting tension and unconfined compression) is the stress-strain response of unconfined compression tests. Examples of stress-strain curves from data set #1 are presented in a)
b)

Figure 5-21. Evident from the figure, the low strength materials with q_u < 5 MPa (725 psi), which are classified as IGM typically exhibit ductile behavior (minimal loss of strength with increased axial strain) or transition between brittle and ductile. This is unique characteristic of Florida porous rocks, as most rocks cited in literature (Schwartz 1964, Hoek and Brown 1980 and 1988, Gowd and Rummel 1980) would display brittle rupture response when there is no confinement. The higher strength rocks with q_u > 9 MPa (1,305 psi) typically exhibit brittle behavior (a significant drop in strength after the peak). As shown by various above authors - this brittle behavior typically transitions to ductile behavior under increasing confining pressure in triaxial testing (presented in Chapter 6). This type of behavior is helpful to the engineers when selecting an applicable stress-strain model for Florida carbonate-rocks, for example, a finite element method analysis.

5.6 Summary

Florida carbonate-rocks are among the youngest sedimentary rocks in the world. As seen in this study, they are of relatively low strengths, which can be explained by their index parameters. Florida carbonate-rocks are generally very porous, some of them with porosity exceeding 50%, i.e., more voids than solids. In addition, some Florida carbonate-rock formations have very low carbonate contents, which reduces the binding cementation and, in-turn, reduce the rock strengths.

The unconfined strengths – both in splitting tension and in unconfined compression – are strongly correlated to the material bulk porosity, which is inversely represented by the bulk dry unit weight, γ_{dt}. The relationships to γ_{dt} are presented in Eqs. 5-1 and 5-7. The unconfined strengths are also functions of rock formations, which are represented by the porosity structures (portions of vug, permeable, and impermeable porosities), and average carbonate contents. For each formation, the carbonate content can vary from specimen to specimen. The relationship between unconfined strengths and three key parameters (bulk dry unit weight, formation factor, and carbonate content) are presented in Eqs. 5-6 and 5-17.

Since Florida rocks are highly variable, with intermixing of hard and soft lenses with highly variable recoveries and rock quality designation (RQD), obtaining a significant number of core pieces of sufficient length for strength testing for a particular stratum can be difficult. However, index rock parameter testing as discussed is an attractive alternative where it is not feasible to do strength tests due to L/D requirement. Therefore, a comprehensive and continuous rock strength profile with depth can be established using strength correlations to index parameters. The established correlations are not only helpful in explaining the behaviors of Florida carbonate-

rocks in unconfined strength tests, but also crucial in economical and safe design of shallow or deep foundations relying on continuous strength profiles.

The significant of the results from this chapter is that: i) it examines large volume of data of Florida carbonate-rocks that are much more porous than other carbonate-rocks typically cited in literature, ii) the correlations involve with three input parameters, which improve the reliability of the correlations, and iii) the input parameters are relatively easy to obtain.

Table 5-1. Splitting tension formation factor (F_t)

Formation	Ft	
Anastasia	1.3	
Key Largo	1.5	
Shallow Ft. Thompson	0.6	
Miami, poor induration	0.75	Average 0.9
Miami, moderate induration	0.9	for the
Miami, moderate/well induration	1	Miami
Miami, well induration	>1	formation
Arcadia dolostone	0.8	
Hawthorn	0.7	

Table 5-2. Average carbonate content from data set #2

Formation	Key Largo	Anastasia	Miami	Shallow Ft. Thompson	Arcadia	Hawthorn dolostone
Average Carbonate Content	99.5%	87.0%	93.9%	73.6%	84.9%	81.7%

Table 5-3. Compression formation factors (F_u)

Formation	Key Largo	Anastasia	Miami	Shallow Ft. Thompson	Arcadia dolostone	Hawthorn
Fu	1.5	1.0	0.85	0.5	0.7	0.7

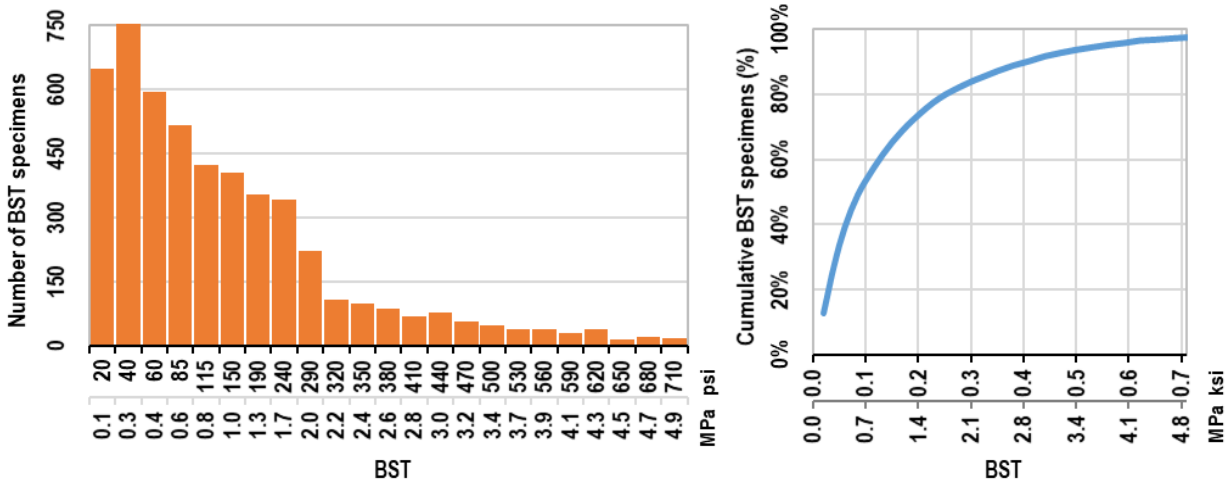

Figure 5-1. Data set #1 – Histogram of Brazilian splitting tension strength BST

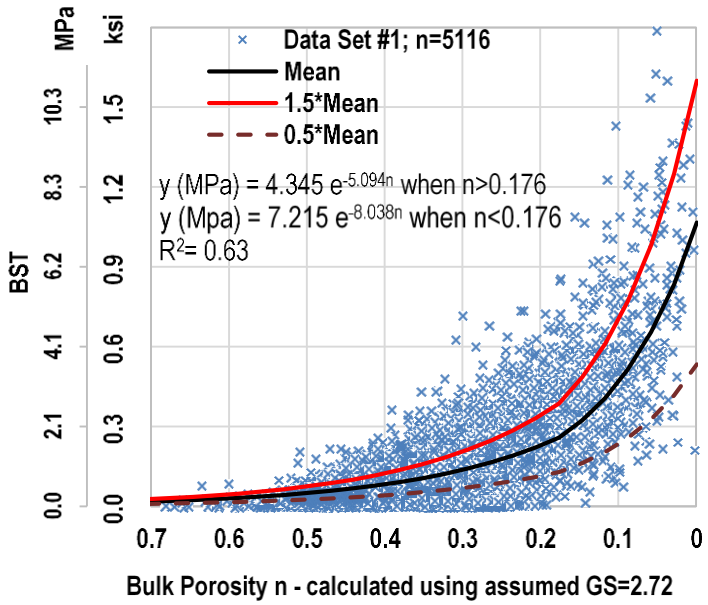

Figure 5-2. Data set #1 - BST results versus bulk porosity

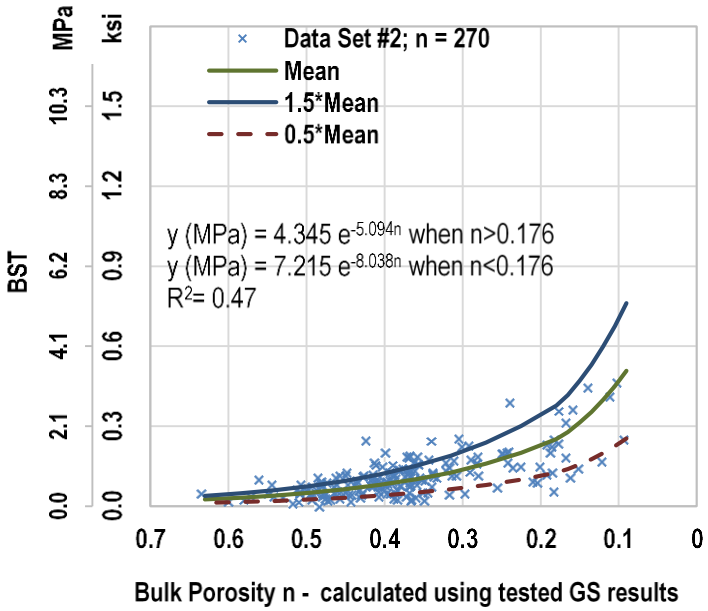

Figure 5-3. Data set #2 - BST results versus bulk porosity

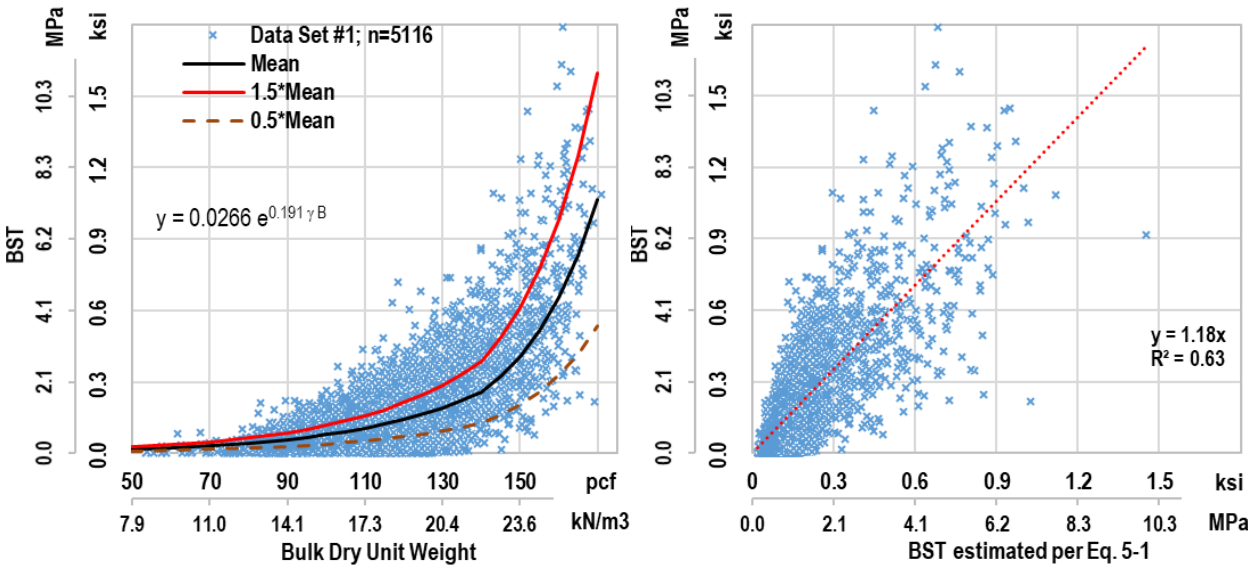

Figure 5-4. Data set #1 - BST results versus bulk dry unit weight

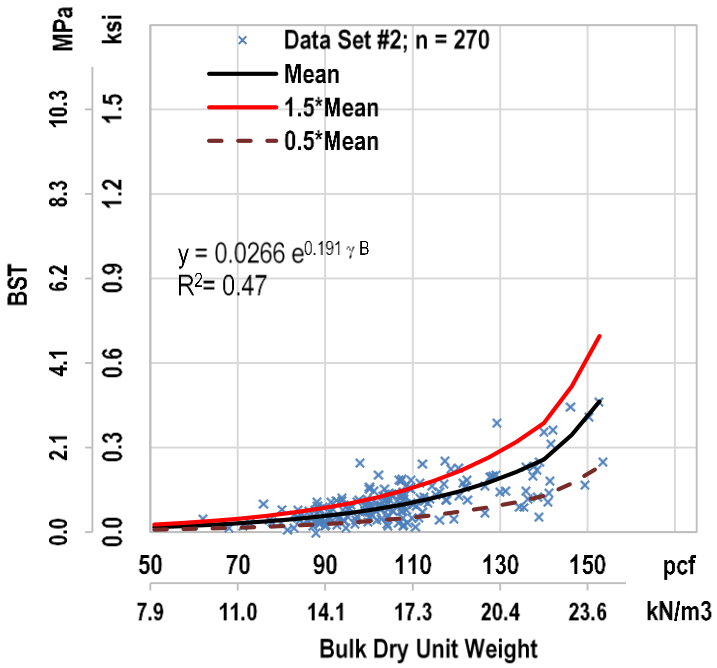

Figure 5-5. Data set #2 - BST results versus bulk dry unit weight

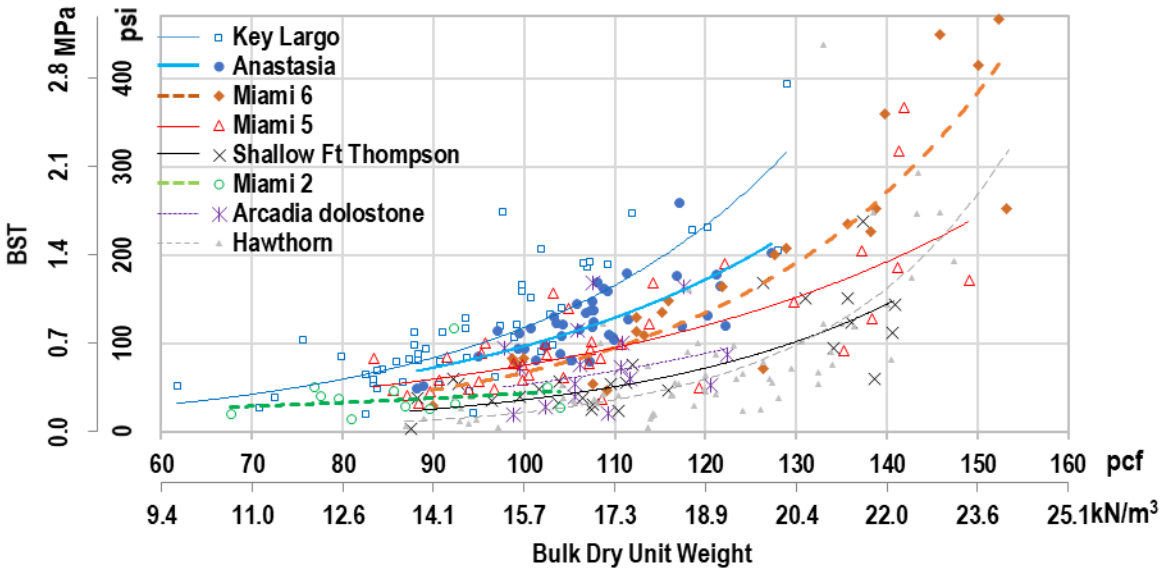

Figure 5-6. Data set #2 - BST and bulk dry unit weight for different formations

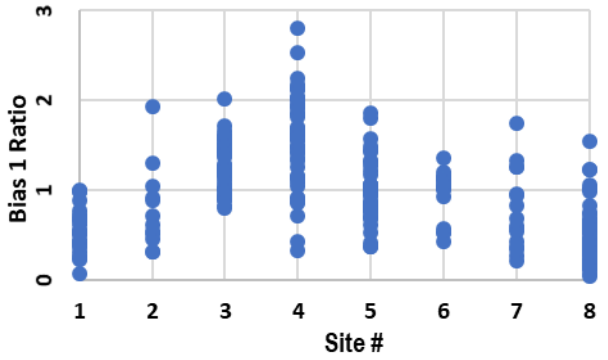

Figure 5-7. Data set #2 - $Bias_1$ for each project site

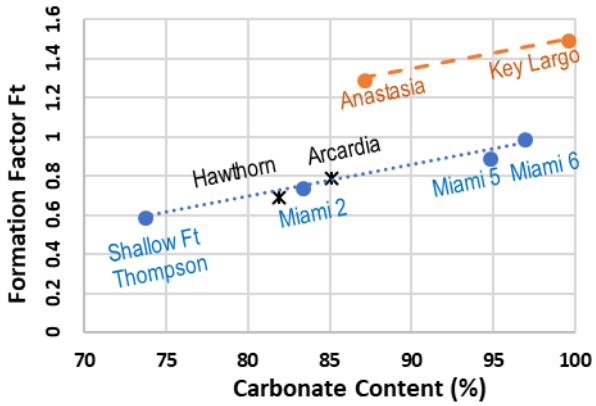

Figure 5-8. Splitting tension formation factor F_t

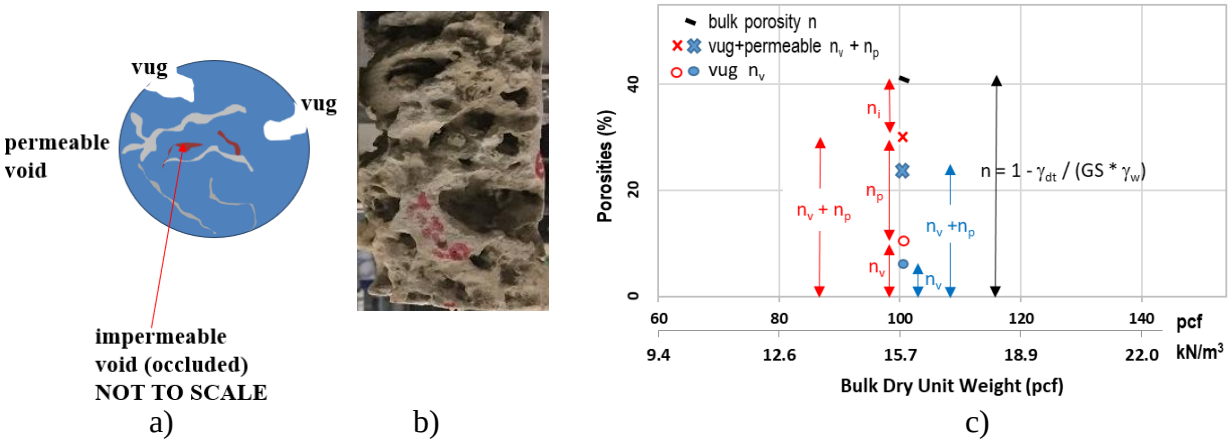

Figure 5-9. Types of porosities: a) Sketch of porosity types, b) Vuggy specimen, c) Example of porosities at γ_{dt} = 15.7 kN/m^3 (100 pcf)

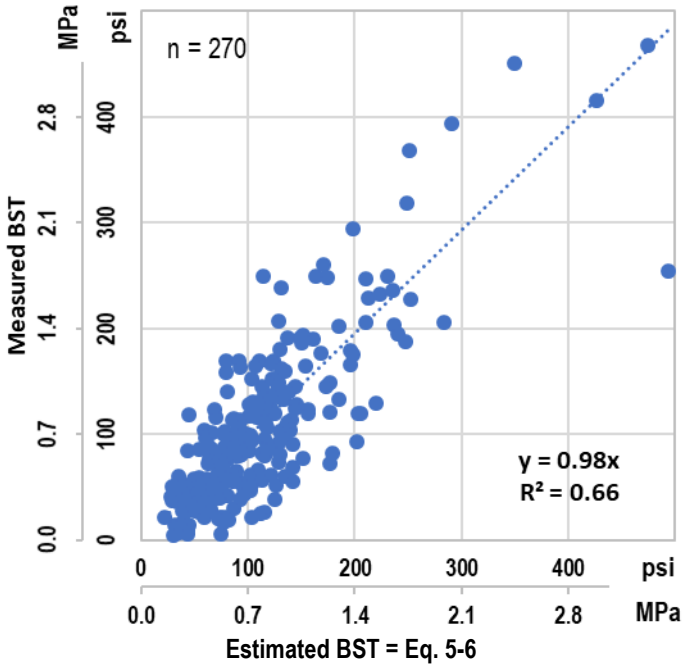

Figure 5-10. Data set #2 - BST correlation with γ_{dt}, F_t, and C

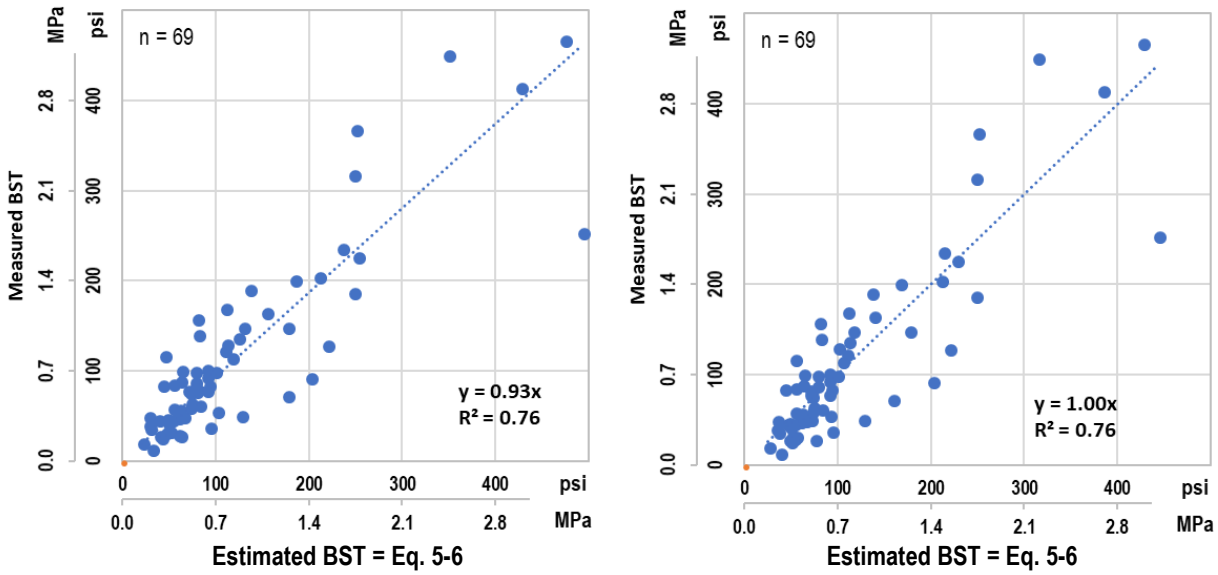

Figure 5-11. Statistical results for Miami formation only - BST correlation with γ_{dt}, F_t, and C: a) F_t = 0.75, 0.9, and 1.0, b) F_t = 0.9 for all 3 sites

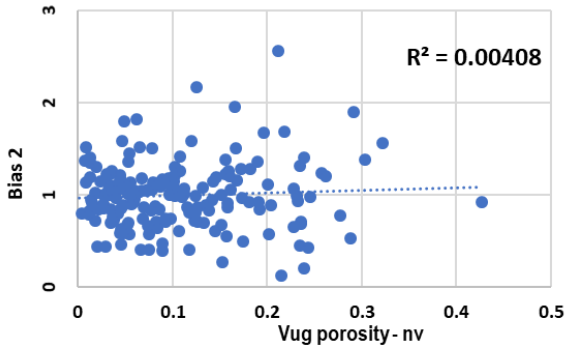

Figure 5-12. Data set # 2 - $Bias_2$ and n_v

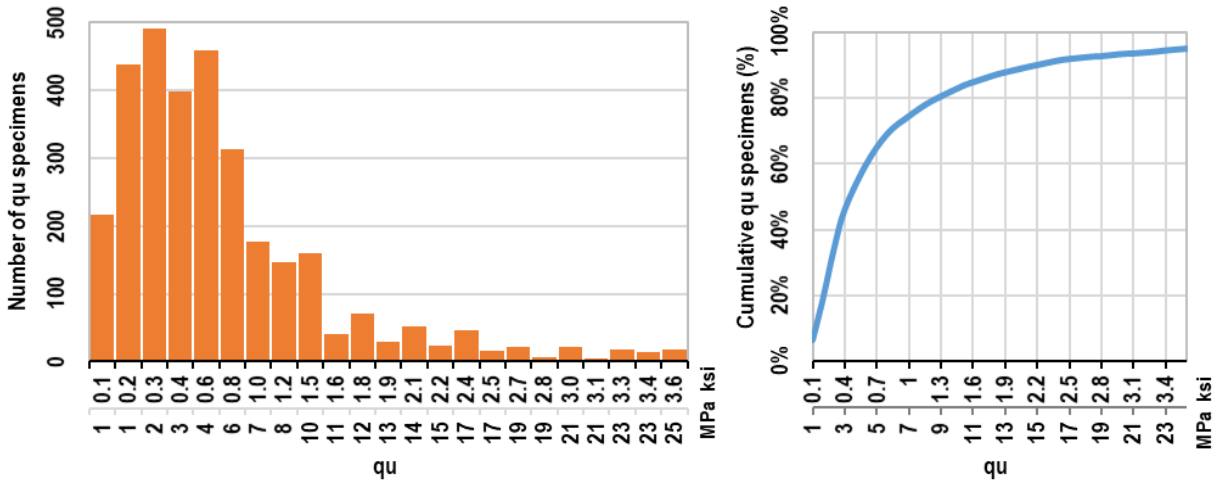

Figure 5-13. Data set #1 – Histogram of unconfined compression strength q_u

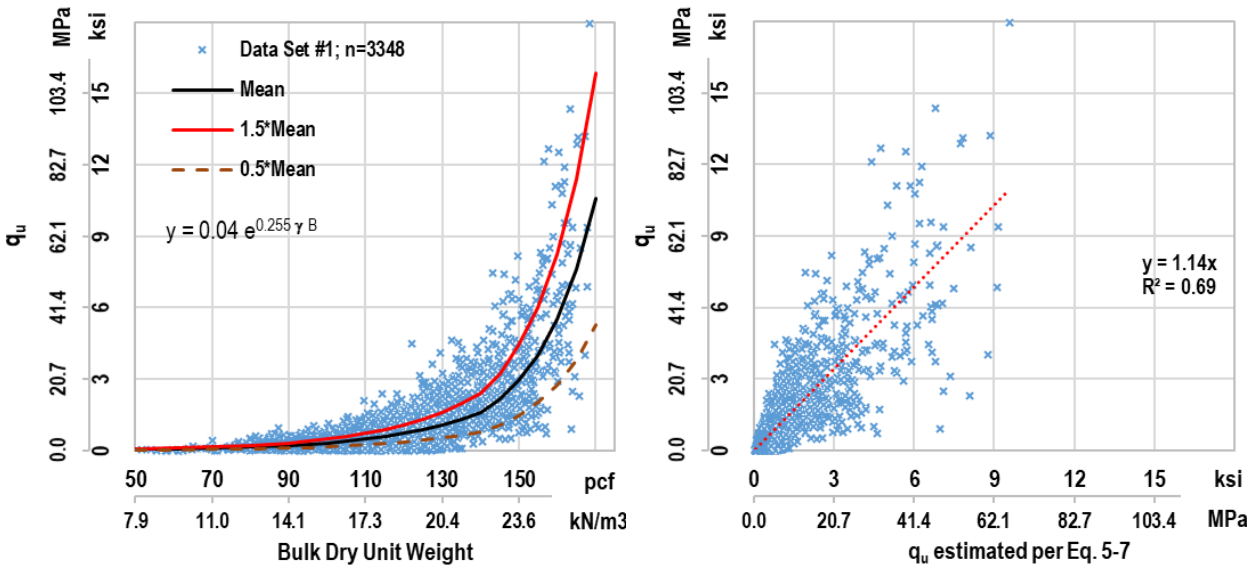

Figure 5-14. Data set #1 - q_u results versus bulk dry unit weight

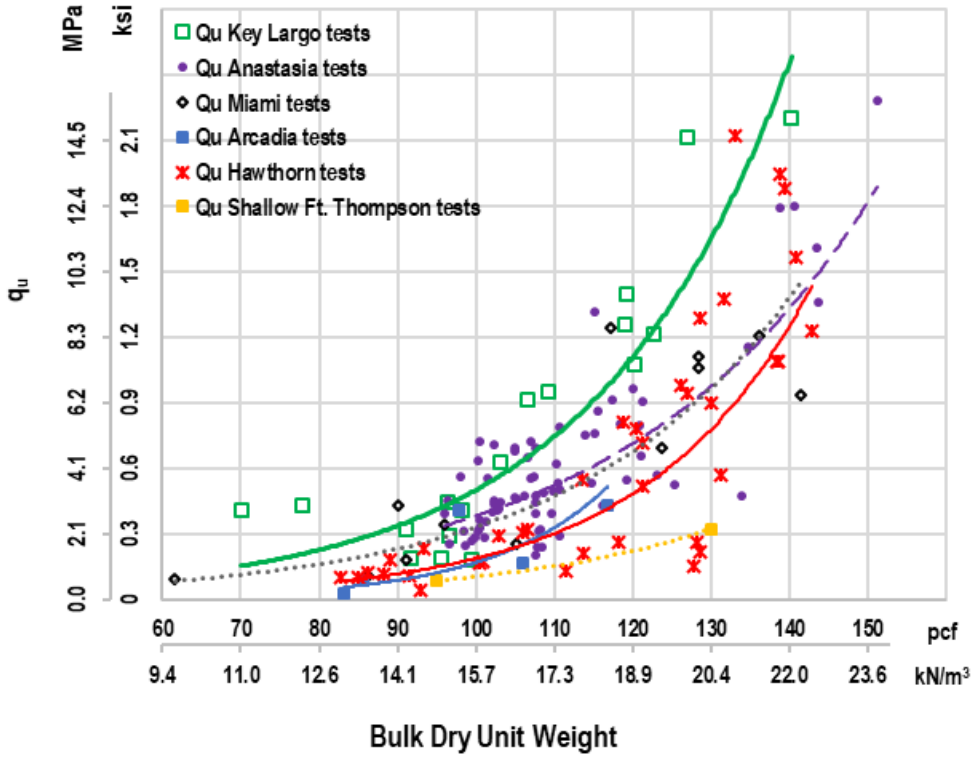

Figure 5-15. Data sets #1a and 2 - q_u and bulk dry unit weight for different formations

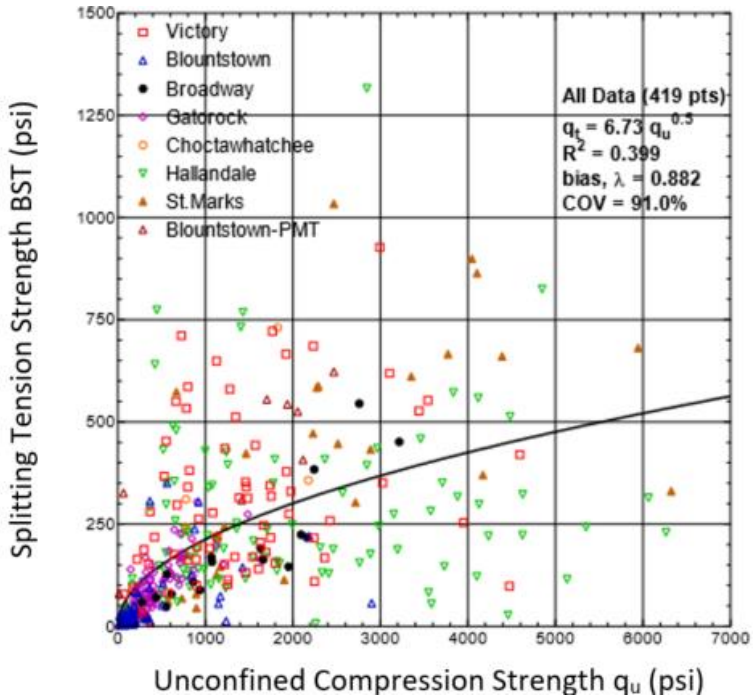

Figure 5-16. Bullock (2004) q_u versus BST relationship (FDOT Public Report)

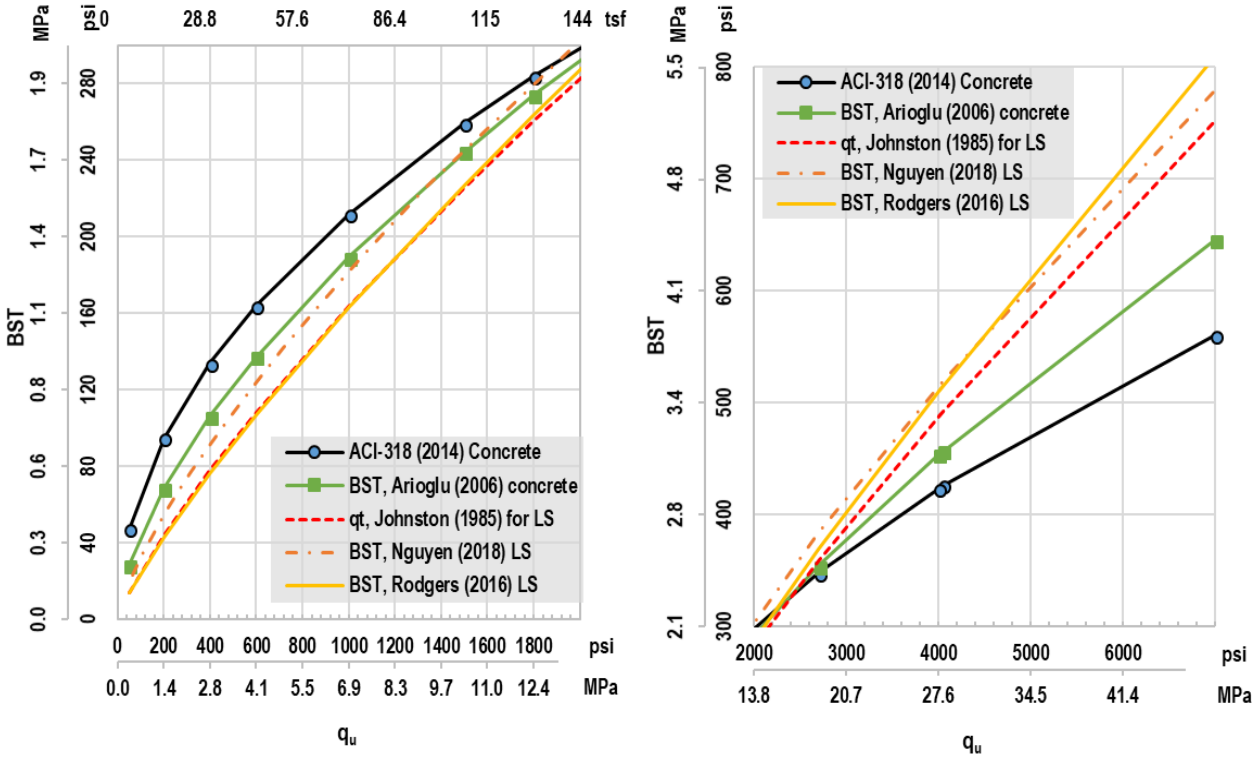

Figure 5-17. q_u versus BST relationship: a) For typical Florida rocks, b) For rocks outside of typical Florida strengths. Notes: 1, LS – Limestone; 2, Johnston relationship is for direct tension test result, q_t.

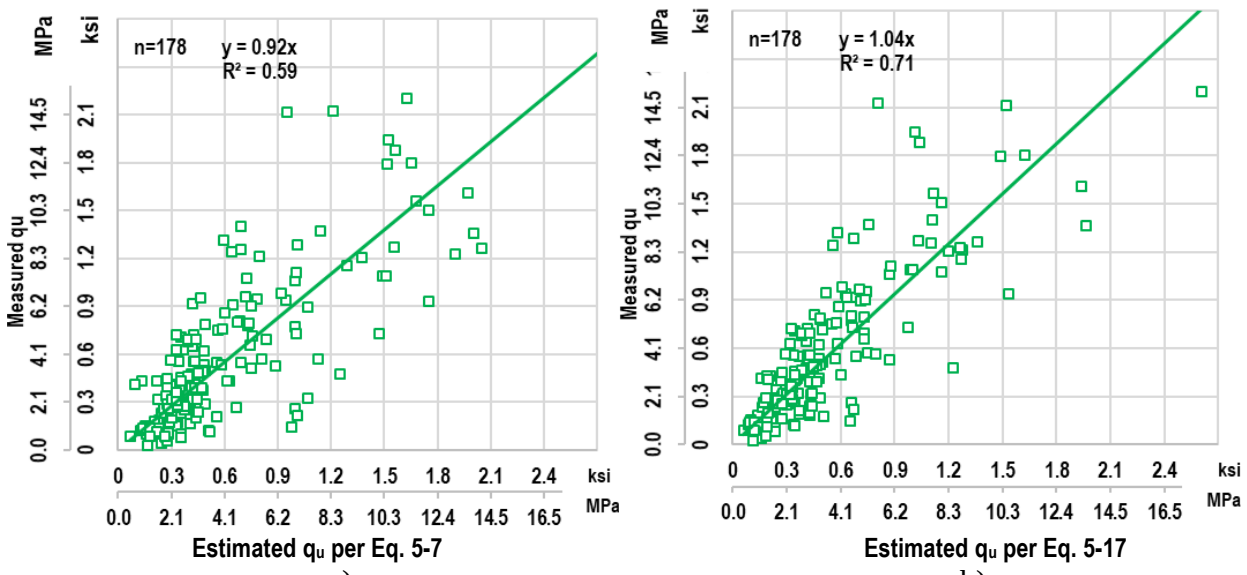

a) b)

Figure 5-18. Data sets #1a and 2 – q_u correlations: a) Correlation against 1 parameter (γ_{dt}), b) Correlation against 3 parameters (γ_{dt}, F_u, and C)

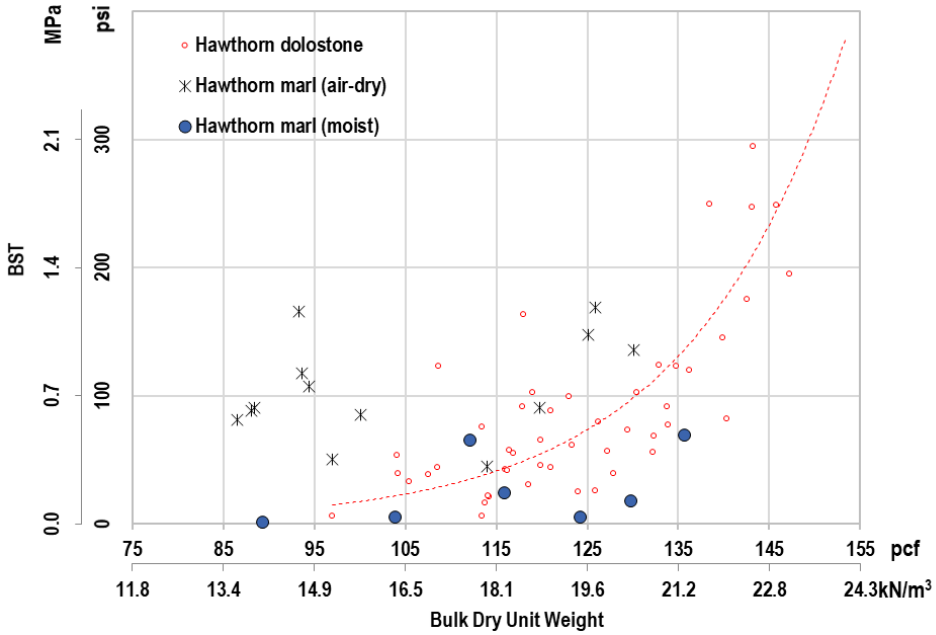

Figure 5-19. BST results for marl

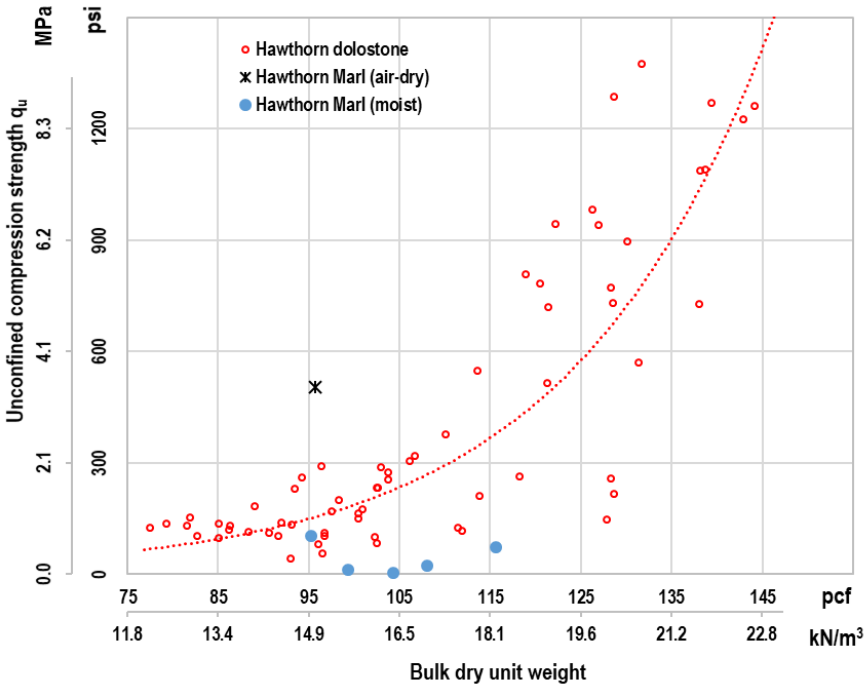

Figure 5-20. q_u results for marl

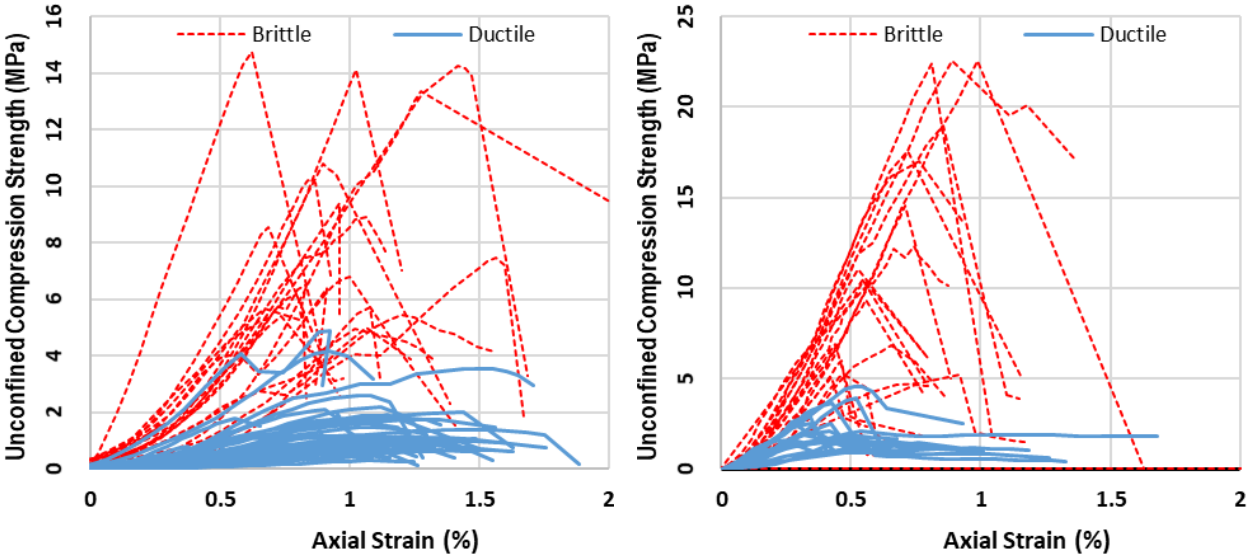

a) b)

Figure 5-21. Example of stress-strain results from q_u tests: a) Site 8-I95/ Fuller Warren Bridge St. Johns River, b) Site 21-SR 8 over Choctawhatchee River

CHAPTER 6
STRENGTH ENVELOPES OF FLORIDA CARBONATE-ROCKS AND IGMS

6.1 Existing Strength Envelopes

Many of the Florida Department of Transportation (FDOT) bridges are supported on deep foundations (drilled shafts, driven piles, and a minority of projects on other types of piles). Most of these foundations derive their bearing capacities from embedment in carbonate-rocks. The design practices for these deep foundations are as follow:

Driven pile resistances are designed not based on laboratory rock testing results, but based on correlations with in-situ testing results, e.g., SPT or CPT (McVay et at. 2017).

Drilled shafts: a) toe bearing capacity of shafts that are not post-grouted is typically ignored, and when utilized it is assigned only a fraction of the anticipated ultimate resistance to account for strain incompatibility between side resistance and end bearing; b) side resistance (f_s) approximately equals to the adhesion between concrete and rocks. McVay et al. (1992) proves that the linear Mohr-Coulomb portion (red continuous line in Figure 6-1), tangent with Mohr circles of unconfined compression results (q_u) and direct tension results (q_t) could be used to calculate the cohesion, which is the intercept between the linear portion and the y axis, and has been shown to have good correlation with the adhesion between drilled shaft concrete and the surrounding rock material in side resistances:

$$f_s = 0.5\sqrt{q_u q_t} \tag{6-1}$$

In a number of locations across Florida, especially south east of the state, shallow rock formations exist (i.e., rocks encountered at a depth less than about 10 m or 30 ft), and designers have recently proposed the use of shallow foundations for support of bridge piers or bents.

Required for design is the assessment of the rocks' bearing capacity which requires strength envelopes for the rock material, as well as identifying the stress-strain response of the rocks to assess foundation deformations, as well as bearing failure modes (general, local, and punching). The dashed black lines in Figure 6-1 is the portion of the strength envelope that had not been explored for the shallow and porous Florida carbonate-rocks. One option is to modify and use existing strength envelope models for the design. One such model is the well-known Hoek and Brown criterion, which is widely accepted and has been applied in a large number of projects around the world (Hoek and Brown 1980, 1988, and 2018), originally developed for rocks of brittle failure (rupture) behaviors:

$$\sigma_1 = \sigma_3 + q_u \left(m\frac{\sigma_3}{q_u} + s\right)^a \tag{6-2}$$

where,

σ_1 and σ_3 = specimen principal stresses.

s = rock mass discontinuity factor.

$$s = e^{(GSI-100)/(9-3D)} \tag{6-3}$$

GSI is the Geological Strength Index, which approaches 80 to 100 for intact or massive rock (blocky, very well interlocked undisturbed rock mass), and reduces to as low as 10 for very weathered, heavily broken rock mass.

$$m = m_i\, e^{(GSI-100)/(28-14D)}. \tag{6-4}$$

m_i ranges from approximately 8±3 to 12±3 for different carbonate-rocks (Table 6-1). A typical value of m_i = 10 for Florida carbonate-rocks when Hoek-Brown criterion is used in this study.

D = disturbance factor caused by the rock removal methodology. For shallow foundation excavation, D=0.

$a = 0.5 + (e^{-GSI/15} - e^{-20/3})/6$; Typically, a = 0.5 (6-5)

Note, setting $\sigma_3 = 0$ in Eq. 6-2 results in:

$\sigma_1 = q_u s^a$ (6-6)

For intact rock, s =1.0 and $\sigma_1 = q_u$. When comparing the strength envelopes to laboratory test results, s is always 1.0 regardless of rock mass qualities as each individual rock piece is intact (otherwise, σ_1 would not equal to q_u at $\sigma_3 = 0$).

When setting $\sigma_1 = 0$ in Eq. 6-2, then σ_3 would be the direct tension strength, $\sigma_3 = 0.5(m - \sqrt{m^2 + 4s})q_u$. Therefore, for intact rock (i.e., s=1 and m = m_i), it becomes $\sigma_3 = 0.5(m_i - \sqrt{m_i^2 + 4})q_u$. Since direct tension strength $q_t = -\sigma_3$ in this case, the direct tension strength over unconfined compression strength ratio for intact rock is:

$$q_t / q_u = 0.5(\sqrt{m_i^2 + 4} - m_i) \approx 0.1 \quad (6\text{-}7)$$

Hoek and Brown (2018) found out that this q_t / q_u ratio per Eq. 6-7 is higher than measured values, when q_t test results were available. Thus, a tension cut-off value was introduced, where the estimated q_t value is reduced to the following value (Hoek and Brown 2018):

$$q_t = q_u / (0.81m_i + 7) \quad (6\text{-}8)$$

In shallow foundation analyses or triaxial testing, it is more convenient to express the strength envelope in the Lambe's p-q diagram (Lambe and Whitman, 1969), as below:

$$p = (\sigma_1 + \sigma_3)/2 \quad (6\text{-}9)$$

$$q = (\sigma_1 - \sigma_3)/2 \quad (6\text{-}10)$$

Therefore, the Hoek-Brown criterion becomes:

$$q = 0.5\, q_u \left(m\frac{\sigma_3}{q_u} + s\right)^a \quad (6\text{-}11)$$

$$p = q + \sigma_3 = 0.5\, q_u \left(m\frac{\sigma_3}{q_u} + s\right)^a + \sigma_3 \quad (6\text{-}12)$$

For intact tested specimens, using typical carbonate-rock parameters of $m_i = 10$, s=1, a=0.5:

$$q = 0.5\, q_u \left(10\frac{\sigma_3}{q_u} + 1\right)^{0.5} \quad (6\text{-}13)$$

$$p = q + \sigma_3 = 0.5\, q_u \left(10\frac{\sigma_3}{q_u} + 1\right)^{0.5} + \sigma_3 \quad (6\text{-}14)$$

Similar to Hoek-Brown criterion, Johnston (1985) developed the following criterion that did not include a recommended range for the rock mass parameter, s, only that for intact rock, s = 1:

$$\sigma_1 = q_u \left(\frac{M}{B}\frac{\sigma_3}{q_u} + s\right)^B \quad (6\text{-}15)$$

$$B = (1\text{-}0.0172\log^2 q_u) \quad (6\text{-}16)$$

$$M = (2.065\text{+}0.170\log^2 q_u) \text{ for limestone} \quad (6\text{-}17)$$

These criteria, as stated, are suitable for rocks with brittle rupture behaviors. Numerous authors have studied the transitions from brittle to ductile flow, characterized as compactive cataclastic flow. These studies generally provide important physical insights into earthquake-related rock mechanics and tectonic processes in relation to faulting (Mogi 1966; Wong et al. 1997). Schwartz (1964) studied four different rocks with void ratio, e, from 0.02 to 0.24, or porosity, n, from 3% to 20%. For the "porous" Indiana limestone with n = 20%, the results indicated that the stress-strain response transitioned from brittle to ductile at confining pressure exceeding 34 MPa (5 ksi) and when the stress ratio of σ_d/σ_3 reduced to approximately 3.0 or

below. Mogi (1967) evaluated the transition from brittle to ductile in 45 different rocks with porosity from 0% to 21.6% and found that the average transition is defined by $\sigma_d/\sigma_3 = 3.4$. It is noted that Mogi (1967) grouped rocks with porosity above 10% as "highly porous". The confining pressure in Mogi (1967) study typically ranged between 30 MPa and 300 MPa (4.3 to 43 ksi) when the rocks change from brittle to ductile flow. For other "highly porous" rocks, where the porosity exceeds 18%, both studies by Elliot and Brown (1985) and Wong et al. (1997) showed that the rock responses changed from brittle faulting to compactive cataclastic flow at or above confining pressure of 10 MPa (1.5 ksi). In term of unconfined compression strength, q_u, the original Hoek and Brown (1980) study consisted of 923 data points, with majority of q_u exceeding 100 MPa (14.5 ksi), and the remaining minority all exceeding 40 MPa (5.8 ksi). The q_u = 23 MPa (3.3 ksi) for the Bath oolitic limestone in Elliot and Brown (1985) study was among the lowest unconfined compression strengths in the above studies. These rock properties are characterized in Figure 6-2.

Considering the aforementioned results in the literature, it is logical to adopt the Hoek-Brown criterion for the evaluation of shallow foundation (spread footing) bearing capacities as most rocks are expected to be in brittle zone. That is: (i) the overburden lateral stress within the spread footing influence zone only ranges from 0 to 0.2 MPa (0 to 30 psi); (ii) due to the expected foundation load and spread footing size, the vertical stress under a spread footing is typically 0.2 to below 5 MPa (30 to 725 psi). To give some perspectives: (i) the 169-m (555-ft) Washington Monument had a shallow foundation loading stress of approximately 0.5 MPa (70 psi) (Briaud et al. 2009), (ii) The 110-story World Trade Center Towers 1 and 2 were not on shallow foundations, however based on the dead weight of 4,900 MN (500,000 tons) and a foot print of 4,100 m^2 (44,000 ft^2), Eagar and Musso 2001), the dead-weight pressure would be 1.2

MPa (170 psi). All of these values are well below the threshold of between 10 and 300 MPa (1.4 to 43 ksi) found above for rocks to start changing to ductile flow. The conclusion to adopt Hoek-Brown criterion can also be justified by using the ductile threshold of $\sigma_d/\sigma_3 \approx 3$, which was found in the above studies. With low confinement under spread footings, σ_d/σ_3 ratio would overwhelmingly exceed 10 for typical rocks with strength exceeding 20 MPa (2.9 ksi), which means the rocks are expected to be in the brittle zone. Consequently, Carter and Kulhawy (1988) utilized the Hoek-Brown criterion in recommending Eq. 6-18 to evaluate the ultimate bearing capacity (p_u) of shallow foundation on rock, which is cited in Transportation Research Board (TRB) Report 651 (Paikowsky et al 2010).

$$p_u = \left[\sqrt{s} + \sqrt{m\sqrt{s} + s}\right] q_u \qquad (6\text{-}18)$$

Carter and Kulhawy (1988) method is the only semi-empirical bearing capacity evaluation method for rocks that is referenced in the current FHWA publication for shallow foundations (Kimmerling 2002) as well as in the current AASHTO LRFD Bridge Design Specification (AASHTO 2017).

As the ductile stress-strain behavior, or the compactive cataclastic flow, would typically never occur under minimal confining pressure (shallow foundation bearing capacity scenario), this ductile regime has never been explored under low confining pressure for rocks.

In contrast, Florida carbonate-rocks are generally much weaker as a result of their recent deposition in the Florida peninsula and their porous nature. Based on more than eight thousand data points from 1990 to 2017 in data set #1 (Chapter 5), the median q_u value is 3 MPa (435 psi) and the median porosity is 37%. The cementation of Florida rocks is apparently significantly lower than carbonate-rocks reported in other regions. For example, at a same porosity of n = 20%

to 21%, the Bath limestone and Indiana limestone are anticipated to have q_u at three times higher than that for Florida ones (Figure 6-2). Given this difference, it is critical to explore the ductile zone in regard to lower confining pressure along with the strength parameters suitable for Florida carbonate-rocks. In this chapter, 223 triaxial tests on Florida rocks were performed using innovative method to measure the volumetric behaviors of the porous specimens. The study results expand the knowledge on the σ_d/σ_3 threshold for ductile response in the low confinement pressure zone, suitable for shallow foundation application in soft rocks and IGM. Finally, it leads to the development of rock strength envelopes for many of the Florida rock formations that may be used for shallow foundation design.

6.2 Triaxial System for Rock Testing

Directly under a spread footing, the lateral stress may be 50% of the applied vertical stress, whereas at the edge of the footing, it could be greater than the vertical stress at the center (i.e. extension loading, σ_1 = lateral stress, and σ_3 = vertical stress). To capture these loading scenarios, a triaxial testing device is required, which is capable of testing material under different confining pressures. Typical soil triaxial cells (e.g., at universities, SMO, etc.) have maximum confining pressures (lateral stress) of approximately 0.9 MPa (130 psi) or less and employ air and water for confinement. The rock triaxial device must be capable of testing in both compression and extension (higher lateral vs. vertical stress). Also, the device must be capable of strain control for measuring strain softening (i.e. loss of strength), as well as measuring volumetric behavior.

The triaxial system for testing Florida limestone has been setup to satisfy the above objectives. The system is modular and consists of (1) a 180-kN (40,000-lb) capacity strain-

controlled Sigma-1 load frame by GEOTAC, (2) GEOTAC Sigma-1 CU SI software and instrumentation for controlling the load frame strain rate and sample monitoring (load, deformation, cell pressure, etc.), (3) a Hoek cell by RocTest with cell pressure rated for 69 MPa (10,000 psi), and (4) a volume change measurement device.

The modular system offers the greatest flexibility of testing any material (soil and rock). For instance, under lower cell pressures, the Hoek cell may be replaced with a standard soil triaxial cell for testing soil and intermediate geomaterials (IGM). A discussion of each component as well as their integration is presented next.

6.3 Triaxial Hoek-cell

The Hoek-cell, made of hardened stainless steel, was acquired from RocTest, Ltd. of Industry, Pennsylvania. The parts and dimensions of Hoek cell for this study are shown in Figure 6-4 and Figure 6-5. The Hoek cell system consists of:

1. One main steel cylindrical body with end caps, Figure 6-4, that screw onto the body. The manufacturer recommends white grease on the cap's thread (Lubriplate white lubricant l0034, Dow Corning Molykote 33 light grease, or Kleen-Flo #907);
2. One set of steel platens (top and bottom), which include a set of concave and convex end platens (to center the load);
3. One specimen membrane made of Adiprene urethane and is capable of withstanding 69-MPa (10,000-psi) hydraulic cell pressure.

Once the central section of the cell is attached to the bottom end cap, Figure 6-5, the rubber membrane is placed within the cell (greased top and bottom) and the top end cap is screwed onto the central section. Next, two quick-release self-sealing Simplex hydraulic couplings are screwed into the cell to provide for circulation of the hydraulic fluid and for the coupling of a pressure transducer. This device allows the hydraulic fluid to stay, without the need to drain it

nor dismantling of the cell between tests of different specimens. Dismantling of the cell is only needed to replace the worn out or damaged membrane, which typically lasts for about 20 to 30 triaxial tests. Figure 6-6 shows the hydraulic fluid filling the annulus between the outer cell steel wall and the rubber membrane. Finally, the operator inserts the specimen into the cell, place the top platen with the spherical seats. The spherical seats are provided so that the rock core ends do not need to be parallel – they only need to be flat and the spherical seats – without lubricant - will help minimize bending to the specimen.

It is noted that the cell pressure in a Hoek cell is only acting on the membrane surrounding the specimen, but not the top and bottom of the specimen. Therefore, during the initial pumping of the oil to reach the target confining pressure in the isotropic loading phase, axial load should also be gradually applied to maintain initial vertical stress σ_1 equal to the confining pressure σ_3. The procedure to perform a rock triaxial test is presented in Appendix C.

6.4 Displacement or Strain Measurements

To measure the vertical displacement of the rock specimen during shear, a Direct Current Displacement Transducer (DCDT) is attached to the top of the Hoek cell assembly. Hoek and Franklin (1968) recommended lateral strains to be measured via strain gauges, which are typically glued to the surface of the rock specimens. However, due to the vugs and large amount of shells in Florida carbonate-rocks, it is typically infeasible to attach strain gauges to the rock surfaces, such as the specimen in Figure 6-4 or other specimens previously presented in Chapter 4. To overcome this challenge, innovative methods to capture the hydraulic oil movement inward or outward were implemented. In Figure 6-7, the volume measurement device is simply an inactive piston, moving in or out depending on the oil flow direction. The piston is attached to a

linear variable displacement transducer (LVDT), which is correlated to the oil volume (ΔV). Also shown in this figure, a dry inert gas accumulator is used to stabilize the oil pressure (i.e. confining pressure) at the prescribed pressure, σ_3. Later in the study, the volume measurement mechanism was improved to the configuration shown in Figure 6-8, where a Digiflow pump - custom made for the project was used. The Digiflow pump is an active piston, where upon any change in oil pressure, a signal is sent to the piston to run in or out to get the pressure back to the target pressure. Similarly, the piston displacement is correlated to the volume change (ΔV) of the supplied hydraulic oil. The lateral strain and volumetric strain are as follow:

$$\varepsilon_L = \Delta R/R = \frac{\Delta V}{A_{surface}} \; / \; R = \frac{\Delta V}{2\pi HR^2} \tag{6-19}$$

$$\varepsilon_v = \varepsilon + \varepsilon_L + \varepsilon_H = \varepsilon + 2\varepsilon_L \tag{6-20}$$

where,

R, ΔR, and H: dimensions as shown in Figure 6-9.

ΔV: oil volume change.

$A_{surface}$: Surface area of specimen.

ε, ε_L, ε_H, ε_V: axial, lateral, horizontal, and volumetric strains during triaxial shearing test, respectively.

6.5 Range of Triaxial Confining Pressures

Due to the limited depth of a shallow foundation, the initial confining stress is minimal. However, as the major principal stress (σ_1) is increasing under the foundation loading, the confining stress (σ_3) is increasing along as well. In Zone 1 (outside of the footing) in Figure 6-10.a, at ground surface (i.e., depth = 0), $\sigma_{3\_zone\ 1} = \sigma_v = 0$ and $\sigma_{1\_zone\ 1} = q_u\, s^a$ using the simple approximation by Carter and Kulhawy (1988). Using the median undrain shear strength value for

Florida rock and IGM of q_u = 3 MPa (435 psi) and typical s = 0.3 to 0.8, then $\sigma_{1\_zone\ 1}$ = 1.6 to 2.8 MPa (230 to 400 psi). The q_u value for Florida material frequently reaches up to 9 MPa (1300 psi), and it is not uncommon for certain formations to exceed that value. In this case, $\sigma_{1\_zone\ 1}$ can exceed 5 MPa (700 psi), potentially reaching 10 to 20 MPa (1500 to 3000 psi).

In Zone 2 (underneath of the footing), the confining pressure, $\sigma_{3\_zone\ 2}$, in equilibrium will be equal to $\sigma_{1\_zone\ 1}$. The confining pressure under a footing starts at a minimal value (such as 0.0 to 0.2 MPa, depending on the rock's depth). However, as foundation loading increases, the stress-path induced confining pressure can eventually reach 2.0 to 6.9 MPa (300 to 1000 psi), and could exceed those values, either during extreme event conditions, or due to concentrated contact pressure that is higher than the average pressure as in the diagram depicted in Figure 6-10.b, or both.

The above discussion can also be illustrated using the stress paths in Figure 6-11. In a triaxial test, the σ_3 is maintained to be constant. However, σ_3 under a footing will keep going up along with the applied load (σ_1). As such, depending on Finite Element Method (FEM) simulation, the possible stress path under a footing could be such as the dashed line example in Figure 2. The final confining pressure for this dashed line example would be 4 MPa (580 psi), despite having a minimal starting confining pressure. Therefore, a majority of the triaxial tests were performed at a chamber pressure at or less than 6.9 MPa (1000 psi), and a small portion of the triaxial tests were performed at a chamber pressure up to 20.7 MPa (3000 psi).

6.6 Triaxial Stress-Strain and Volumetric Responses of Florida Carbonate-rocks

In this study, the rock specimens were cored at 7 different sites across the state of Florida. The encountered Florida rock formations are: Key Largo, Miami, Anastasia, Hawthorn, and Ft. Thompson. Triaxial tests were performed using confining pressures ranging from 0.35 to 20.7 MPa (50 to 3,000 psi), which covers the expected shallow foundation range of stresses, yet less than the typical threshold of 20 to 300 MPa (3 to 43 ksi) for the response to change from brittle to ductile for rocks found in literature. Pictures of rock specimens after triaxial tests are presented in Appendix D and representative individual triaxial test results are presented in Appendix E. Typical normalized deviatoric stress (σ_d / σ_3) versus vertical strain, ε, plots of the triaxial results are shown in Figure 6-12, where $\sigma_d = \sigma_1 - \sigma_3$ is the deviatoric stress. It was found that a few of Florida carbonate-rocks have brittle rupture failure (Figure 6-12.a), with a sharp rise in stress versus strain, then a sudden drop in deviatoric stress at failure. A large number of specimens have ductile responses (Figure 6-12.b), where the stress is rising gradually with strain, and there is no sudden drop in deviatoric stress at failure. Shown in Figure 6-13 are the stress-strain response from 223 triaxial specimens obtained from different Florida formations utilizing the improved triaxial system:

1. The red curves represent triaxial results for low confining pressure of σ_3 = 0.35 MPa (50 psi). It was discovered that:

    a) 30% of the specimens had brittle rupture failures, they experienced moderate to large volumetric dilation. The latter specimens were all dense rocks, with bulk dry unit weight (γ_{dt}) typically exceeding 20 kN/m^3 (127 pcf), associating with high rock strengths. Note, bulk dry unit weight is the ratio between the dry weight of specimen and its cylindrical core volume.

    b) 42% of the specimens experienced ductile failures, and it was found that ductile stress-strain behavior would be indicative of contractive volumetric responses. Also, some of the specimens' behavior would be described as "transition" (Figure 6-13.b), where there

is a sharp rise in stress in the first part of the curve, but in the subsequent parts, the deviatoric stress only drops within 0% to 20% compared to the previous peak.

2. In the case of higher confining pressure of σ_3 = 0.9 MPa (130 psi, black curves), more (76%) specimens experienced ductile behavior. As the confining pressures exceeded 4.1 MPa (600 psi, purple and orange curves), almost no specimen experienced brittle rupture failure. Even in unconfined pressure condition, Chapter 5 results indicate that the very porous Florida rocks already exhibit transition and ductile behavior when the unconfined strength q_u is approximately less than 5 MPa (725 psi), i.e., $\sigma_d/\sigma_3 = 50$, using atmospheric pressure of σ_3 = 0.1 MPa.

The above observations are summarized in Tables 6-2 and 6-3, where ductile/ brittle responses are categorized per confining pressure ranges and σ_d / σ_3 ratios or rock porosities. It is evident that Table 6-2 supplements the σ_d / σ_3 thresholds to cover all range of confining pressures, not just at high pressures (i.e., at or above 20 MPa, or 3000 psi) as was previously studied. For example, a weak rock with $\sigma_d / \sigma_3 = 10$ at $\sigma_3 = 0.3$ would be in the ductile flow zone per Table 6-2. However, if the existing threshold ratio of 3 were to be used, it would mistakenly be categorized as brittle. It is noted that depending on carbonate content, mineral structure, and rock grain size, some rock specimens would behave more or less ductile than the indicated ranges in Table 6-3.

Discussion regarding compactive cataclastic flow of porous carbonate-rocks:

One of the phenomena of the triaxial response when testing porous carbonate-rocks is the crushing or breaking of the rock's cemented grain structure, leading to structural rearrangement with appreciable porosity reduction, evident by the contractive volumetric strains in Figure 6-12.b. When the rocks have very high porosity (low bulk dry unit weight), under high isotropic (all around) stress, the rock grain cementation break and subsequently crush due to the extent and size of the void structure. Consider the case of Figure 6-14.a, the deviatoric stress is $\sigma_d = 0$, i.e. the sample is subject to an isotropic stress state. As confining pressure is increased, several

drops in stress are observed at vertical strains of 1.1%, 1.4%, and 1.7%, which are due to crushing of some cementation structure. At which times, the strain-rate controlled loading frame and the hydraulic oil could not initially maintain the confining stress during the crushing but recovered when crushing stopped. However, as the confining pressure increased, the crushing resumed, and collapse ensued.

In the case of medium isotropic stress states, the sample will still exhibit shearing resistance. That is the rock structure may crush forming granular assemblages within the sample and they will exhibit friction between granular particles as well as cementation within the non-crushed zones. For example, consider Figure 6-14.b which shows isotropic loading followed by deviatoric (shear) loading. Under isotropic loading, crushing is observed at strains of 1.1%, 1.4%, and 1.7%. Subsequently under triaxial shearing phase, the sample carried an increasing deviatoric stress and observed further crushing and shear failures at axial strains of 2.7% and 3.5%.

It should be noted that porous Florida carbonate-rocks generally do not experience natural crushing under their own overburden pressure due to their limited depths as well as due to the recent rock deposition (i.e., pre-consolidation pressure is about the same order of magnitude as the current overburden pressure). The formations investigated in this research were typically encountered at depths of 1 to 10-m (3 to 30-ft), thus the overburden pressure is only less than 0.2 MPa (30 psi). In summary, the very porous Florida rock formations likely experience breaking of cemented grain structure and a collapse of some void structure under high isotropic or deviatoric stress applications. This phenomenon may result in the steep downward curvatures of the strength envelopes as function of dry unit weight or porosity (Section 6.8).

The crushing phenomena, especially at confining pressure only at 0.1 to 4.1 MPa (10 to 600 psi), is less frequently encountered in rocks cited in literature due to their low porosities, thus, the perception of "porous" rocks is very different to that of Florida rocks. For instance, Fereidooni and Khajevand (2018) indicated travertine samples with n of 7% were porous; Schwartz (1964) considered the Pottsville sandstone and Indiana limestone as porous rocks, with porosities of n = 14% to 20%, respectively. Gowd and Rummel (1980) considered n = 15% as porous. In Mogi (1966), rocks with n = 1% to 10% were grouped as porous, and n > 10% as very porous, with a highest porosity cited as n = 21.6%. In comparison, 90% of Florida carbonate-rocks has porosity n ≥ 20% and only 10% of Florida carbonate-rocks has porosity between 5% and 20% (Chapter 4), i.e., the rocks that are typically considered porous in literature are considered "dense" and "outlier" data for Florida in general.

6.7 Extension Test Results

In a conventional compression triaxial test, the cell pressure, σ_3 is applied, and then the vertical stress, σ_1, is increased to failure. In the case of extension loading, the isotropic pressure is applied initially all around as in the above case. However, while the vertical stress is maintained fixed, the cell pressure is increased, i.e. shearing. For the shearing phase, the cell pressure is the major principal stress, σ_1, and the constant vertical stress is now σ_3.

For the extension test results at vertical stress of $\sigma_3 = 0$, the failure value of σ_1 is called q_e. The q_e value is generally at least the same or higher than the unconfined compression strength (q_u) trendlines as shown in Figure 6-15.

Similarly, for extension tests at higher vertical stress (such as σ_3 = 0.35 MPa = 130 psi), the failure normalized stress (σ_d/σ_3) is approximately at least the same as, or a little higher than, the compression test normalized results, as shown in Figure 6-16.a.

There are outlier points where the extension test results have lower normalized stress ratios (σ_d/σ_3) than those from the compression triaxial tests:

For the orange dot in Figure 6-16.a for a Miami specimen: the specimen had a large vug (hole) within the specimen (Figure 6-18.a). As the cell pressure (σ_1) was increasing on the flexible membrane, the cell pressure failed the sample at this location, splitting the specimen and damaged the membrane without failing the hard rock above and below this splitting surface. Thus, the strength of this specimen is lower than expected. In conventional compression tests, under a constant chamber pressure of 130 psi, the membrane would survive even if there are anomalies in the specimens.

For the two solid dots in Figure 6-16.b for two Hawthorn specimens: The specimen had a very soft end (Figure 6-18.b), while the remaining section of the specimen was of harder rock. As pressure was being increased, the membrane kept squeezing in, thus the lateral pressure reached a limit and would not increase – as seen in Figure 6-17. The test was stopped to prevent membrane puncture.

If these specimens for the above cases were to be tested in a conventional compression, the very rigid loading steel platen would transfer the axial load in a wider area, instead of being localized as in the case of the flexible membrane, which could lead to membrane puncture due to excessive displacement.

In summary, the extension test strengths and envelopes are generally expected to be at least the same as those of compression test results, with occasional outlier results due to inhomogeneity of specimens and the flexible nature of the membrane, which would be punctured and damaged due to the anomalies of the specimen under high pressure.

6.8 Intact-rock Strength Envelope

Construction of a typical strength envelope requires a series of triaxial tests, as well as tension strength tests, and unconfined compression strength tests to be performed (Figure 6-19). Ideally, all the specimens are supposed to have the same, or at least similar index properties. For Florida carbonate-rocks, it is difficult and sometimes impossible to find a pair of specimens that have similar index properties (i.e., same mineral components, porosities, dry weights, etc.) at the same depth. As identified in Chapter 4, within short vertical distances (cm or inches) of one another, one Florida rock specimen may have a bulk dry unit weight (γ_{dt}) of 20.5 kN/m^3 (130 pcf) and the adjoining rock specimen may have γ_{dt} of 12.5 kN/m^3 (80 pcf). Thus, pairing these two specimens is not recommended despite being at almost the same depth.

Furthermore, assuming a pair of specimens with same index properties were to be found, the results of the triaxial tests could still exhibit scatter from the mean value (due to orientation and distribution of vugs within each specimen), yielding less-meaningful strength envelopes. For example, specimen A and B in Figure 6-20 - both are of Key Largo formation, both have the same carbonate content of approximately 99.5%, both have the same bulk dry unit weight of approximately 12.7 kN/m^3 (81 pcf). Due to point A being lower than the mean value line for the 345-kPa (50-psi) tests (blue dash line in Figure 6-20) and point B being higher than the mean value line for the 900-kPa (130-psi) tests (green continuous line in Figure 6-20), the constructed

strength envelope (blue continuous line in Figure 6-21.a) would have an illogical slope-up curve instead of downward curve, or at least a straight line as in Mohr-Coulomb envelope. In an opposite example, specimen C and D also in Figure 6-20 - both are again of Key Largo formation and all have the same index properties. However, the paring of C and D would result in an extreme and illogical downward curve in the strength envelope (blue continuous line in Figure 6-21.b)

To resolve this issue of incompatible paring when constructing strength envelopes, the following procedures were followed:

The mean values for the normalized stress are utilized by establishing individual correlation between the normalized stress (σ_d/σ_3) at failure along with the bulk dry unit weight (γ_{dt}) for each formation, at each level of confining pressure (e.g., Figure 6-20). As identified in Chapter 4, it is simple for practitioners to obtain bulk dry unit weight (γ_{dt}), which is directly related to porosity: $n = 1 - \gamma_{dt}/ (GS*\gamma_w)$, where GS is the sample specific gravity and γ_w is water unit weight. Therefore, instead of correlating to porosity (n), Florida test result correlations were established based on the bulk dry unit weight as the primary parameter.

The correlations (e.g., Figure 6-20) were then used to calculate the σ_d/σ_3 at failure for each increment of dry unit weight (e.g., 5 pcf). The resulted values are presented in individual graphs for each of the formations (Figure 6-22 through Figure 6-26, with detailed descriptions presented in the subsequent discussion). Shown in Figure 6-22 are strength envelopes for Key Largo formation. Also shown in this figure are two curves obtained using Hoek-Brown criterion, for comparison purposes with Florida materials:

- The red continuous Hoek-Brown curve corresponds to an unconfined compression result of q_u = 7.9 MPa = 1112 psi and bulk dry unit weight of 18.8 kN/m^3 = 120 pcf, which is among the densest Key Largo limestones. This Hoek-Brown curve matches well with the tested

results, which is expected as these very dense Key Largo limestone specimens had brittle rupture responses in the triaxial test (Figure 6-12.a).

- The red dash Hoek-Brown curve (Figure 6-22) corresponds to an unconfined compression result of q_u = 4.3 MPa = 630 psi and bulk dry unit weight of 16.5 kN/m^3 = 105 pcf. The Florida test result for this rock (at 105 pcf) indicates a much lower strength envelope than the Hoek-Brown one. The triaxial tests of these specimens typically show ductile behavior (Figure 6-12.b), which explains why the Hoek-Brown criterion does not apply for the more porous Florida materials.

Similarly, shown in Figure 6-23 are strength envelopes for Anastasia formation. As shown in Chapter 5, Florida rock formations that have a high proportion of vug and permeable porosities (i.e., low proportion of impermeable porosity) within the bulk porosity have a lower unconfined strength. Higher proportion of impermeable porosity, such as of Key Largo or Anastasia formations, will have a higher unconfined compression strength at a given bulk porosity (i.e., at a given bulk dry unit weight) than other Florida formations. However, at sufficiently high confining pressures in triaxial tests, all the different zones of porosities in a specimen will collapse (i.e., crush), not just the vug and permeable portions as in the case of unconfined strength tests. Therefore, the strength envelopes for the porous specimens of these two formations have very steep downward slopes (Figure 6-22 and Figure 6-23). For other formations (Hawthorn, Miami, and Ft Thompson), due to the low carbonate content or low proportion of impermeable porosity, their starting points on the strength envelopes (from q_u results) are already low, thus the downward slopes in Figure 6-24 to Figure 6-26 for these formations are not as steep as in the case of Key Largo or Anastasia formations. Based on Figure 6-22 through Figure 6-26, dense Florida rocks with q_u higher than 9 MPa (1.3 ksi) are typically in the brittle zone when loaded under minimal confinement, e.g., under shallow foundations. Thus, the Hoek-Brown envelope would be applicable. More than 80% of Florida specimens (Chapter 4), however, are more porous and have q_u less than 9 MPa (1.3 ksi). As shown in Figure 6-22 through Figure 6-26, they are in the ductile zone – even under minimal confinement – and

the strength envelopes of these porous rocks have much steeper downward slopes than those in the brittle zone.

a) Discussion regarding data variability

In addition to rock crushing, which is already discussed in Section 6.5 there is an additional dip in the middle of several constructed envelopes such as in Figure 6-23 for γ_{dt} = 14 to 16 kN/m^3 (90 to 100 pcf) when σ_3 = 2.1 MPa (300 psi). This concavity in the strength envelopes could be the result of a lower bias at σ_3 = 2.1 MPa (300 psi), or it could be a result of a higher bias at $\sigma_3 \neq$ 2.1 MPa (300 psi). This is due to the scatter of the test results and the statistical population (the number of tests performed) for the data set.

The bias ratio, $(\sigma_d/\sigma_3)_{measured}$ / $(\sigma_d/\sigma_3)_{predicted}$, has a standard deviation of 0.33 from the triaxial test results. Therefore, the upper bound and lower bound of the σ_d/σ_3 value can be calculated as $(1.00 \pm 0.33) * (\sigma_d/\sigma_3)_{predicted}$. The strength enveloped constructed based on the lower bound of σ_d/σ_3 value, with example presented in Figure 6-27, would be ideal in a conservative design.

b) Discussion regarding Brazilian splitting tension (BST) and direct tension (q_t) relationship

The direct tension test is difficult to perform (Perras and Diederichs 2014). This is especially true for Florida carbonate-rocks with porosity commonly ranging from 25% to 50% (Chapter 4), as it would be practically infeasible to reshape the vuggy and poorly cemented rock specimens to the dog-bone shape for direct tension tests. Thus, BST has become the de factor laboratory test - it is the only test method listed in the FDOT Soil and Foundations Handbook (FDOT 2018) - to evaluate tension strengths for Florida materials. Perras and Diederichs (2014) tabulated that q_t / BST could vary from 0.4 to 1.2, with a mean value of 0.7 for sedimentary rocks. Therefore, a q_t

value of 0.7BST for Florida carbonate-rocks was used as starting point in our study. Figure 6-28 plots the early portions of the strength envelopes, connecting three values of q_t (of 0.7BST), q_u, and triaxial test results at low confinement of σ_3 = 0.345 MPa (50 psi) on the Lambe's p-q diagram. Figure 6-28.a and Figure 6-28.b, as examples, are essentially the zoom-in portions to the lower left corners of Figure 6-22 and Figure 6-23, respectively, where the early portions of the strength envelopes are practically linear. As shown in lower left corners of Figure 6-22 through Figure 6-26, as well as the zoom-in portions presented in Figure 6-28, a few lines could be straighter if one of the following scenarios occur: i) the q_t values are higher, such as to q_t = (1.0 or 1.2) BST; or ii) the q_u values are lower, or the triaxial strengths are higher at σ_3 = 0.345 MPa (50 psi), while q_t = 0.7BST. Either of these scenarios are possible due to the scatter of the test results and the population (the number of tests performed) of the data, which is similar to discussion (a) above. In summary, Florida carbonate test results support q_t = 0.7BST as a reasonable and conservative assumption.

6.9 Simplified Intact-rock Strength Envelope

Hoek et al. (2002) stated that it is necessary to determine equivalent Mohr-Coulomb angles of friction and cohesive strengths for each rock mass and stress range. This is done by fitting an average linear relationship to the Hoek-Brown curve, involving balancing the areas above and below the Mohr-Coulomb plot. Thus, the slightly curved Hoek-Brown envelope becomes a straight-line Mohr-Coulomb envelope. The reason for this simplification necessity is for geotechnical applications employed by various bearing capacity theories and numerical models, such as finite element method (FEM). Hoek et al. (2002) derived the equivalent Mohr-Coulomb envelope as follow:

$$\varphi = \arcsin\left[\frac{6am(s+m\sigma_{3n})^{a-1}}{2(1+a)(2+a)+6am(s+m\sigma_{3n})^{a-1}}\right] \quad (6\text{-}21)$$

$$c = \frac{q_u[(1+2a)s+(1-a)m\sigma_{3n}](s+m\sigma_{3n})^{a-1}}{(1+a)(2+a)\sqrt{1+(6am(s+m\sigma_{3n})^{a-1})/((1+a)(2+a))}} \quad (6\text{-}22)$$

where s, m, a are from Eqs. 6-3 to 6-5, and σ_{3n} is σ_{3max} / q_u, with σ_{3max} as the maximum confining stress over which the Hoek-Brown curve is approximated to the linear Mohr-Coulomb envelope.

Similarly, there is a need to simplify strength envelopes for Florida carbonate-rocks for finite element simulation of boundary value problems (e.g., bearing capacity of spread footings). Due to the general shape of the Florida strength envelopes, a bilinear simplification is proposed which allows a general modeling of Florida carbonate-rocks at a specified dry unit weight in a finite element method simulation. For Florida carbonate-rocks, rock heterogeneity is one more reason that necessitate the bilinear simplification for a practical engineering project. For one project site, one rock layer (for example, at 5-m or 15-ft thick) will have a wide range of bulk dry weights. As such, either that there will not be enough specimens (required 30 to 50 specimens) to perform triaxial tests for all different confining pressures at different bulk dry unit weights, or that it will be expensive for the designer to complete all 30 to 50 triaxial tests. Thus, it is anticipated that only 5 to 8 triaxial tests to be performed at one specific confining pressure. This pressure is suggested to be 4.1 MPa (600 psi) to cover the typical range of confining pressure under shallow foundation (Appendix F).

The four parameters that define the bilinear strength envelopes are: initial friction angle (φ), location of slope change (p_p), which can be considered as the onset of cementation breakage and crushing (onset of the ductile flow), 2nd slope of the envelope (ω), and cementation (c). The term cementation is used because unlike cohesive, the cementation strength is not recoverable once

the rock grains have been disintegrated. It is noted that the strength envelopes are presented in Lambe's p-q diagram (Figure 6-29), and the relatable geotechnical terms have direct relationships to Lambe's p-q diagram parameters as follow:

$$c = a / \cos\varphi \text{ or } a = c\cos\varphi \tag{6-23}$$

$$\sin\varphi = \tan\alpha \text{ and } \sin\omega = \tan\beta \tag{6-24}$$

These output parameters are obtained via four input parameters: q_t, q_u, γ_{dt}, and Florida carbonate formation identification, as identified below:

The cementation c (or a in Lambe's p-q diagram) is the intercept between the initial straight portion of the envelope (between q_t and q_u results) to the y-axis:

$$c = 0.5\sqrt{q_u q_t} \tag{6-25}$$

The friction angle φ (or α in p-q diagram) is the slope of the initial straight portion of the envelope (between q_t and q_u results):

$$\sin\varphi = \frac{q_u - q_t}{q_u + q_t} \qquad \text{(in p-q diagram: } \tan\alpha = \frac{q_u - q_t}{q_u + q_t}\text{)} \tag{6-26}$$

The p location at the peak of the initial straight portion of the envelope corresponds to a triaxial chamber pressure of 0.35 MPa (50 psi, Figure 6-29). This is a conservative representation of the peak points, since Figure 6-22 to Figure 6-26 indicate that the initial straight portion of the envelopes extends a little further out to a triaxial chamber pressure σ_3 of between 0.35 and 1.40 MPa (50 psi and 200 psi).

$$p_p \text{ (psi)} = \frac{50 + a}{1 - \tan\alpha} = \frac{50 + c\cos\varphi}{1 - \sin\varphi} \tag{6-27}$$

The 2nd slope on the strength envelope (β in p-q diagram, or ω in σ-τ diagram) is calculated between the above peak point and the end of the curve, presented in Figure 6-30 through Figure

6-34. The ω value is best fitted using bulk dry unit weight and rock formations due to (i) different proportions of vug, permeable, or impermeable porosities within the bulk porosity; (ii) mineral bonds (i.e., calcite, dolomite, and/or the sum of them – represented as carbonate content); (iii) rock grain size. The ω correlation is then presented in Table 6-4. In the case where formation identification is not known, a general value (approximately lower bound value) for ω is also suggested in Table 6-4 under Generic Florida formation. Using the above parameters, the simplified bilinear envelopes for the formations tested in this study are presented in Figure 6-35 through Figure 6-39.

A bias statistical analysis was performed to evaluate the scatter of the triaxial test results compared to the recommended bilinear strength envelopes on 223 tested specimens. One example of bias calculation is presented below using the trigonometry from Figure 6-29:

- Key Largo test specimen results: bulk dry unit weight γ_{dt} = 80.1 pcf, carbonate content of 98.2%, and the measured triaxial normalized stress $(\sigma_d/\sigma_3)_{measured}$ = 3.37 at chamber pressure of σ_3 = 130.5 psi. Thus, the triaxial stress path is:

  $$q = -130.5 + p \quad (6\text{-}28)$$

- Unconfined compression strength q_u = 230.4 psi and tension strength q_t = 46.8 psi.
- Per Eq. 6-25, c = 51.9 psi
- Per Eq. 6-26, $\tan\alpha = 0.66$, $\varphi = 41.5^0$, $\cos\varphi = 0.75$
- Per Eq. 6-23, a = 38.9 psi
- Per Eq. 6-27, p_p = 263.2 psi
- Per Table 6-4, $\omega = 0.69\,\gamma_{dt} - 68 = -12.7^0$, thus $\sin\omega = \tan\beta = -0.22$
- Therefore, the recommended bilinear strength envelope is:

  For $p \le p_p$: $q = 38.9 + 0.66p$ (6-29)

  For $p > p_p$: $q = 38.9 + 263.3\,(0.66+0.22) - 0.22p = 271.3 - 0.22p$ (6-30)

- Eq. 6-28 intersects with Eq. 6-30 at p = 328.8 psi and q = 198.3 psi, therefore the predicted deviatoric stress based on the bilinear envelope is $\sigma_d = 2q = 396.6$ psi, and $(\sigma_d / \sigma_3)_{predicted} = 3.04$.
- The (σ_d/σ_3) bias for this specimen is $(\sigma_d/\sigma_3)_{measured} / (\sigma_d/\sigma_3)_{predicted} = 3.37 / 3.04 = 1.11$.

Figure 6-40 shows the (σ_d / σ_3) bias scatter representation for all 223 tested specimens, which indicates that the bilinear strength envelopes are quite acceptable ($R^2 = 0.88$, with a conservative bias higher than 1.0) in representing the Florida rock strengths.

6.10 Rock Mass Strength Envelope

In engineering practice, there is a great need in the characterizing Florida's rock masses from intact rock specimens and coring information. In the cases of a jointed rock mass, the overall Hoek-Brown envelope for the rock mass is lower than that for intact rock, via parameters m, s, and a as shown in Eq. 6-2. The resulting $q_{rock\text{-}mass} = (\sigma_{1rock\text{-}mass} - \sigma_3)/2$ value on the rock mass strength envelope is reduced by a factor approximately proportional to GSI/100 value, compared to the $q = (\sigma_1 - \sigma_3)/2$ of intact rock, with examples presented in Figure 6-41. For jointed rock, the GSI/100 value is approximately proportional to the RQD or REC value. Therefore, the rock mass strength envelope is expected to be proportional to RQD or REC with respect to the intact rock strength.

For Florida rocks and IGMs, the materials appear jointless (Truzman 2016): the appearance of intact or massive rock mass can be misinterpreted and it is not feasible to directly evaluate the GSI index. Therefore, further studies are needed regarding the reduction of rock mass strength envelopes for Florida materials. Pending further studies, a provisional procedure is suggested below:

6.10.1. Weight-adjusted Strength Envelope

Bulk dry unit weights are performed on as many specimens (Length, L_i) as possible from the recovered rocks, and a weighted average unit weight is found:

$$\gamma_{dtw} = \Sigma(\gamma_{dti}\, L_i) / \Sigma L_i \quad (6\text{-}31)$$

The three subscripts are: d for dry, t for total (or bulk, to differentiate with apparent dry unit weight, obtained from ASTM D6473 method, presented in Eq. 3-3), and w for weighted average.

For the rock layer that is being evaluated, the weighted average dry unit weight for those specimens that are tested for strength is γ_{dts} (the three subscripts are: d for dry, t for total, and s for strength tested specimens). The same procedure can be done for carbonate content to arrive at the weighted average carbonate content C_w and strength test only carbonate content C_s. Despite varying a lot from one formation to the next, the carbonate content may not vary much within a site-specific rock layer and it can be assumed that for a specific investigated rock layer, $C_w \approx C_s$. For the porous Florida rocks, BST is estimated to be $2.468F_t e^{0.03\gamma_{dt}} e^{0.5C}$ and q_u is estimated to be $3.24F_u e^{0.04\gamma_{dt}} e^{2C/3}$ (Chapter 5). Therefore, the weighted BST (thus q_t) and q_u values for the evaluated rock layer are reduced from the values of the intact specimens as:

$$q_{tw} = q_t * e^{0.03(\gamma_{dtw}-\gamma_{dts})} e^{0.5(C_w-C_s)} \approx q_t * e^{0.03(\gamma_{dtw}-\gamma_{dts})} \quad (6\text{-}32)$$

$$q_{uw} = q_u * e^{0.04(\gamma_{dtw}-\gamma_{dts})} e^{2/3(C_w-C_s)} \approx q_u * e^{0.04(\gamma_{dtw}-\gamma_{dts})} \quad (6\text{-}33)$$

where q_t (based on 0.7*BST) and q_u are site specific test results for the evaluated rock layer (when many specimens are tested for BST and q_u, then the statistical procedure in Appendix A of FDOT Soil and Foundations Handbook can be followed to arrive at a single mean value of BST and q_u for the rock layer). So after step 1, instead of strength envelope based

on intact properties of q_t, q_u, and γ_{dts}, a weight-adjusted strength envelope based on q_{tw}, q_{uw}, and γ_{dtw} should be used in Eqs. 6-25 to 6-27 and Table 6-4.

For example, in the last core run of Figure 2-12, REC = 78%, and there are two pieces (labelled as 1 and 2 in the figure) that are tested for strength (BST or q_u) as well as dry unit weight, the other specimens in the core would be tested for index parameters only (no strength test). For the specimens tested for strengths, let says the mean values are: BST = 66.9 psi, q_t = 0.7*66.9 = 46.8 psi, q_u = 230.4 psi, and γ_{dts} = 80.1 pcf. When including all specimens (tested both for strengths and tested only for index parameters, i.e., no strength tests), the weighted value is γ_{dtw} = 70.1 pcf. Thus, we have lower weighted strength values of: $q_{tw} = 46.8 * e^{0.03(70.1-80.1)} = 34.7$ psi and $q_{uw} = 230.4 * e^{0.04(70.1-80.1)} = 154.4$ psi. Then, after step 1, instead of a strength envelope based on intact properties of 46.8 psi, 230.4 psi, and 80.1 pcf, a weight-adjusted strength envelope based on 34.7 psi, 154.4 psi, and 70.1 pcf should be used in Eqs. 6-25 to 6-27 and Table 6-4.

6.10.2. Recovery-adjusted Strength Envelope

In the Florida Department of Transportation practice (FDOT 2018), the rock mass strength is reduced by rock recovery (REC%) compared to the intact specimen strength to account for uncoreable materials. For example, $q_{um} = q_u * REC$ and $q_{tm} = q_t * REC$, thus $f_{su\_design} = REC * 0.5\sqrt{q_u * q_t}$ for drilled shaft side resistance calculation. This strength reduction accounts for the uncorable weak rock or soil within the core run. Additional advantages of using REC to reduce the rock strength estimation during the design phase include:

i) If low recovery indicates suspected voids, it forces the designers to evaluate the negative impact the suspected voids may have to the foundations.

ii) If low recovery is simply a product of the out-of-maintenance drilling equipment or the skill of the drilling crew, resulting in no or not enough specimens available to be tested, then it would be an incentive for the designers to rework the subsurface exploration plan in order to achieve higher rock recovery and thus, have a more economical yet reliable foundation design based on realistic rock recovery.

It is therefore recommended that the Florida strength envelope for the rock mass to be reduced by a factor of REC as illustrated in Figure 6-42 and in the equation below:

$$q_m = q * REC \tag{6-34}$$

which would result in the following parameters, based on the weighted values from Step 1:

$$a_m = REC*a = REC*0.5\sqrt{q_{uw}q_{tw}}\cos(\arcsin\frac{q_{uw}-q_{tw}}{q_{uw}+q_{tw}}) \tag{6-35}$$

$$tan\alpha_m = REC*\tan\alpha = REC\frac{q_{uw}-q_{tw}}{q_{uw}+q_{tw}} \tag{6-36}$$

$$tan\beta_m = REC*\tan\beta = REC*\sin\omega \tag{6-37}$$

$$p_{pm} = p_p \tag{6-38}$$

It is noted that the above Eq. 6-34 and its derivations for rock mass would yield slightly more conservative rock mass's cementation value than the conventional $REC*\ 0.5\sqrt{q_{uw} * q_{tw}}$ value:

$$c_m = a_m / cos\varphi_m = REC*\ c\ *\cos\varphi / \cos\varphi_m$$

$$c_m = REC*\ 0.5\sqrt{q_{uw} * q_{tw}}\ *\cos\varphi / \cos\varphi_m \le REC*\ 0.5\sqrt{q_{uw} * q_{tw}} \tag{6-39}$$

Therefore, the simplicity yet conservative form of Eq. 6-34 makes it ideal to model the rock mass envelope in finite element method software.

6.11 Summary

The main focus of this chapter is the development of strength envelopes for the shallow Florida rock formations, with the ultimate goal of estimating shallow foundation (spread footing) bearing capacity. Because of the limited depth of exploration for such subsurface, the encountered Florida carbonate-rocks are porous, with some porosities exceeding 50%, or bulk dry unit weight less than 13.4 kN/m^3 (85 pcf). Their strengths are low, with the median value for unconfined compression strength of 3 MPa (435 psi). Due to the difficulty in attaching strain gages to the vuggy and shelly surface of Florida carbonate-rocks, innovative volume measurement device was added to the Hoek cell triaxial system, enabling the researchers to easily measure the volumetric responses of Florida carbonate-rocks in triaxial tests. It is demonstrated that when the unconfined compression strength, q_u, is higher than 9 MPa (1.3 ksi), the material typically exhibits brittle stress-strain behavior for shallow foundation loading conditions. In this case, the well-known Hoek-Brown criterion, developed for brittle rupture failure, is applicable. However, most of the porous Florida carbonate-rocks have weaker strengths with ductile stress-strain response, associated with contractive volumetric behavior. The σ_d/σ_3 threshold for the material to transition from brittle to ductile responses have been expanded beyond the conventional ductile pressure range (i.e., toward the minimal confining pressure range), presented in Table 6-2. Accordingly, the strength envelopes for these materials are sloping downward at a much steeper rate than those in the brittle zone. Moreover, the envelopes vary between formations, due to different cementations (different minerals, carbonate contents, and rock grain sizes) as well as different proportions of void structures (vug, permeable, and impermeable voids). Consequently, it is recommended that different Florida carbonate-rock formations have their own prior established strength envelopes based on dry unit

weights, or sufficient specimens be collected, and strength envelopes be established based on triaxial testing as discussed herein. Furthermore, it is not recommended to reduce the strength envelope of Florida carbonate-rocks using the GSI index since it is not readily available. Pending further study, a provisional procedure is recommended to develop Florida rock mass strength envelope from the intact strength envelope, weighted-average value for dry unit weight, and rock recovery ratio (REC).

Table 6-1. Values of the constant mi for carbonate-rocks
(after Marinos and Hoek 2000; with updated values from Rocscience, Inc. 2007)

Texture	Coarse	Medium	Fine	Very Fine
Rock	Crystalline Limestone	Sparitic Limestone	Micritic Limestone	Dolomite
m_i	12 ± 3	10 ± 5	8 ± 3	9 ± 3

Table 6-2. Approximate behavior type table of Florida carbonate-rocks based on σ_d/σ_3 ratio

σ_3 (MPa)	σ_3 (psi)	σ_d/σ_3 for transitional response	σ_d/σ_3 for ductile response
0.1	15	50	20
0.3	50	17	10
0.9	130	10	7
1.4	200	9	6
2.1	300	8	5.5
4.1	600	7	5
6.9	1000	6.5	4.5
20.7	3000	*	3
**	**	**	**

Note: * Florida carbonate-rock specimens tested at σ_3 = 20.7 MPa all had $\sigma_d/\sigma_3 \leq 3$

** For $\sigma_3 > 20$ MPa, the transitional and ductile thresholds of $\sigma_d/\sigma_3 \approx 3$, as in Schwartz (1964) and Mogi (1967) could be applicable.

Table 6-3. Approximate behavior type table of Florida carbonate-rocks

		Bulk Dry Unit Weight Range (pcf)					
σ_3 (MPa)	σ_3 (psi)	60-65	66-85	86-110	111-120	121-130	130-135
0.1	15	Transition	Transition	Brittle	Brittle	Brittle	Brittle
0.3	50	Ductile	Transition	Transition	Brittle	Brittle	Brittle
0.9	130	Ductile	Ductile	Transition	Transition	Brittle	Brittle
1.4	200	Ductile	Ductile	Ductile	Transition	Transition	Brittle
2.1	300	Ductile	Ductile	Ductile	Ductile	Transition	Transition
4.1-6.9	600-1000	Ductile	Ductile	Ductile	Ductile	Ductile	Transition
6.9-20.7	1000-3000	Ductile	Ductile	Ductile	Ductile	Ductile	Ductile

Table 6-4. Value of 2nd slope (ω) on Florida strength envelopes

Formation	ω value for γ_{dt} in pcf	ω value for γ_{dt} in kN/m^3
Key Largo	$0.69\,\gamma_{dt} - 68$	$4.4\,\gamma_{dt} - 68$
Shallow Ft. Thompson	$1.57\,\gamma_{dt} - 165$	$10\,\gamma_{dt} - 165$
Miami	$0.0136\gamma_{dt}^2 - 2.2\,\gamma_{dt} + 85$	$0.55\gamma_{dt}^2 - 14\,\gamma_{dt} + 85$
Anastasia	$0.0691\gamma_{dt}^2 - 16.45\,\gamma_{dt} + 972$	$2.8\gamma_{dt}^2 - 104.7\,\gamma_{dt} + 972$
	$\omega = -6.7$ for $\gamma_{dt} < 120$ pcf	$\omega = -6.7$ for $\gamma_{dt} < 19$ kN/m^3
Hawthorn	$0.011\gamma_{dt}^2 - 1.72\,\gamma_{dt} + 68$	$0.45\gamma_{dt}^2 - 11\,\gamma_{dt} + 68$
Generic Florida formation	$0.79\gamma_{dt} - 90$	$5\gamma_{dt} - 90$

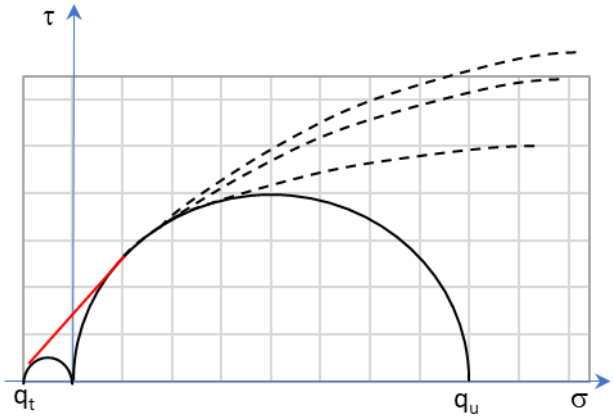

Figure 6-1. Sketch of strength envelopes

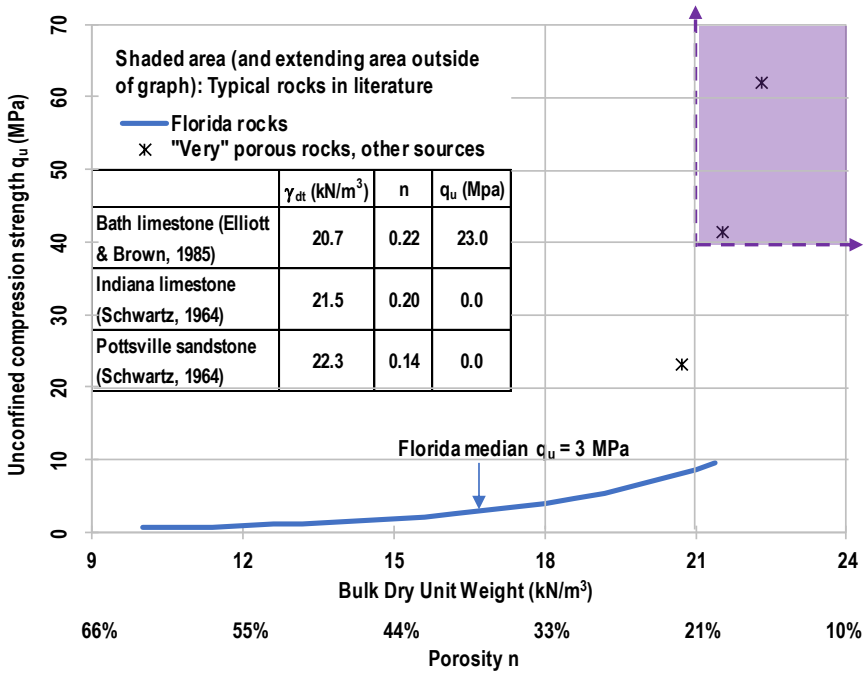

	γ_{dt} (kN/m^3)	n	q_u (Mpa)
Bath limestone (Elliott & Brown, 1985)	20.7	0.22	23.0
Indiana limestone (Schwartz, 1964)	21.5	0.20	0.0
Pottsville sandstone (Schwartz, 1964)	22.3	0.14	0.0

Figure 6-2. Rock unconfined compression strength, bulk dry unit weight, and porosity

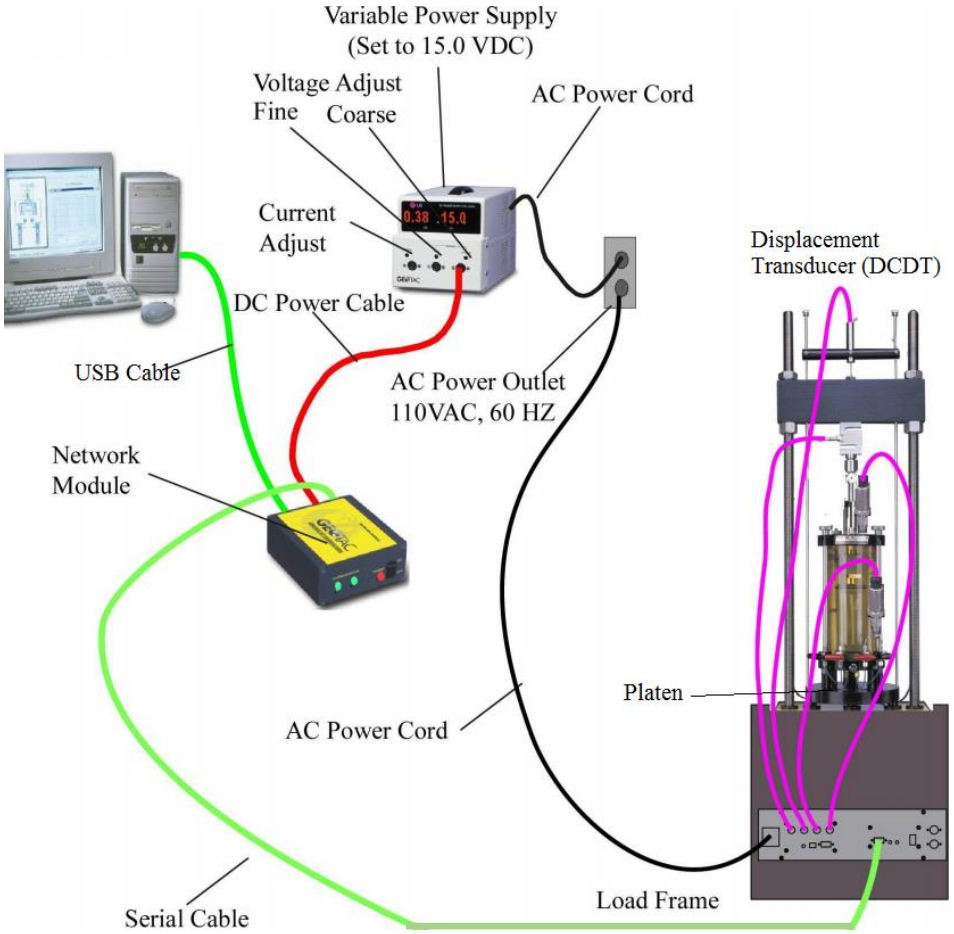

Figure 6-3. Triaxial modular setup

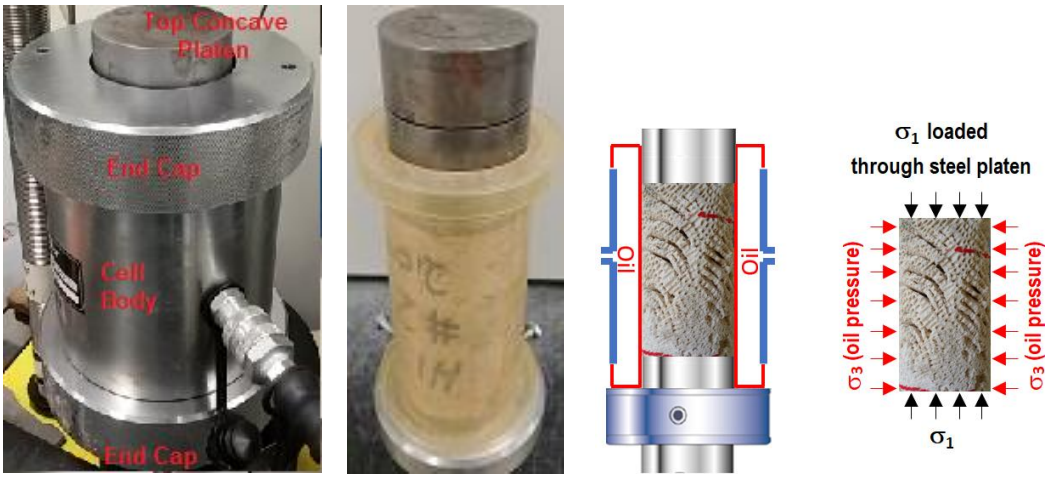

Figure 6-4. Schematic of Hoek-cell triaxial test (Photo courtesy of Thai Nguyen)

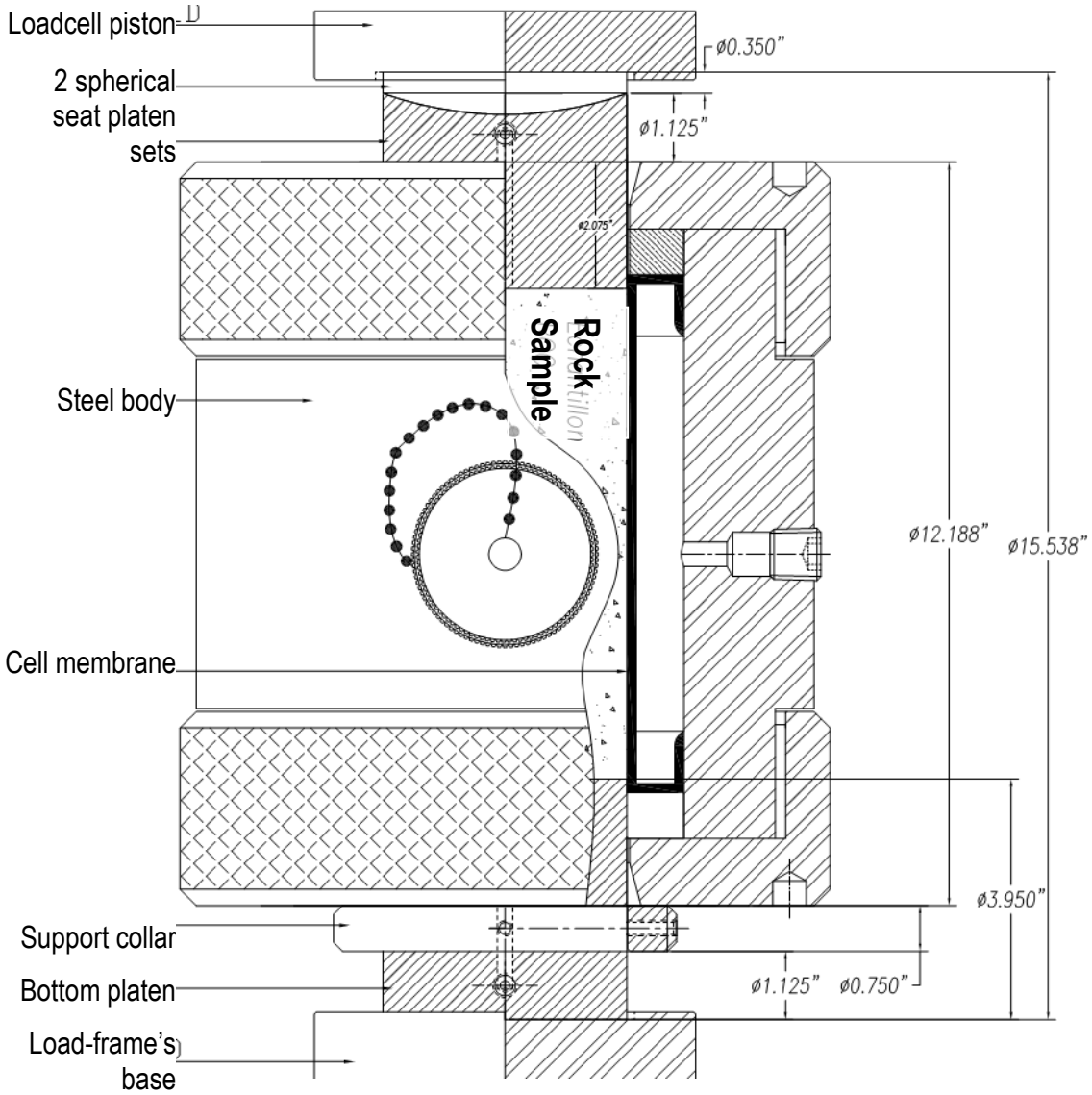

Figure 6-5. Hoek-cell design

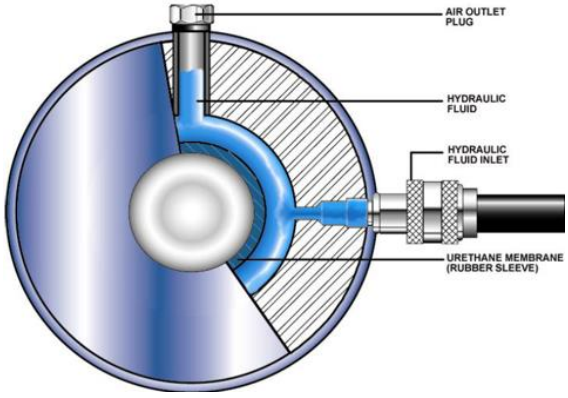

Figure 6-6. Hoek-cell hydraulic fluid filling

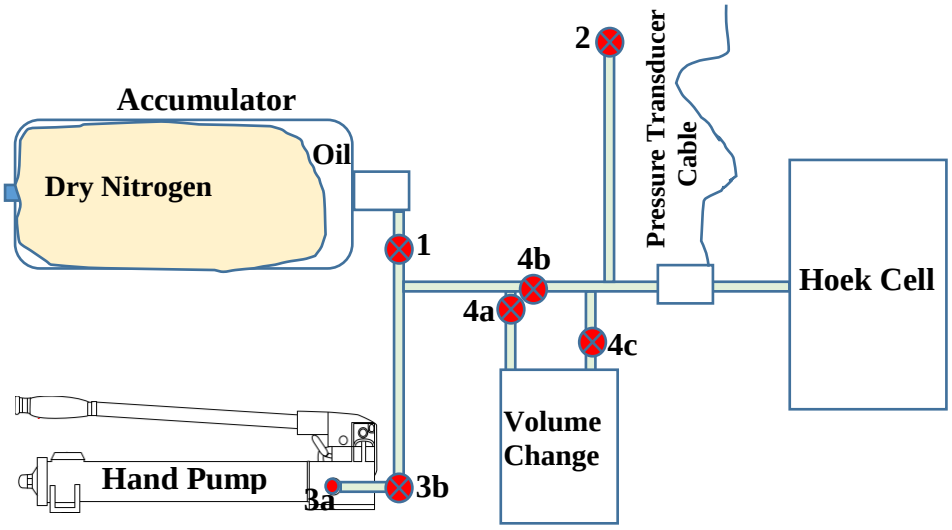

Figure 6-7. Triaxial system with accumulator and volume change device

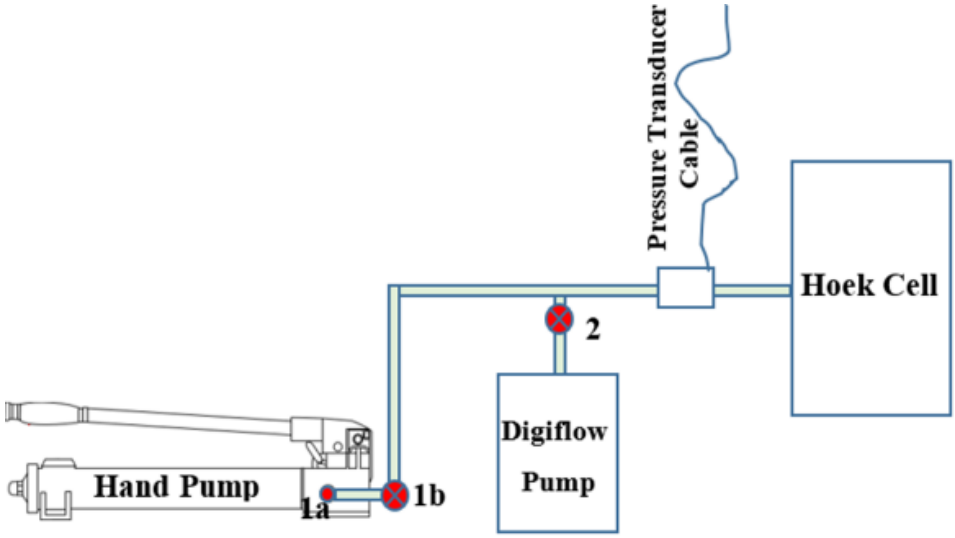

Figure 6-8. Triaxial system with Digiflow pump

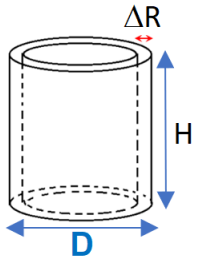

Figure 6-9. Volume change with membrane displacement

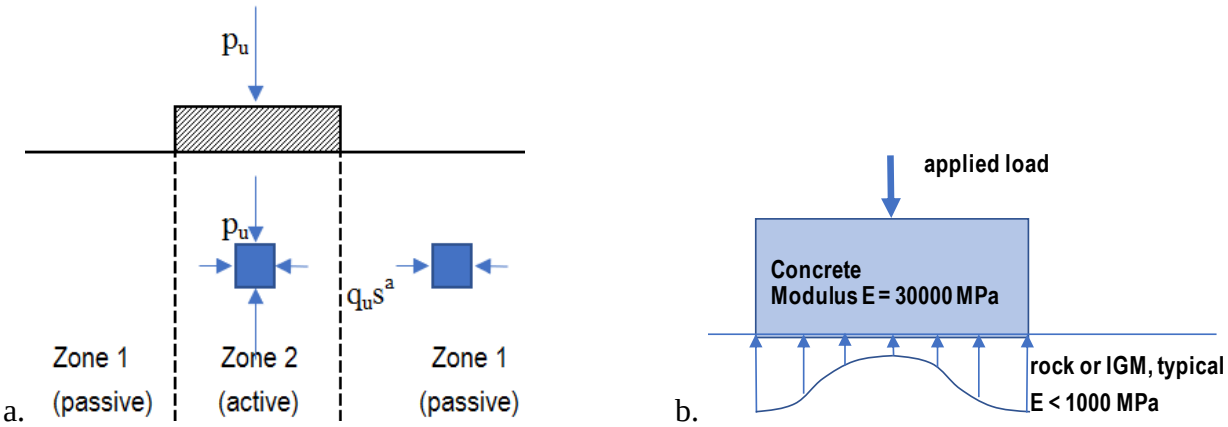

Figure 6-10. Pressure under a footing; a. Active and passive zones (Adapted from Carter and Kulhawy, 1988); b. Possible contact stresses.

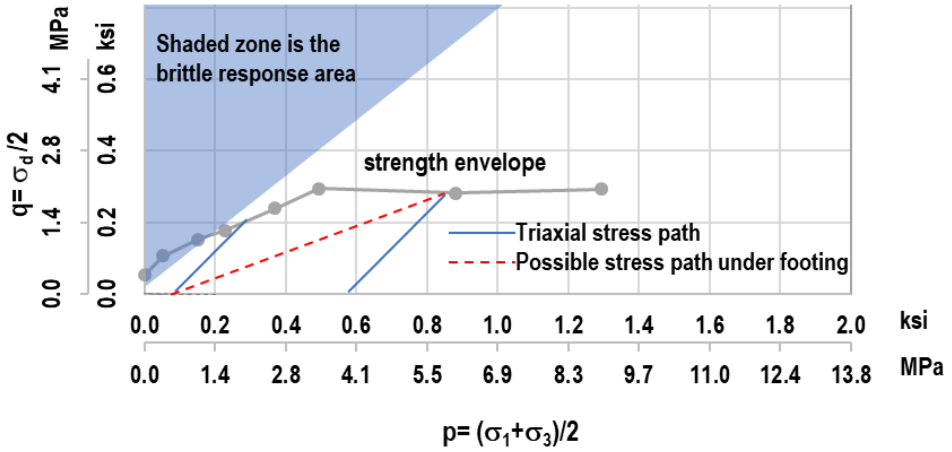

Figure 6-11. Stress paths and strength envelope

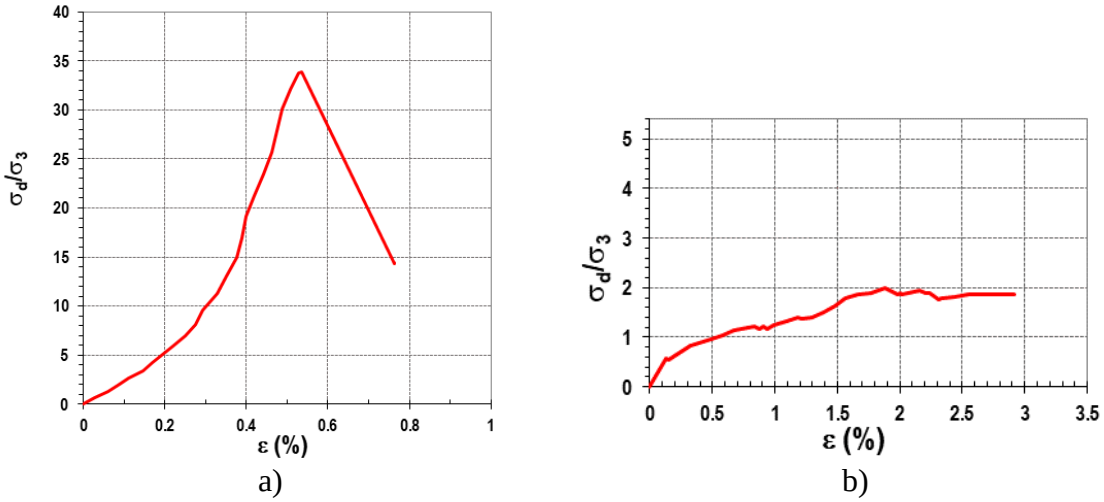

Figure 6-12. Examples of triaxial results - Key Largo formation: a) γ_{dt} = 18.9 kN/m^3 = 120 pcf, σ_3 = 345 kPa = 50 psi, b) γ_{dt} = 15.7 kN/m^3 = 100 pcf, σ_3 = 3100 kPa = 450 psi

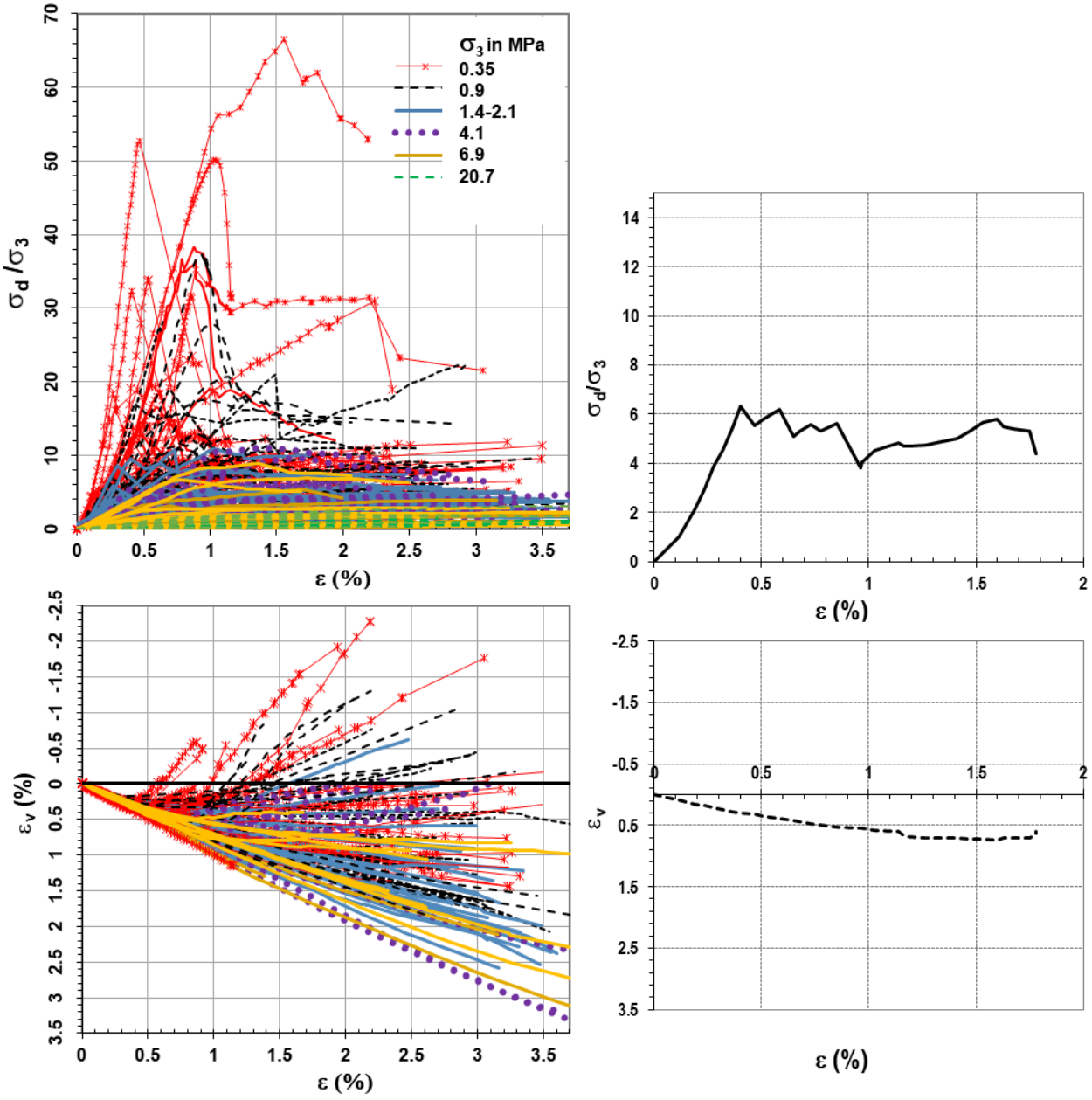

a) b)

Figure 6-13. Normalized deviatoric stress and volumetric strain: a) Combination plots of multiple specimens, b) Example of "transition" behavior

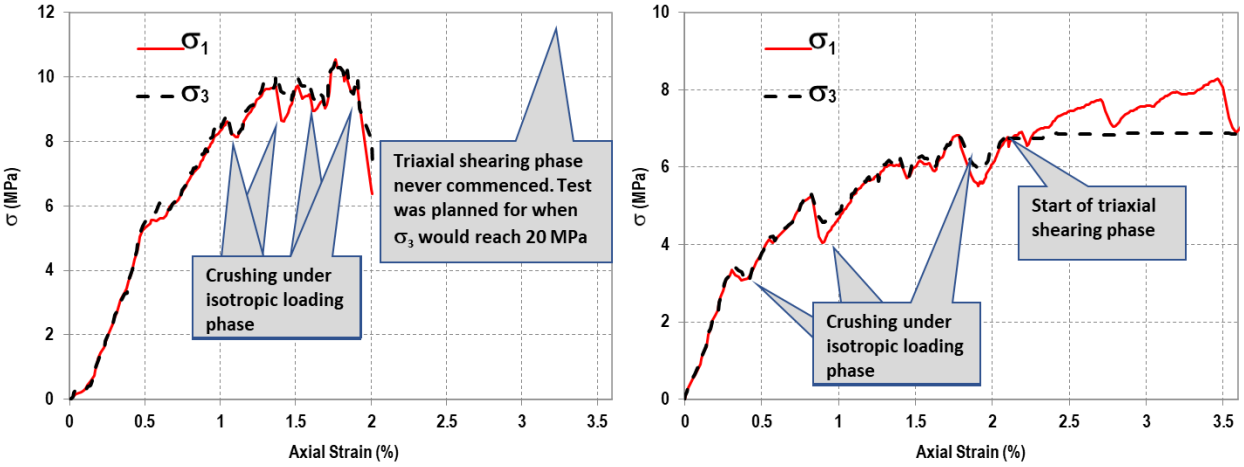

a) b)

Figure 6-14. Crushing of porous rocks: a) isotropic loading, b) isotropic then deviatoric loadings

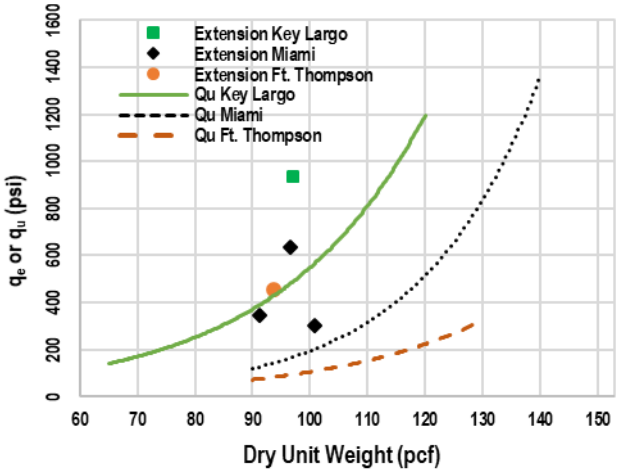

Figure 6-15. Unconfined compression test and extension test results

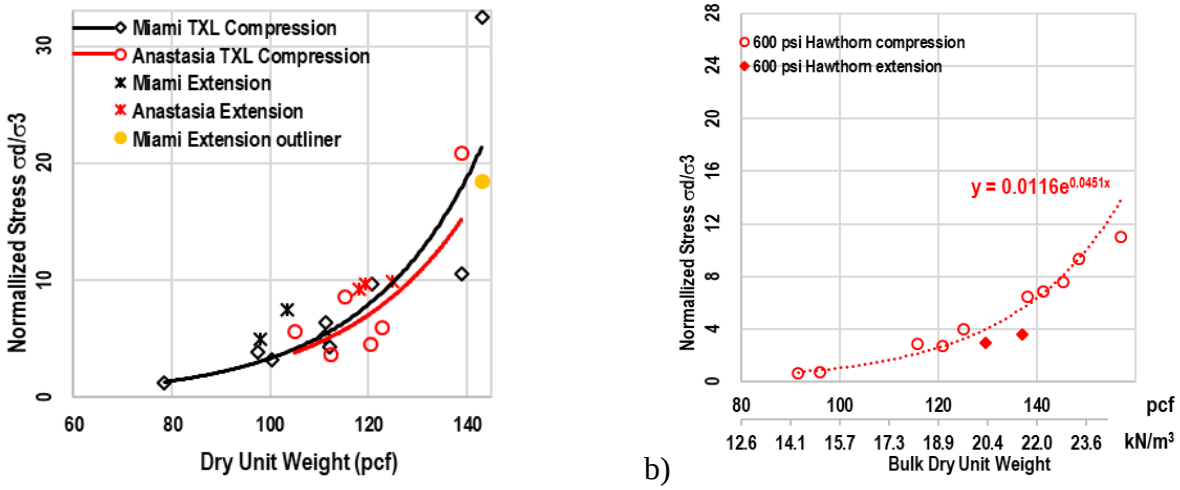

a) b)

Figure 6-16. Triaxial compression test and extension test results. a) σ_3 = 130 psi, b) σ_3 = 600 psi.

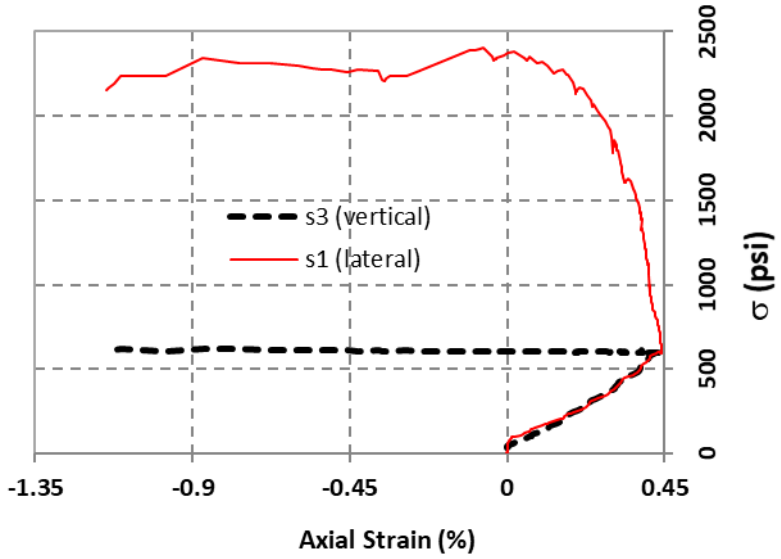

Figure 6-17. Triaxial extension test stress – strain curve for specimen 813

a) b)

Figure 6-18. Outlier extension test specimens: a) Hole on specimen, b) One end of specimen is much softer (Photo courtesy of Thai Nguyen)

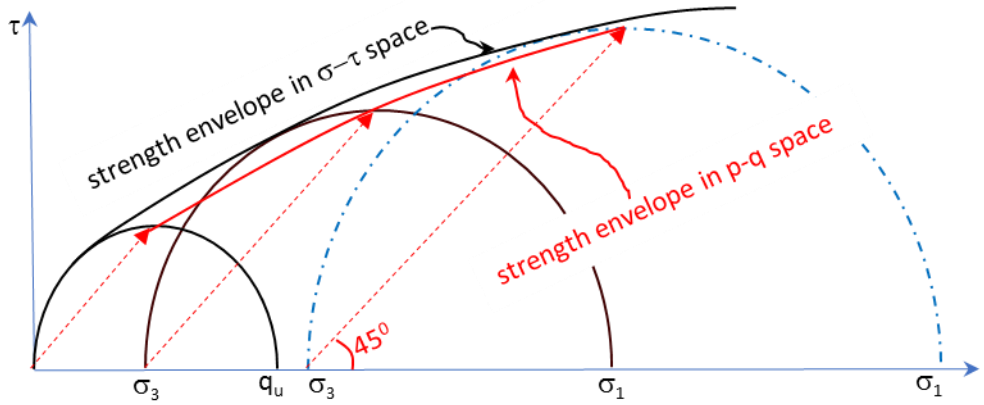

Figure 6-19. Schematic of strength envelope construction

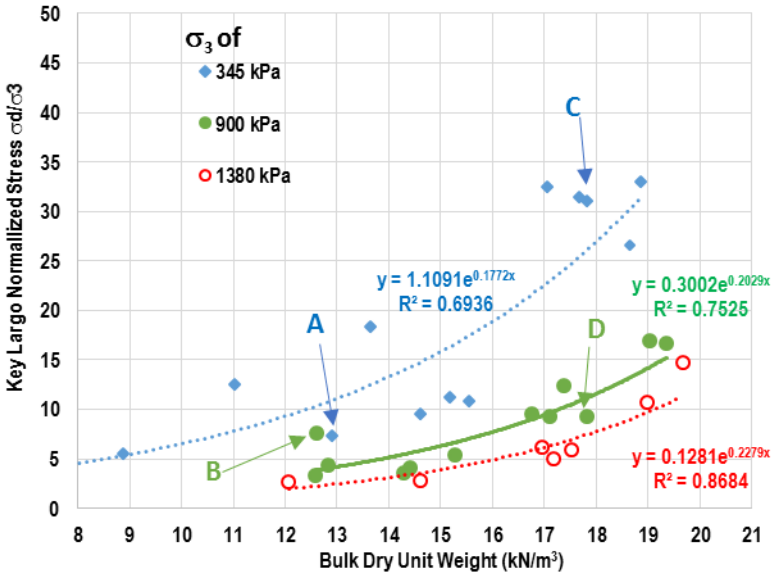

Figure 6-20. Key Largo normalized deviatoric stress results

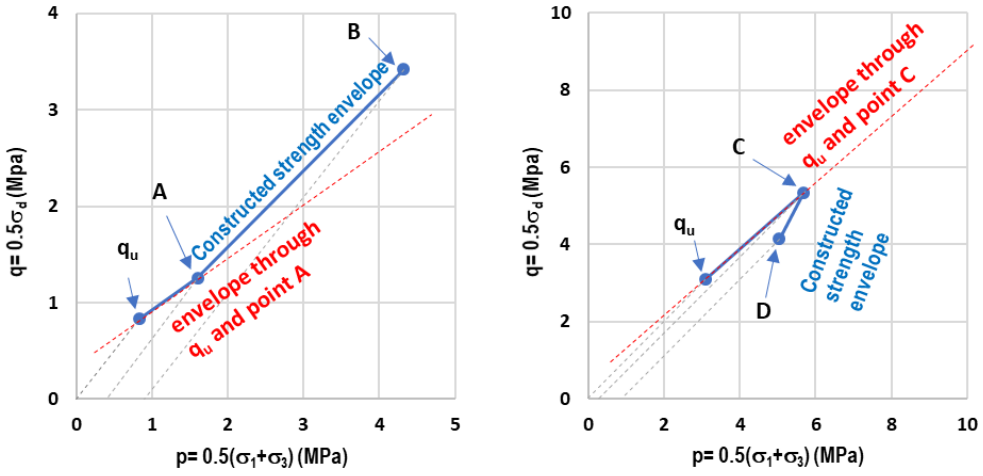

a) b)

Figure 6-21. Examples of incorrectly constructed strength envelopes. a) Specimens A and B pairing, b) Specimens C and D pairing

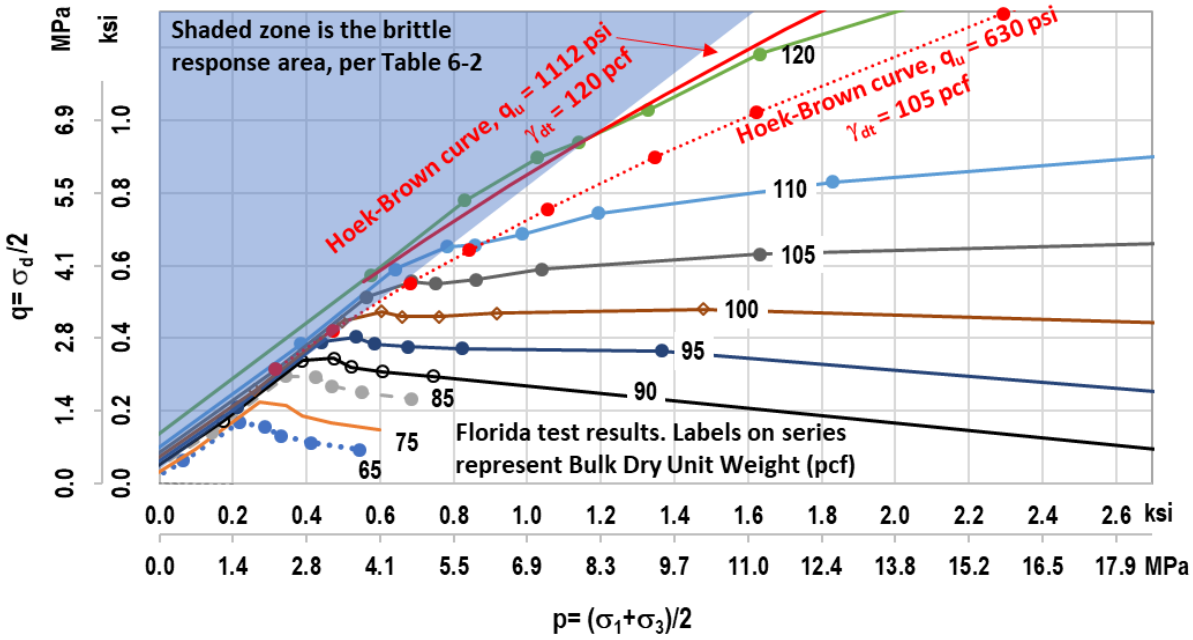

Figure 6-22. Strength envelope – Key Largo formation

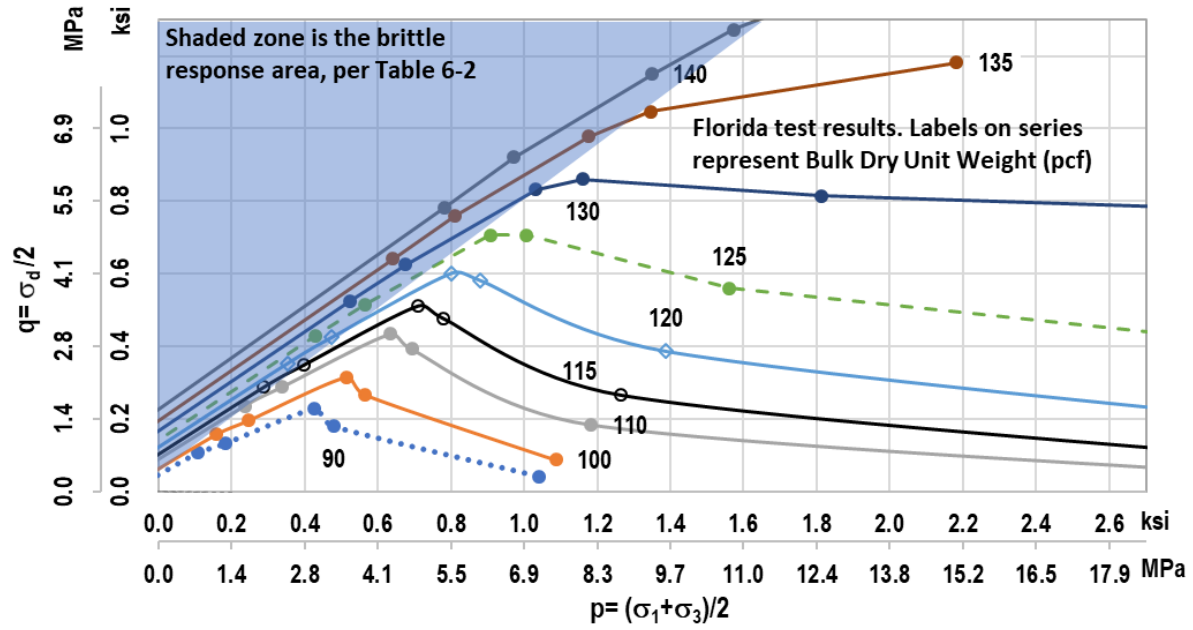

Figure 6-23. Strength envelope – Anastasia formation

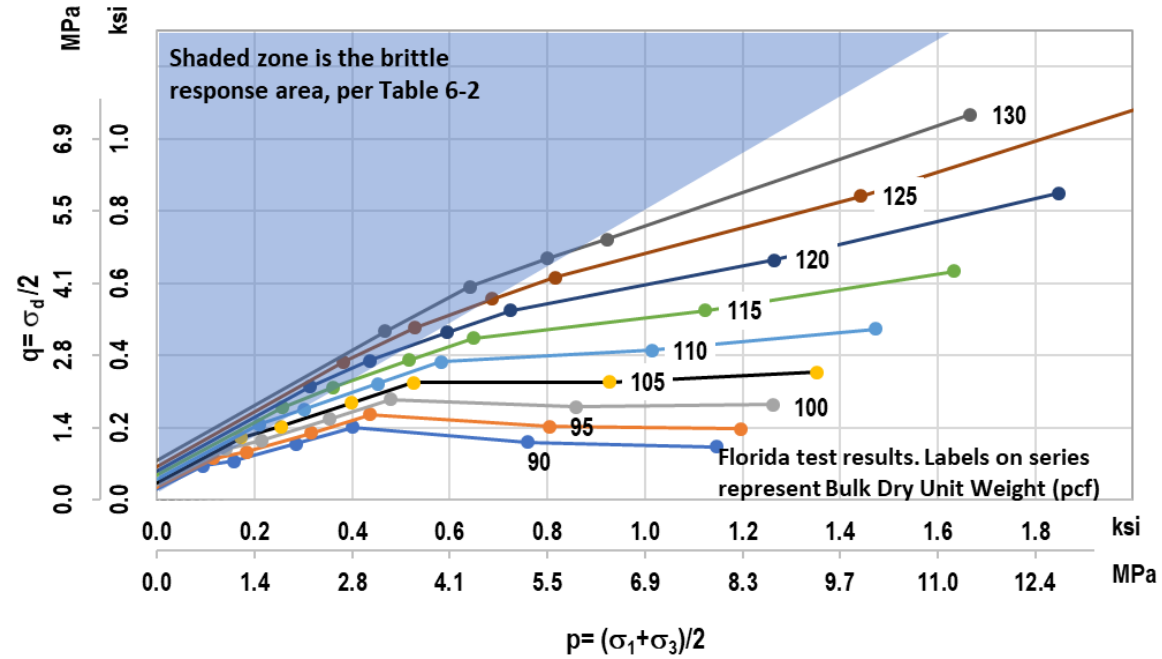

Figure 6-24. Strength envelope – Miami formation

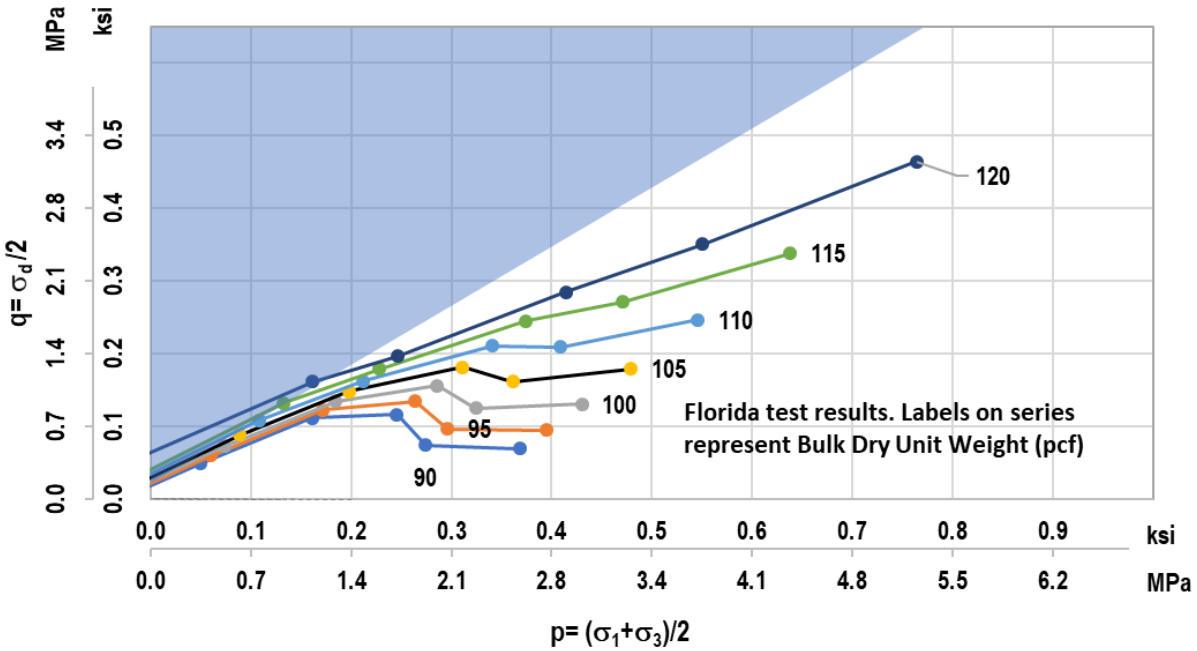

Figure 6-25. Strength envelope – Shallow Ft. Thompson formation

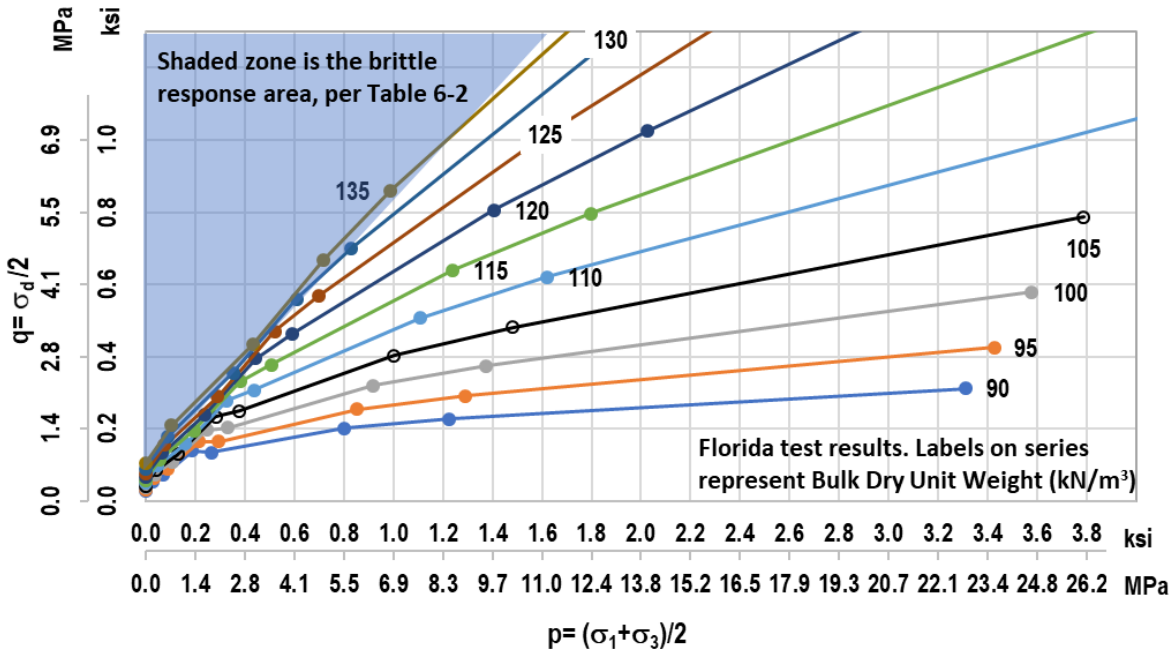

Figure 6-26. Strength envelope – Hawthorn formation

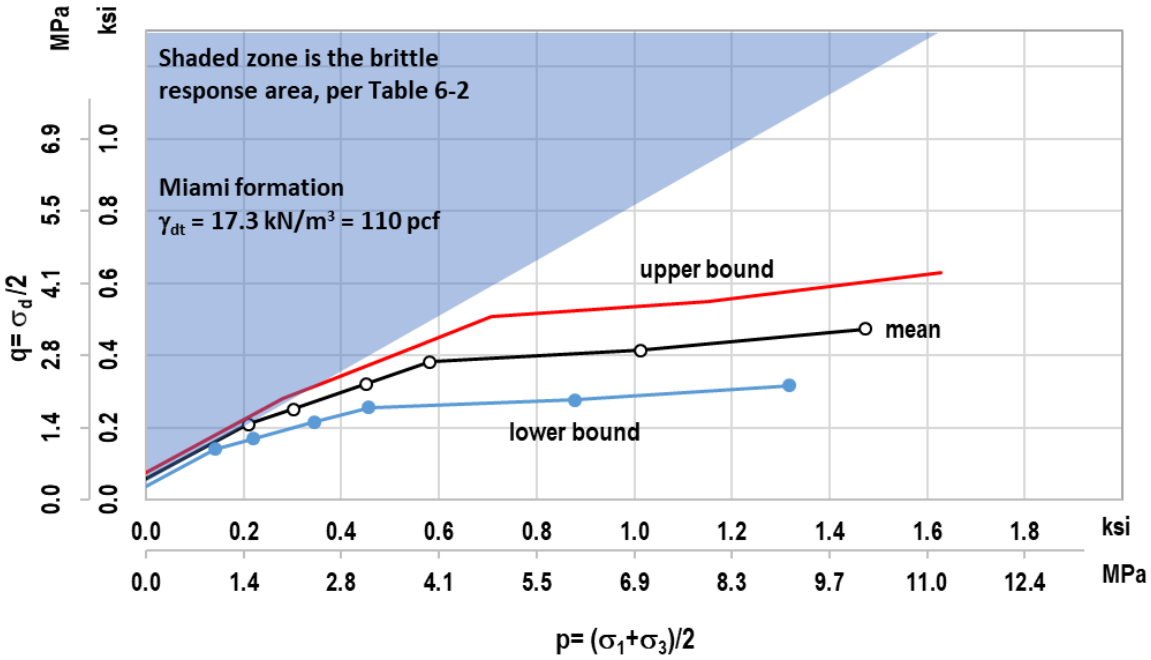

Figure 6-27. Example of lower bound and upper bound of intact rock strength envelope

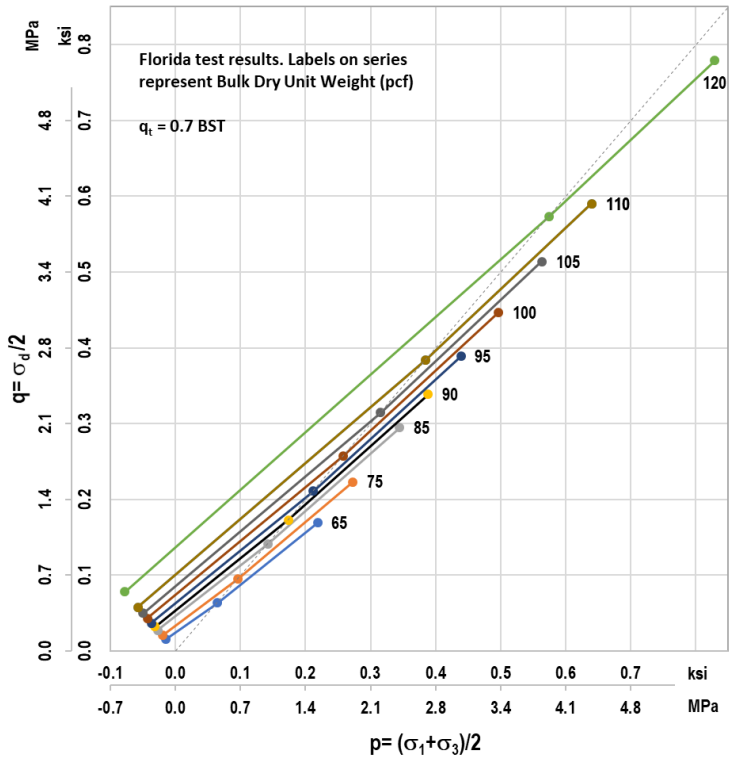

a)

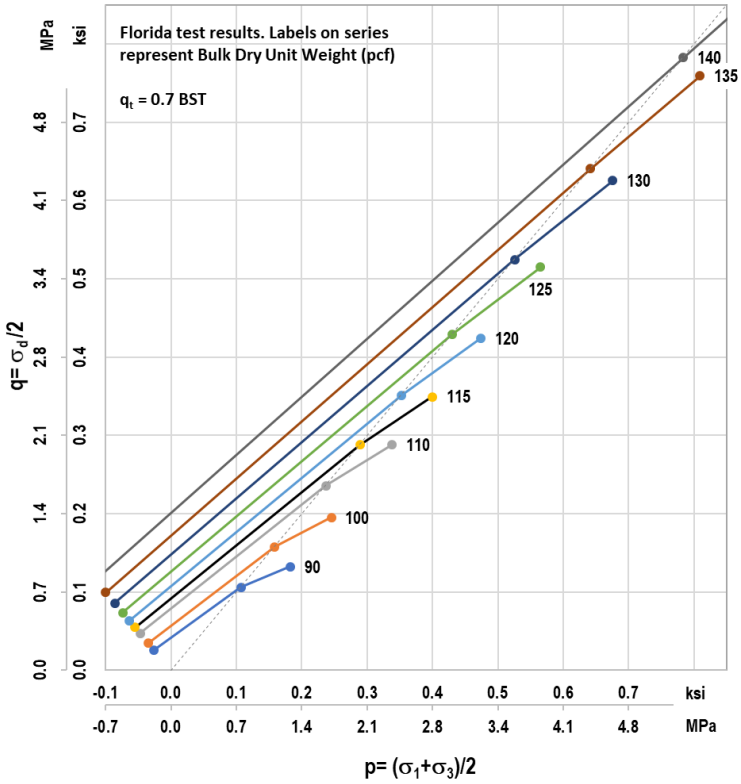

b)

Figure 6-28. Verification for using 0.7BST as q_t value: a) Key Largo formation, b) Anastasia formation

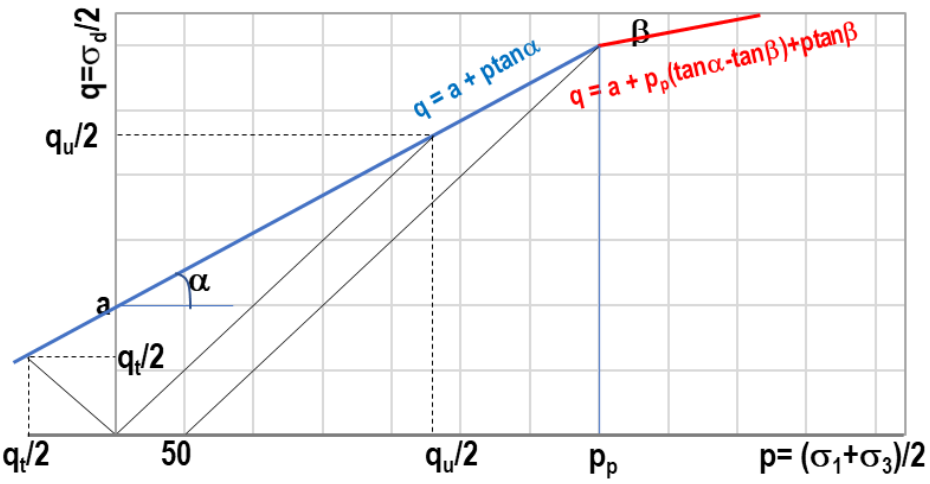

Figure 6-29. Schematic of bilinear strength envelope for intact rock

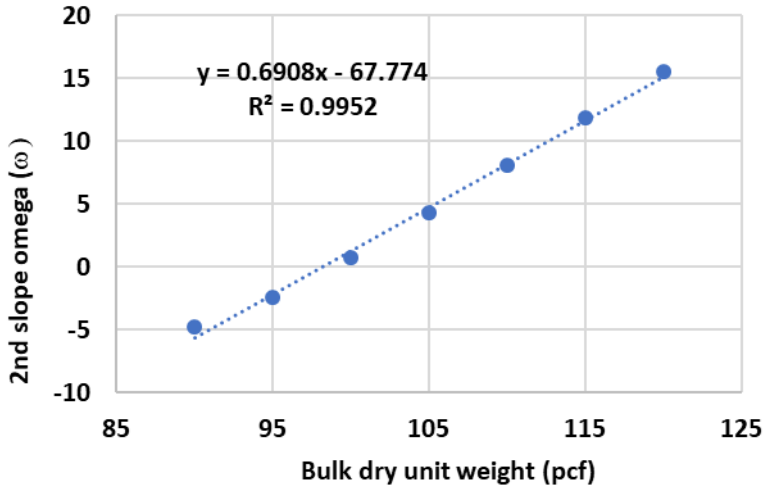

Figure 6-30. 2nd slope ω correlation – Key Largo formation

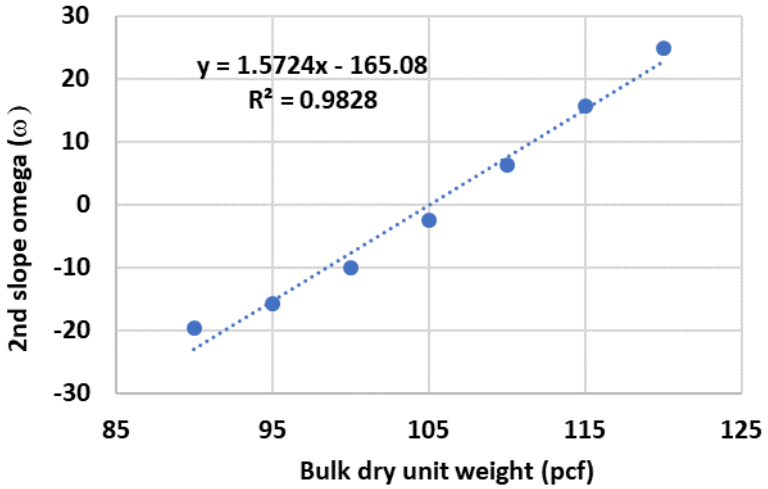

Figure 6-31. 2nd slope ω correlation – Shallow Ft. Thompson formation

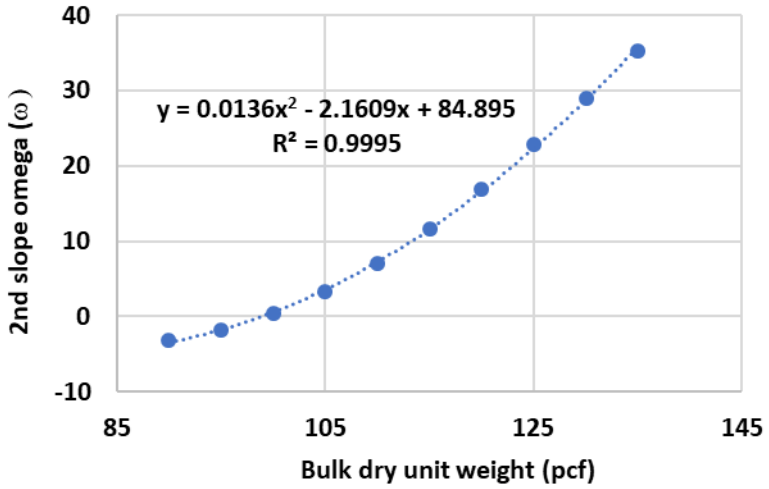

Figure 6-32. 2nd slope ω correlation – Miami formation

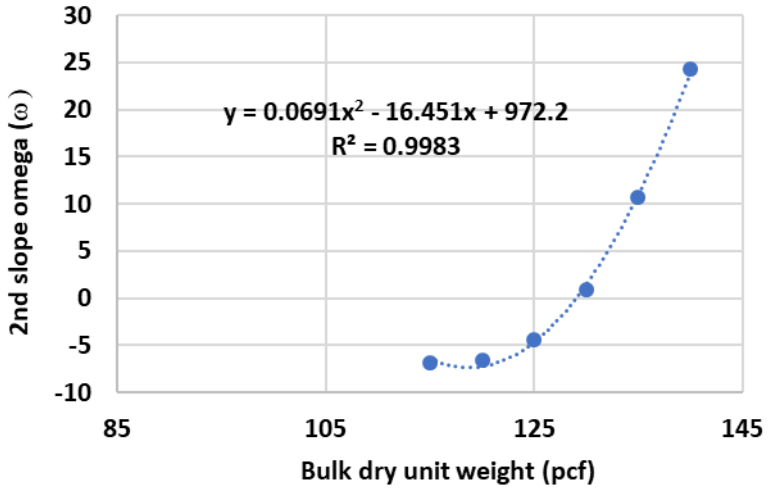

Figure 6-33. 2nd slope ω correlation – Anastasia formation

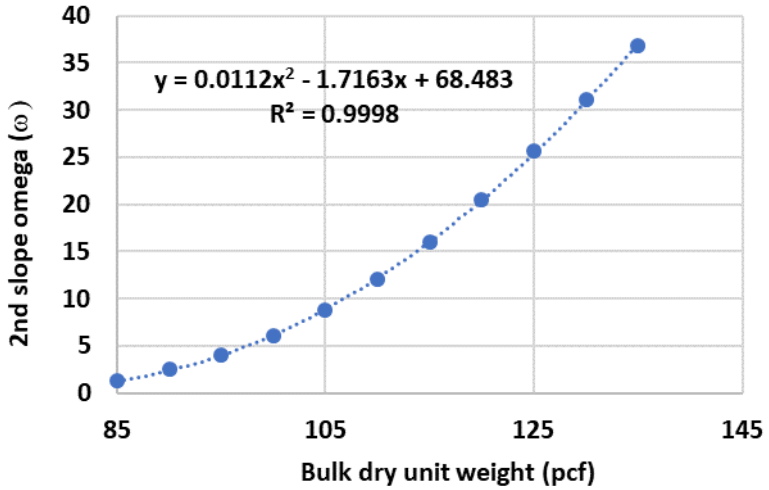

Figure 6-34. 2nd slope ω correlation – Hawthorn formation

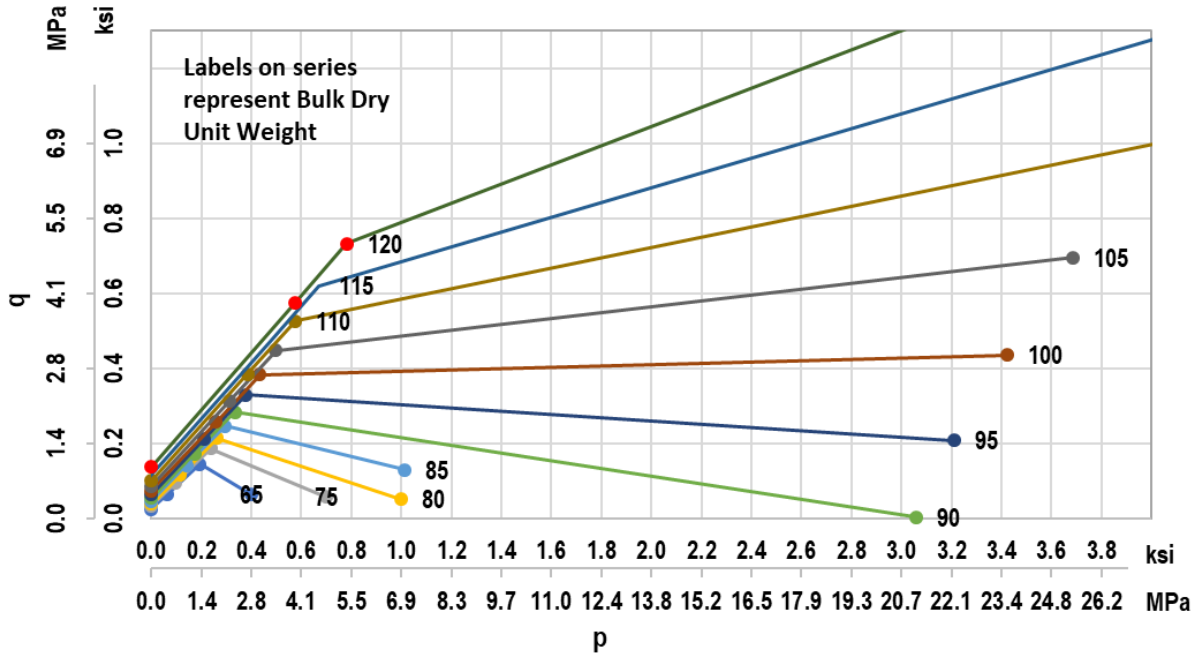

Figure 6-35. Bilinear strength envelope – Key Largo formation

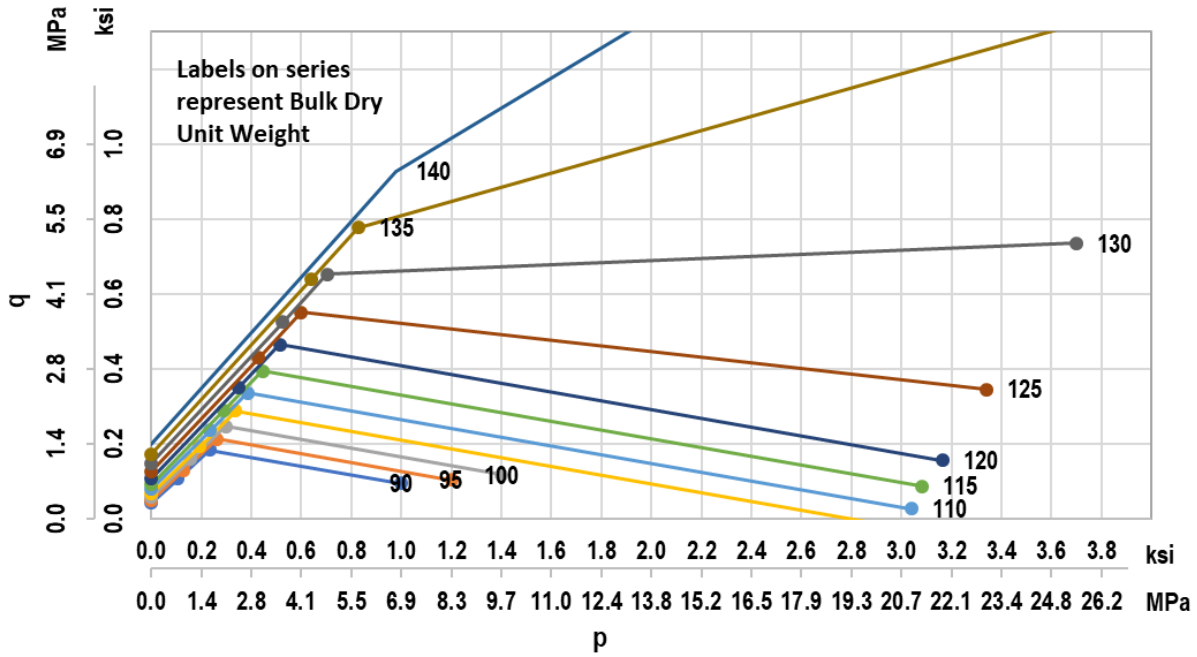

Figure 6-36. Bilinear strength envelope – Anastasia formation

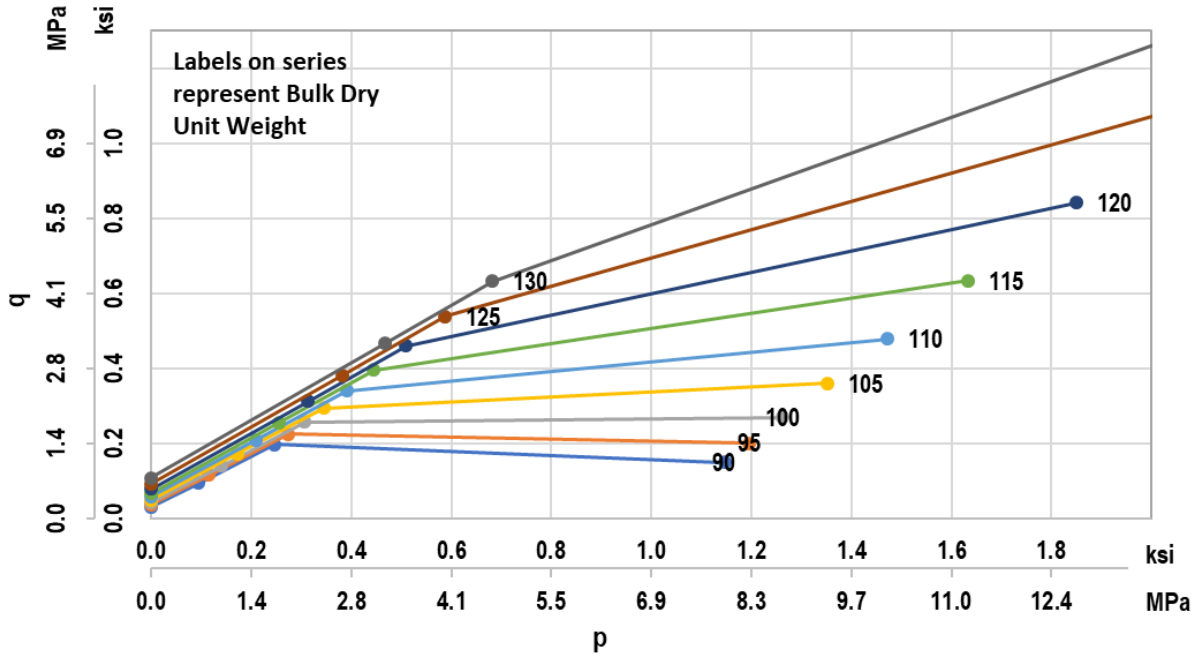

Figure 6-37. Bilinear strength envelope – Miami formation

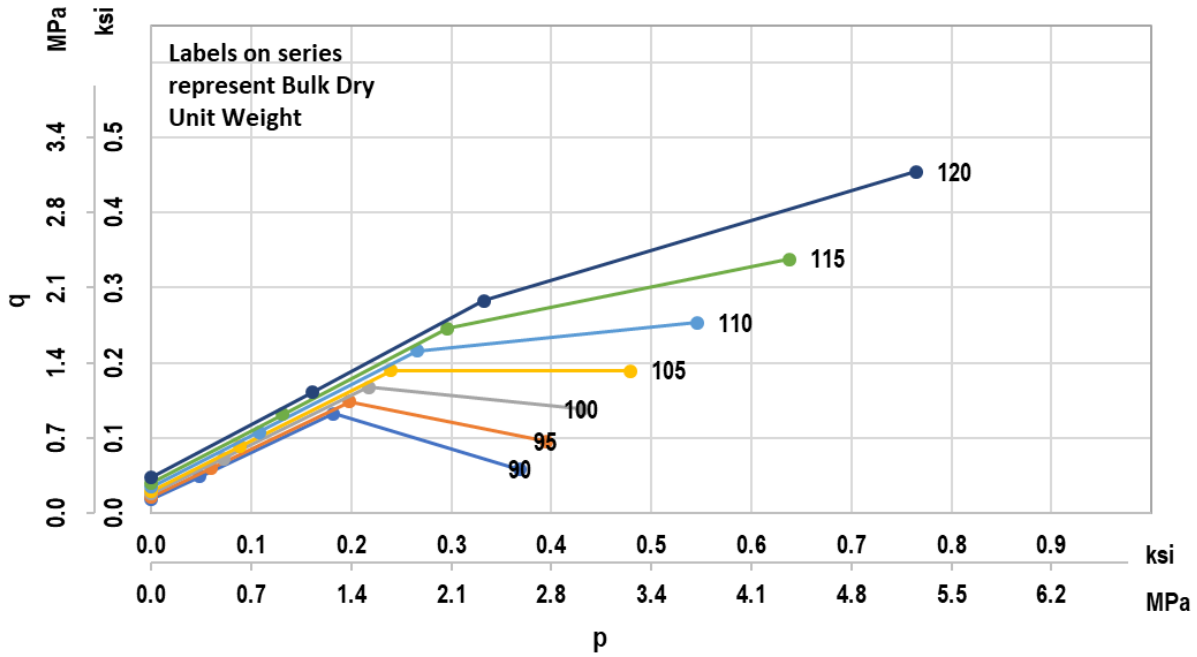

Figure 6-38. Bilinear strength envelope – Shallow Ft Thompson formation

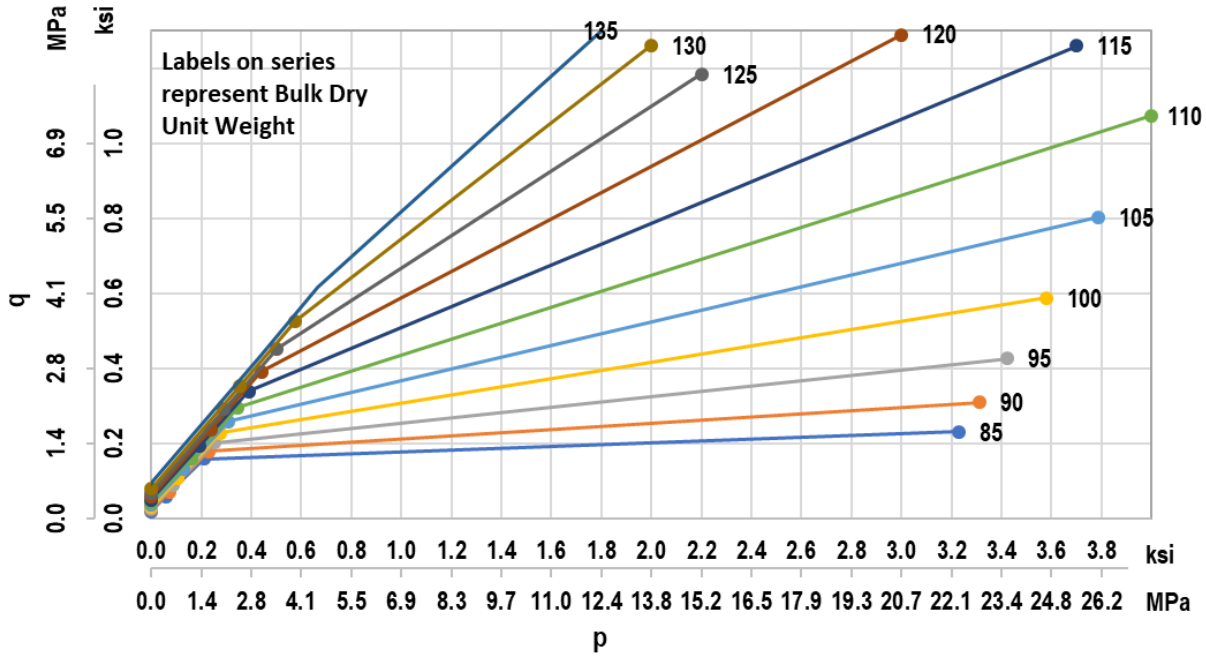

Figure 6-39. Bilinear strength envelope – Hawthorn formation

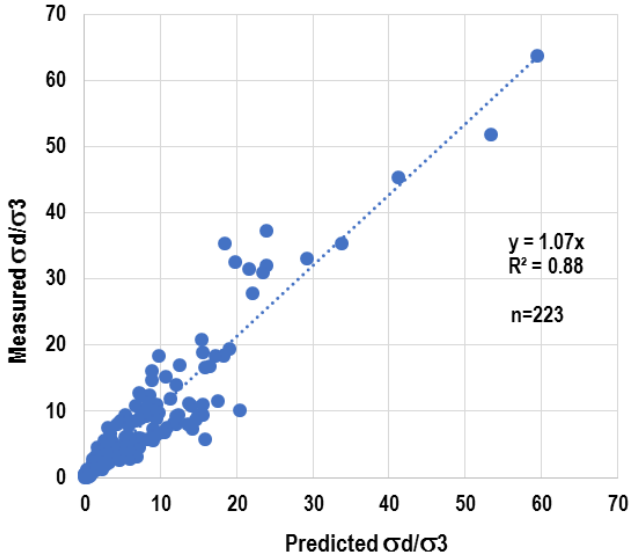

Figure 6-40. Scatter of predicted normalized stresses back-calculated from bilinear envelopes

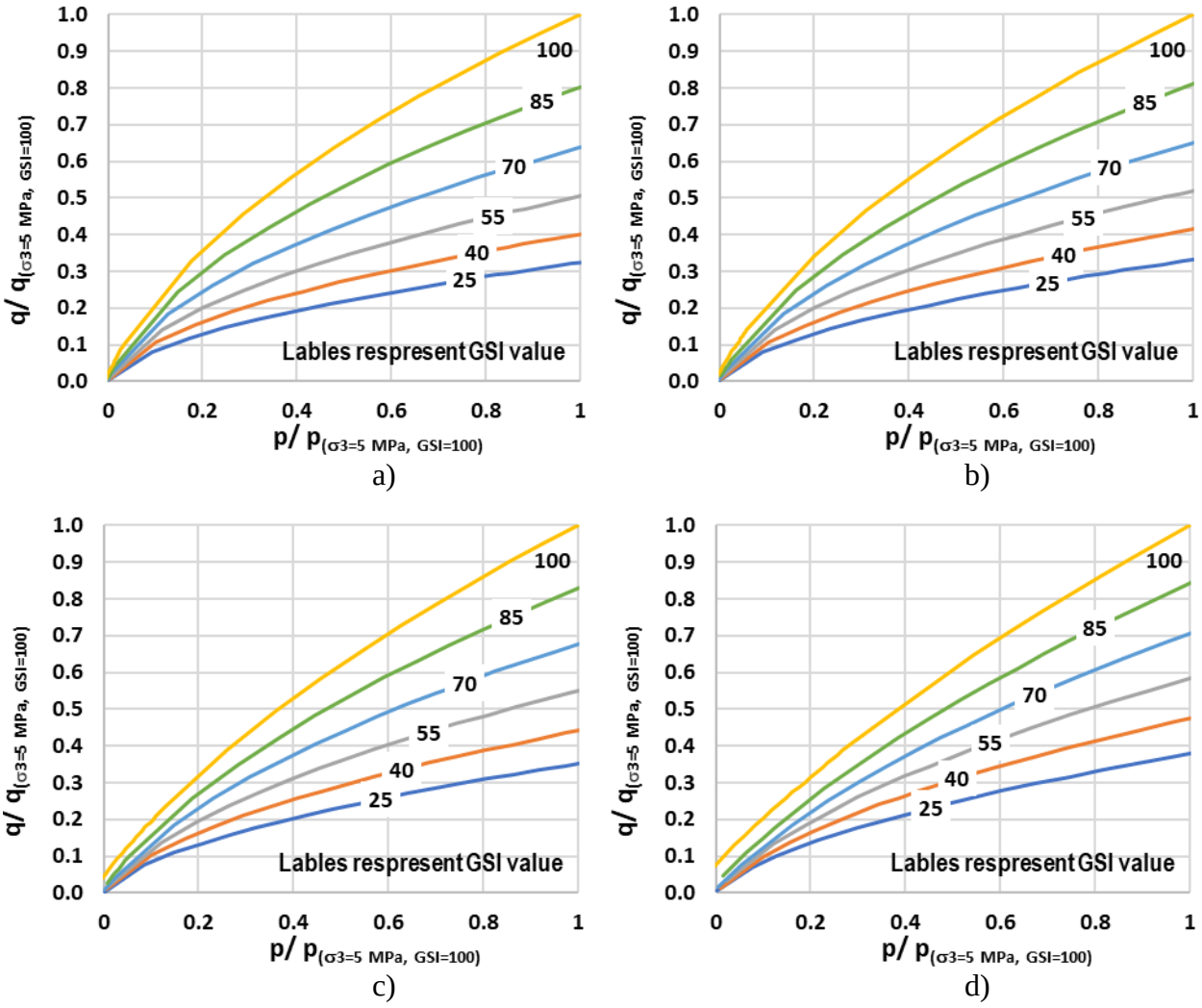

Figure 6-41. Rock mass strength envelopes in relative to intact rock strength envelope: a) q_u = 0.5 MPa, b) q_u = 1 MPa, c) q_u = 3 MPa, d) q_u = 10 MPa

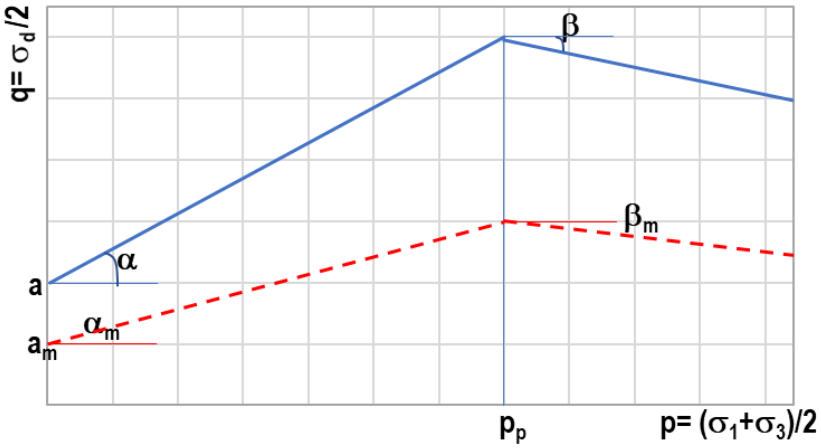

Figure 6-42. Bilinear strength envelope for rock mass from intact rock

CHAPTER 7
CONCLUSIONS AND RECOMMENDATIONS

Florida carbonate-rock strengths are very low: Most of the BST values are less than 1.7 MPa (250 psi, Chapter 5) while most of the q_u values are less than 9 MPa (1.3 ksi, Chapter 5), with q_u median value of only 3 MPa (435 psi, Chapter 5). Cohesive IGM is defined by FHWA as material that exhibits unconfined compressive strengths in the range of 0.5 to 5 MPa (70 to 700 psi). Thus, about 65% of the carbonate-rocks tested in historical FDOT database would be classified as IGM. The carbonate-rocks in other regions reported in literature are typically much stronger, with q_u = 70 to 340 MPa (10 to 50 ksi), including the rocks cited in the development of strength envelops by Hoek-Brown (1980, 1988) and Johnston (1985). The low strengths of Florida carbonate-rocks require unique study and correlations – presented in this study.

There are existing standard test methods for the evaluation of apparent rock index properties (e.g., ASTM D4673 or AASHTO T-85) and standard test methods for the evaluation of specimen solid specific gravity (e.g., ASTM D854 or AASHTO T-100). These standard test methods, however, do not differentiate the proportions of vug and permeable porosities, which are important index parameters for Florida rocks. Based on combinations of these standard test methods, Eqs. 3-7 to 3-9 (Chapter 3) have been derived to differentiate different proportions of porosities:

Impermeable porosity: $n_i = \gamma_{dt}(1/\gamma_{sa} - 1/\gamma_{st})$ (3-7)

Permeable porosity: $n_p = \gamma_{dt}(1/\gamma_{da} - 1/\gamma_{sa})$ (3-8)

Vug porosity: $n_v = 1 - \gamma_{dt}/\gamma_{da}$ (3-9)

where the apparent properties (γ_{sa} and γ_{da}) are obtained from ASTM D4673 or AASHTO T-85 test method, the solid unit weight (γ_t) is obtained from ASTM D854 or AASHTO T-100

test method on rock powder, and the bulk dry unit weight (γ_{dt}) is simply oven-dried weight divided by the cylindrical volume of the specimen.

There is no consistent grading scale in literature to identify a rock as vuggy or porous as each author consider rock as “porous” or “highly porous” at different porosities. Furthermore, there is no grading scale for rock to be described as “slightly vuggy” or “vuggy”. Therefore, Table 3-2 in Chapter 3 is proposed to describe the rocks based on magnitudes of different porosities.

Results from Chapter 4 indicates that rocks in Florida are highly heterogeneous, containing a wide range of bulk dry unit weights (or porosities) within one rock layer. The median porosity of Florida rocks is approximately 37%. In correlating the Florida carbonate-rock strengths, the key parameter is porosity, $n = 1 - \gamma_{dt}/(GS * \gamma_w)$. As GS is relatively a constant, for a given bulk dry unit weight, the porosity, n, fluctuates within a typical margin of 3% depending on value of GS. For example, $\gamma_{dt} = 15.7$ kN/m^3 = 100 pcf, then n could vary from 0.405 to 0.418, or 40.5% to 41.8% when GS = 2.69 to 2.75. GS for rock is difficult to measure while γ_{dt} is very simple to obtain. Therefore, the key parameter to correlate the Florida rock strength is its bulk dry unit weight γ_{dt}.

The BST can be roughly estimated using Eq. 5-1 in Chapter 5, repeated as follows:

$$\text{BST (psi)} = 3.864\, e^{0.03\gamma_{dt} B} \qquad (5\text{-}1)$$

However, Florida rock strengths are highly dependence on rock formations. A more reliable estimate of BST based on two additional parameters - formation factor, F_t, and carbonate content, C, is proposed:

$$\text{BST (psi)} = 2.468\, F_t\, e^{0.03\,\gamma_{dt} B}\, e^{0.5C} \qquad (5\text{-}6)$$

where,

C is the carbonate content, typically ranging from 0.5 to 1.0 (i.e., 50% to 100%), and $e^{0.5C}$ would be 1.28 to 1.65. For C < 0.5, it is considered as soil and is not applicable for this purpose.

F_t is the formation factor, which is influenced by the rock formation identification, which is dependent on the vug or permeable porosity ratio (in relative to the bulk porosity). F_t are referenced in Table 5-1 or Figure 5-9 for rocks in this study. For other Florida formations not included in this study, F_t can be evaluated by using Eq. 5-2.

It is noted that when C = 89.5% and F_t = 1, which are the typical average value for carbonate content and formation factor of Florida rocks, respectively, then Eq. 5-6 turns into Eq. 5-1.

The unconfined compression strength q_u can be estimated using Eq. 5-7 or 5-17 depending on what rock index parameter is available. Eq. 5-17 is based on three index rock parameters; thus, the correlation has better coefficient of correlation than Eq. 5-7:

$$q_u \text{ (psi)} = 5.89\, e^{0.04\, \gamma_{dt}\, B} \tag{5-7}$$

$$q_u \text{ (psi)} = 3.24\, F_u\, e^{0.04\, \gamma_{dt}\, B}\, e^{2C/3} \tag{5-17}$$

The relationship between q_u and BST is:

$$q_u \text{ (psi)} = 0.97 * BST^{4/3} \tag{5-8}$$

The inversion of this relationship is:

$$BST \text{ (psi)} = 1.03 * q_u^{3/4} \tag{5-9}$$

It is demonstrated in Chapter 6 that when the unconfined compression strength, q_u, is higher than 9 MPa (1.3 ksi), the material typically exhibits brittle stress-strain behavior for shallow foundation loading conditions. In this case, the well-known Hoek-Brown criterion, developed for

brittle rupture failure, is applicable. However, most of the porous Florida carbonate-rocks have weaker strengths with ductile stress-strain response, associated with contractive volumetric behavior. The σ_d/σ_3 threshold for the material to transition from brittle to ductile responses have been expanded beyond the conventional ductile pressure range (i.e., toward the minimal confining pressure range), presented in Table 6-2. Accordingly, the strength envelopes for these materials are sloping downward at a much steeper rate than those in the brittle zone. Moreover, the envelopes vary between formations, due to different cementations (different minerals, carbonate contents, and rock grain sizes) as well as different proportions of void structures (vug, permeable, and impermeable voids). Consequently, it is recommended that different Florida carbonate-rock formations have their own prior established strength envelopes based on dry unit weights (Figure 6-22 to Figure 6-26). For finite element method application, simplified bilinear strength envelopes can be used, with four parameters defining each bilinear envelope: cementation c, initial friction angle φ, onset of non-linear stress-strain (which is simplified to a linear line) p_p, and 2nd slope of the bilinear envelope ω. The equations are shown in Eqs. 6-25 to 6-27 with presentations in Figure 6-35 to Figure 6-39. Appendix F describes a procedure to establish a rock strength envelope for a typical design project. Furthermore, it is not recommended to reduce the strength envelope of Florida carbonate-rocks using the GSI index since it is not readily available. Pending further study, a provisional procedure is recommended to develop Florida rock mass strength envelope from the intact strength envelope, weighted-average value for dry unit weight, and rock recovery ratio (REC).

APPENDIX A
ROCK CORE DESCRIPTIONS

This appendix presents the detailed rock core descriptions for 6 sites that were investigated for shallow foundation considerations. At the other sites, where the rocks were obtained for deep foundation design, only rock results (i.e., BST, q_u, and triaxial results) are collected without detail rock core descriptions.

At site 1 near a wet retention pond of the I-75/ I-595 clover-leaf interchange in Davie, the consultant Professional Service Industries, Inc. (PSI) obtained the cores typically from a depth of 3 to 18 feet below ground surface. On the geological surface map, the site lies near the boundary of Miami limestone formation (Qm) and Fort Thompson formation, which is a subset of the Okeechobee shelly sediments group (Tqsu). Typically, the boundary area is where the subsurface is unpredictable and has great lateral variation due to geological formation changes. The consultant identified the acquired rocks as Fort Thompson. The recovery was poor to decent (typically 40% to 80%) and RQD was very poor to decent (typically 0% to 60%). Visually, the rocks are relatively smooth, a few rock cores have minor vugs. Overall, the rocks are relatively friable and weakly cemented.

At site 2 of SW 13th Street underpass in Miami, the consultant HR obtained the cores from typically depths of 3 to 28 feet below ground surface. On the geological surface map, the site is within the Miami formation (Qm). The recovery was very poor to good (typically 0% to 80%) with typically very poor RQD (typically less than 20%). Most of the recovered rocks were broken in pieces indicating very poor cementation.

Site 3 is near one end bent of the SR-80 bridge to Bingham Island in West Palm Beach. On the geological surface map, the site is within the Anastasia formation (Qa). The recovery was

excellent (close to 100%) with decent to excellent RQD (typically 70% to 80%). Visually, the rock specimens compose of cemented shell fossils (calcarenite to coquina) with no vugs.

At site 4 near one end bent of the SR-5 over Marvin Adams Waterway in Key Largo, the consultant HR Engineering Services, Inc. (HR) obtained the cores from typically depths of 3 to 28 feet below ground surface. On the geological surface map, the site is within the Key Largo formation (Qk). The recovery was good to excellent (60% to 100%) with variable RQD (0% to 100%) – the RQD was typically worse with deeper depths. Overall, the rocks are very porous and light weight.

At site 5 of SR 836 Extension near NW 12 Street in Miami, the consultant HR obtained the cores from typically depths of 8 to 33 feet below ground surface. On the geological surface map, the site is within the Miami formation (Qm). The recovery was average to excellent (typically 50% to 90%) with very poor to average RQD (typically 0% to 50%). The rock texture varies greatly from very vuggy to relatively smooth limestone.

At site 6 of SR 997 (Krome Avenue) over a man-made canal in Miami, the consultant HR obtained the cores from typically depths of 3 to 28 feet below ground surface. On the geological surface map, the site is within the Miami formation (Qm). The recovery was very poor near the ground surface (less than 40%), then approached excellent (near 100%) at deeper depths. Similarly, the RQD was very poor (0%) near the ground surface, then become average to good (50% to 80%) at deeper depths. Similar to site #5, the rock texture varies greatly from very vuggy to relatively smooth limestone.

APPENDIX B
ROCK CORE PICTURES

Figure A-1. Site 1, Bore hole RC-1

Figure A-2. Site 1, Bore hole RC-2

Figure A-3. Site 1, Bore hole RC-3

Figure A-4. Site 1, Bore hole RC-4

Figure A-5. Site 1, Bore hole RC-5

Figure A-6. Site 1, Bore hole RC-6

Figure A-7. Site 1, Bore hole RC-7

Figure A-8. Site 2, Bore hole RC-1

Figure A-9. Site 2, Bore hole RC-2

Figure A-10. Site 2, Bore hole RC-3

Figure A-11. Site 2, Bore hole RC-4

Figure A-12. Site 3, Bore hole RC-1

Figure A-13. Site 3, Bore hole RC-2

Figure A-14. Site 3, Bore hole RC-3

Figure A-15. Site 4, Bore hole RC-1

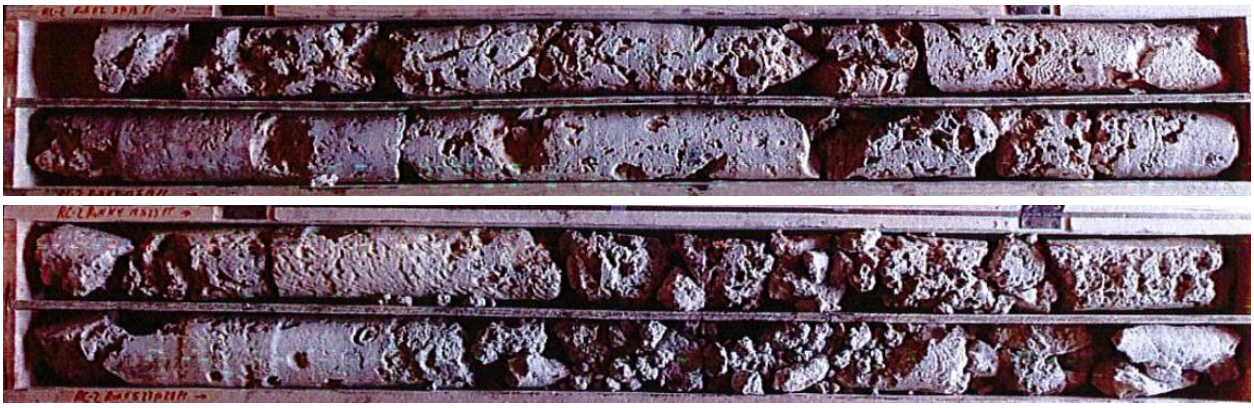

Figure A-16. Site 4, Bore hole RC-2

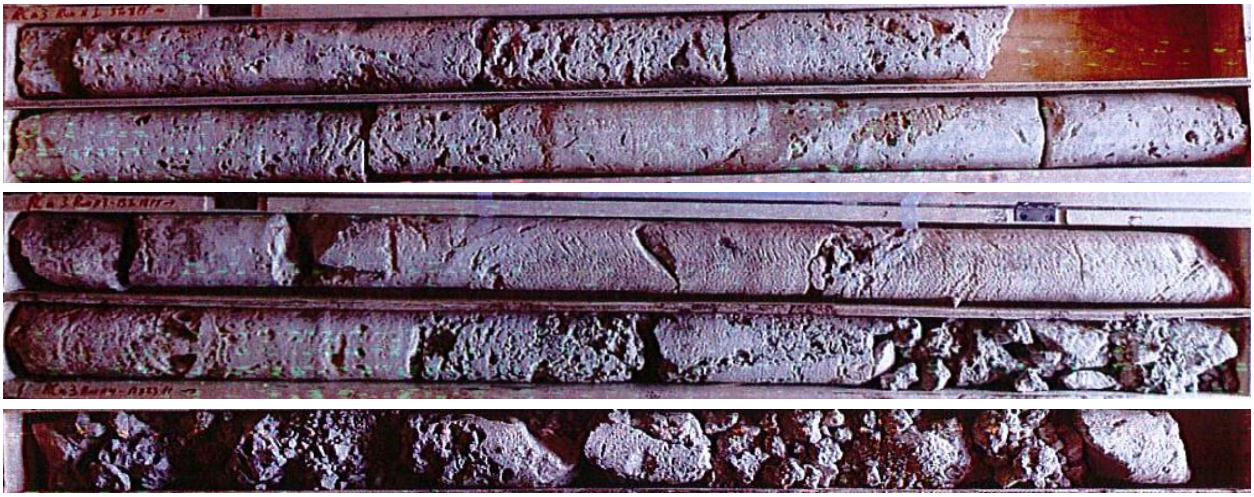

Figure A-17. Site 4, Bore hole RC-3

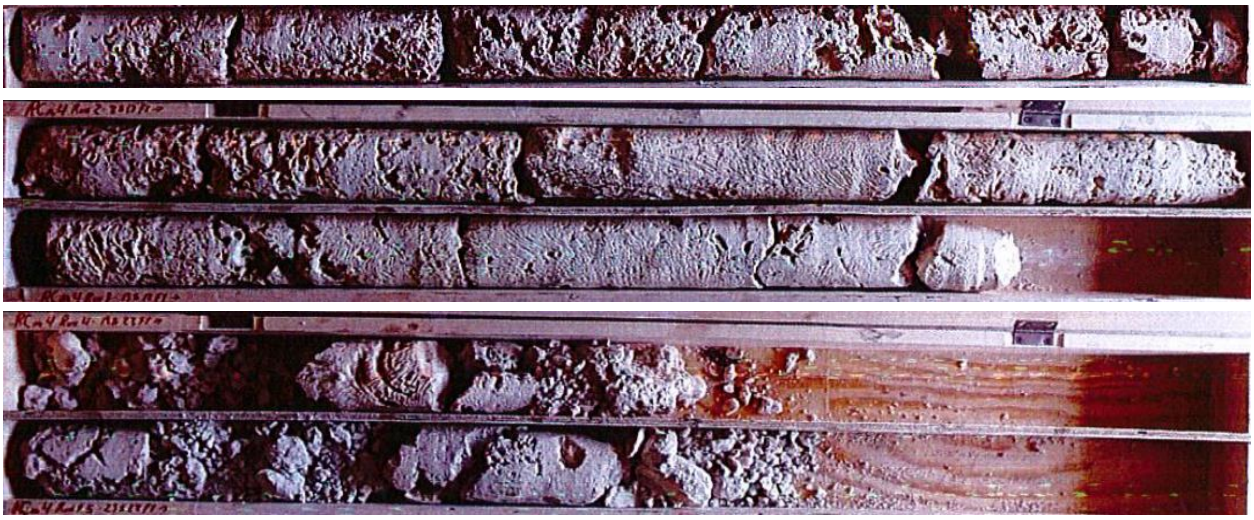

Figure A-18. Site 4, Bore hole RC-4

Figure A-19. Site 5, Bore hole RC-1

Figure A-20. Site 5, Bore hole RC-2

Figure A-21. Site 5, Bore hole RC-3

Figure A-22. Site 5, Bore hole RC-4

Figure A-23. Site 6, Bore hole RC-1

Figure A-24. Site 6, Bore hole RC-2

Figure A-25. Site 6, Bore hole RC-3

Figure A-26. Site 6, Bore hole RC-4

APPENDIX C
ROCK TRIAXIAL TEST PROCEDURE

C.1 Sigma-1 Features

The triaxial test can be terminated upon reaching any of the following action:

1. the button “END TEST” is manually clicked,
2. or the platen reaches its limit (per internal optical encoder),
3. or the load-cell reaches its limit (40,000 lbs, which is the limit of the frame even though the load-cell is rated for 50,000 lbs),
4. or the DCDT reaches its end of travel (maximum travel is 3 inches),
5. or the vertical strain ε reaches its shear strain limit, typically set at 3.5%.
6. or the stress drops by a user input threshold, typically 30% stress.

There are 2 different data recording modes:

1. Data acquisition mode: data is recorded into a with file name “*.dat” whenever “new task” submenu is clicked. The data is recorded per time schedule, for example 1 read per every 10 seconds, regardless of whether the actual triaxial test is being run or not.
2. Triaxial test mode: data is recorded into a with file name “*.trx” only when the “START TEST" button is clicked. The data is recorded per strain schedule, for example 1 read per every axial strain of 0.01%.

The hand-pump, shown in Figure C-1, is fitted with 2 valves. Valve 1 on the side of the pump is a one-way valve: when closed, Valve 1 only closes oil from coming back into the pump, but still allows oil to travel one-way from the pump out. Therefore, the seal on pump 1 is not 100% seal. Therefore, when there is no need to hand-pump, then valve 2 would be closed to prevent oil leaks back to the pump.

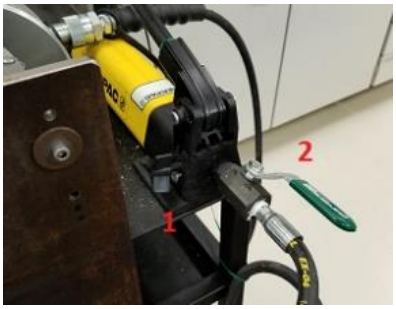

Figure C-1. Hand pump valves

C.2 Sample Preparation

1. Determine specimen dimensions and weight prior to test.
2. Insert rock sample into Hoek-cell with the cell laying horizontal on the working cart.
3. When inserting sample, or removing sample from Hoek-cell, make sure to have the oil not trapped by opening both Valves 1 and 2 of hand-pump.
4. Place bottom steel platen into Hoek-cell
5. Stand the Hoek-cell upright on its bottom platen
6. Place top steel platen into the cell
7. Using "Load Control" tab (Figure C-2.a), make the Load-Cell to contact the top platen for a seating load of about 10 to 20 lbs. Be sure to re-center the Hoek cell before contact.
8. While the loading frame is in the process of moving to automatically reach that 20 lbs of seating load, type in the specimen data, using Menu File – Specimen Data (Figure C-2.b). Specify a maximum strain rate of 3.5% for the Deviatoric (shear) loading phase (the software identifies the moment the "START TEST" is clicked as the start of the Deviatoric loading).
9. Close Valve 1 on hand-pump (Valve 2 still open).

a) 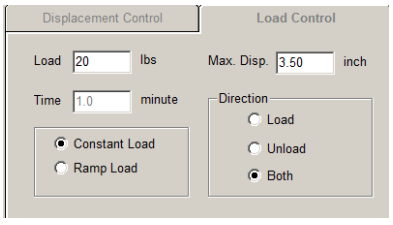

b) 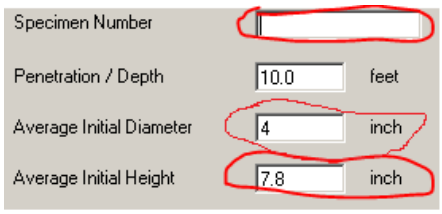

Figure C-2. Sample preparation screen: a) Load-control tab, b) Sample dimensions

C.3 Isotropic Loading to σ_{3max}

1. Prepare the DigiFlow pump (The pump total volume is 73 ml oil):

    c) Make sure the DigiFlow pump piston is at the bottom position (i.e., the DigiFlow is full of oil), otherwise it would not have enough oil to supply to Hoek cell during isotropic loading.

    d) If DigiFlow pump piston is not at the bottom position yet: Need to move the pump piston down by using "Volume Control" (Figure C-3) and move the piston down to the target of Volume = 1.0 mL. At the same time that the piston is moving down, make sure to use hand-pump to supply oil to the upper chamber of the DigiFlow pump, so that the cell or pump pressure to be between 1 to 5 psi while hand pumping

2. Close valve 2 on hand-pump. (Valve 1 was already closed earlier)

3. On DigiFlow, use "Pressure Control" tab, set DigiFlow pump = σ_{3max}

4. On Main window, use "Load Control" tab, set Load = Specimen Area (A) * $\boldsymbol{\sigma_{3max}}$ (example 2.38-in rock specimen, A = 4.45in^2)

5. Set Ramp Pressure and Ramp Load, both to same times as in Figure C-4.

6. Hit Start Pump for both the DigiFlow and Start for Load to increase. That way, the σ_3 (from Digiflow) and σ_1 (from loading frame) would gradually increase to the targets set above during the ramping time.

7. Once the σ_{3max} target has reached, the pressure would stay at σ_{3max}

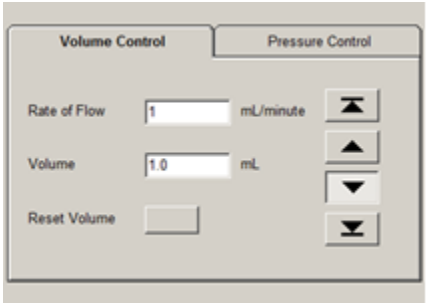

Figure C-3. Volume control tab

σ_{3max}	Target Ramp Time
50-100	2
100-200	3
200-500	5
500-1000	10
1000-1500	12-15

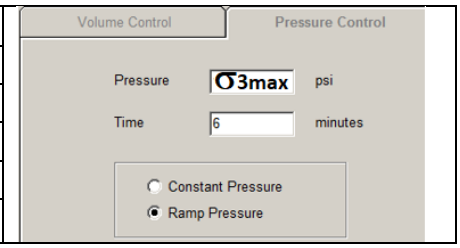

Figure C-4. Pressure ramp schedule

C.3 Deviatoric (Shear) Loading

1. Start the shearing process by hitting the "START TEST", the load frame would increase axial load beyond the load specifying in step 9 to begin the deviatoric loading.

2. Sometimes, the technician would have to interfere to end the test prematurely by hitting "Pause" button if:

   e) There is oil leak (for example, due to membrane is damaged)

   f) Or if the rock is too porous, and when it is crushed unevenly (only on 1 side of the specimen), the top platen may be excessively inclined.

3. The test would automatically "Paused" if a 30% drop in stress is detected, or if maximum strain (of 3.5%) has reached.

C.4 End Test

1. Hit End Test on the Load frame, also, Hit Stop on DigiFlow Pump so that it won't maintain the σ_{3max}

2. Unload to 0 lbs using Full Speed on the load frame

3. When load is about 0 lbs, there would be confining pressure left (possibly around 100 to 200 psi). Use "Pressure control" on the Digiflow pump to bring the pressure down to 1 psi.

4. Gradually opening Valves 2 and 1 on hand-pump to release pressure.

5. Remove rock specimen

6. Weight the specimen after test

7. Dry the specimen in oven, and determine dry weight.

APPENDIX D
PICTURES OF SPECIMENS AFTER TRIAXIAL TESTS

Many rock specimens had a number of inclusions within each piece, especially for some of the longer specimens which were up to 8 inches long. The shear failure surface then would typically go through the softest portion of the specimen – see Figure D-1 for some examples. As the dry unit weight of the softest portion of the specimen is typically lower than that of the denser portion of the specimen, shear strength correlations of the highly variable Florida rocks and IGM would naturally exhibit more scatter and poorer coefficient of determination R^2 than correlations of uniform rocks.

Most specimens would become stuck within the Hoek-cell membrane and require an extruder to push the specimens out after shearing. In that case, there would be many mechanical breaks in the specimens. A small number of specimens could be extruded by hand, and examples of the failure surfaces of those specimens are presented in Figure D-1 and Figure D-2.

Figure D-1. Rock at failure surface apparently weaker than overall rock specimen (Photo courtesy of Thai Nguyen)

Figure D-1. Continued

a) 

Figure D-2. Specimens tested at 130-psi chamber pressure: a) γ_{dt} > 130 pcf (Photo courtesy of Thai Nguyen)

b) 

c) 

Figure D-2. Continued: b) γ_{dt} = 120 - 130 pcf, c) γ_{dt} = 110 - 120 pcf

Figure D-3. Specimens deformed at 3000-psi chamber pressure (Photo courtesy of Thai Nguyen)

APPENDIX E
REPRESENTATIVE INDIVIDUAL TEST RESULTS

The following sign convention is used: compression is positive. Thus, the vertical strain, ε, is always positive, while the lateral strain ε_L is negative as the specimen diameter increases during triaxial shearing ($-\varepsilon_L$ is positive). The slope of the volumetric ε_v curve is positive when rock contracts and negative when rock dilates. Triaxial tests, whenever performed with a volume control device, are presented with ε_v results. In the beginning of the study, when the volume control device was not yet ready, no volumetric strain (ε_v) was recorded. However, as demonstrated in the study, an adequate number of specimens have later been tested for the generalization of the volumetric behavior of Florida carbonate-rocks.

Figure E-1. Test results at σ_3 = 3000 psi

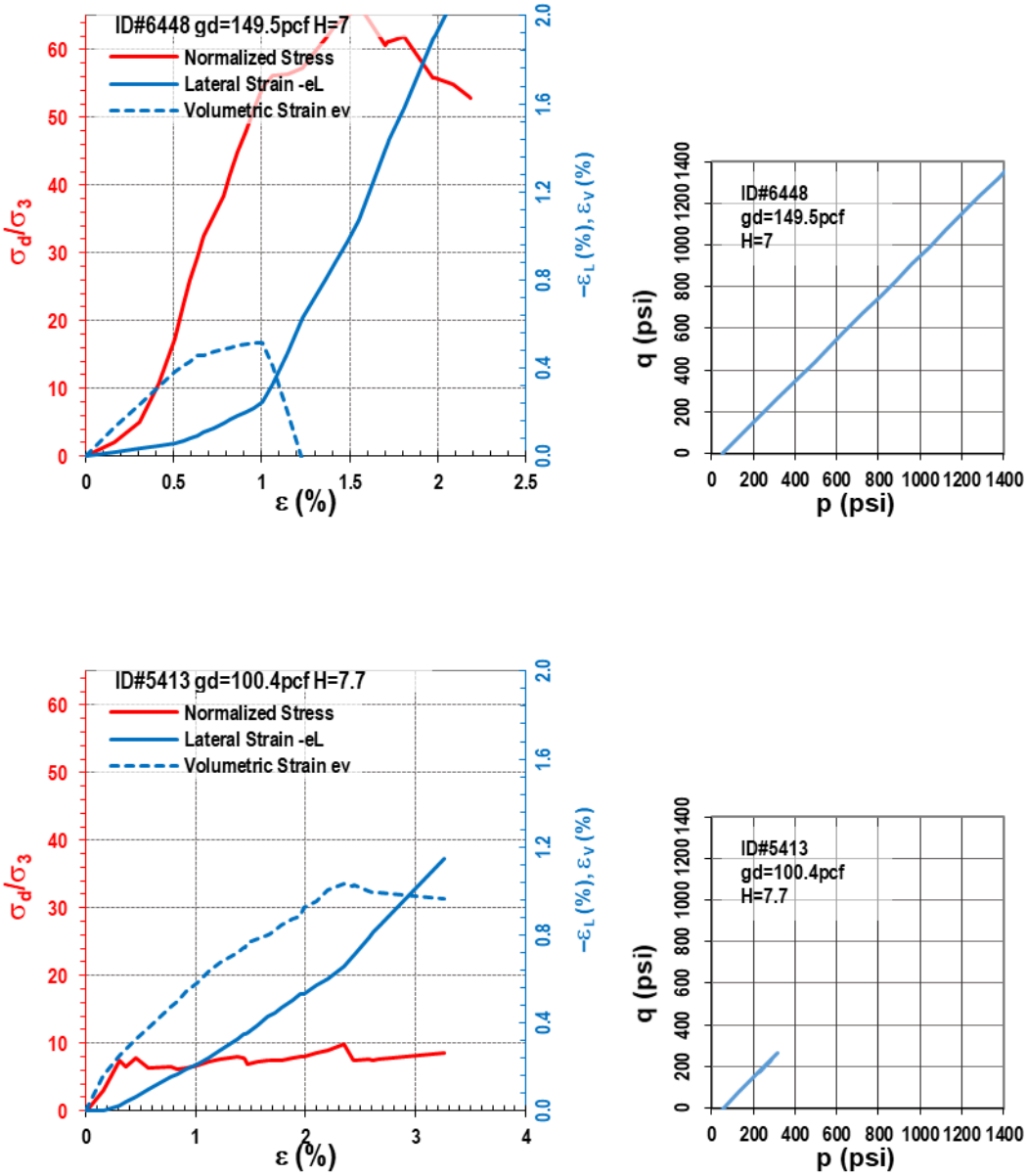

Figure E-2. Test results at σ_3 = 50 psi

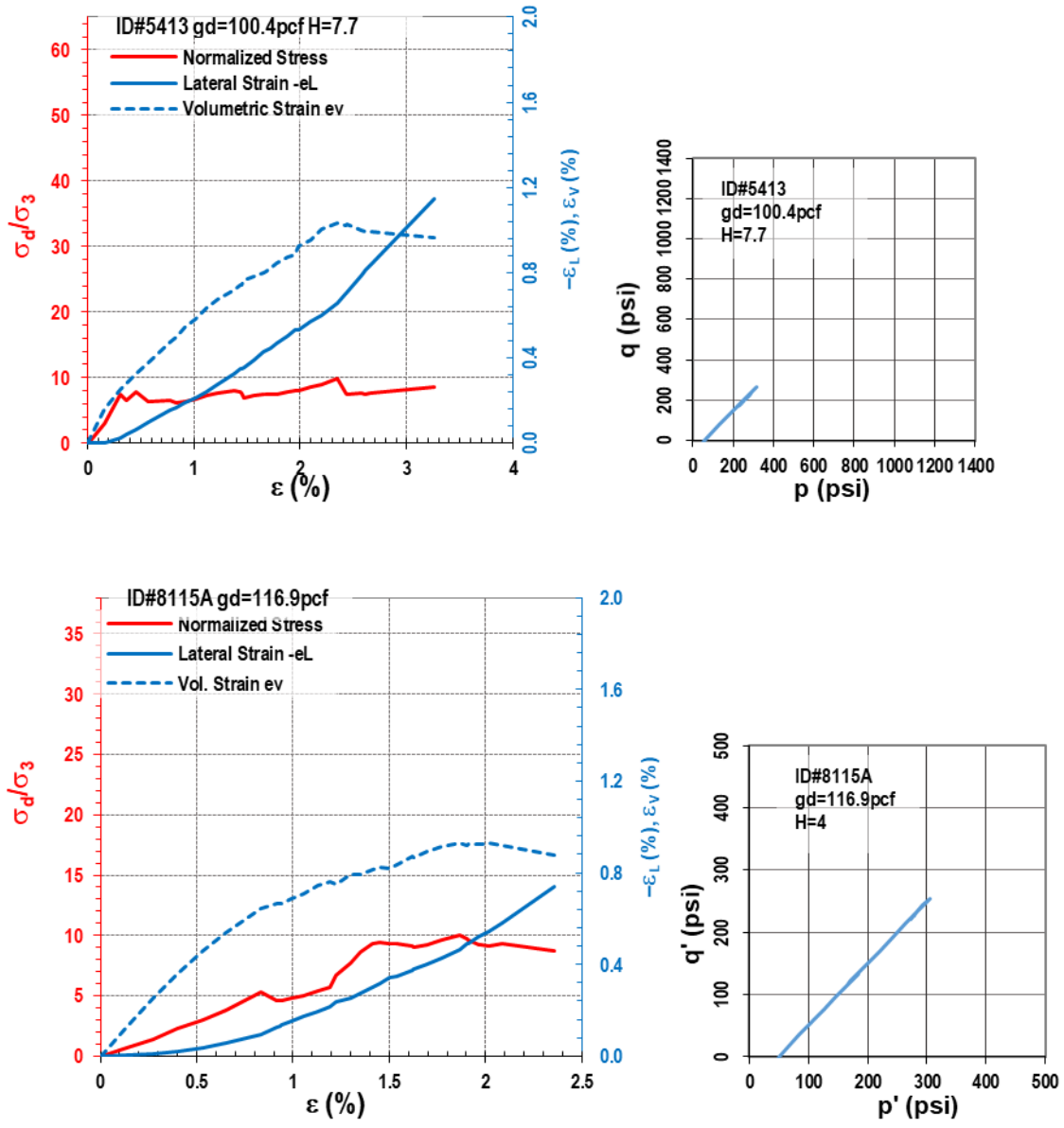

Figure E-2. Continued

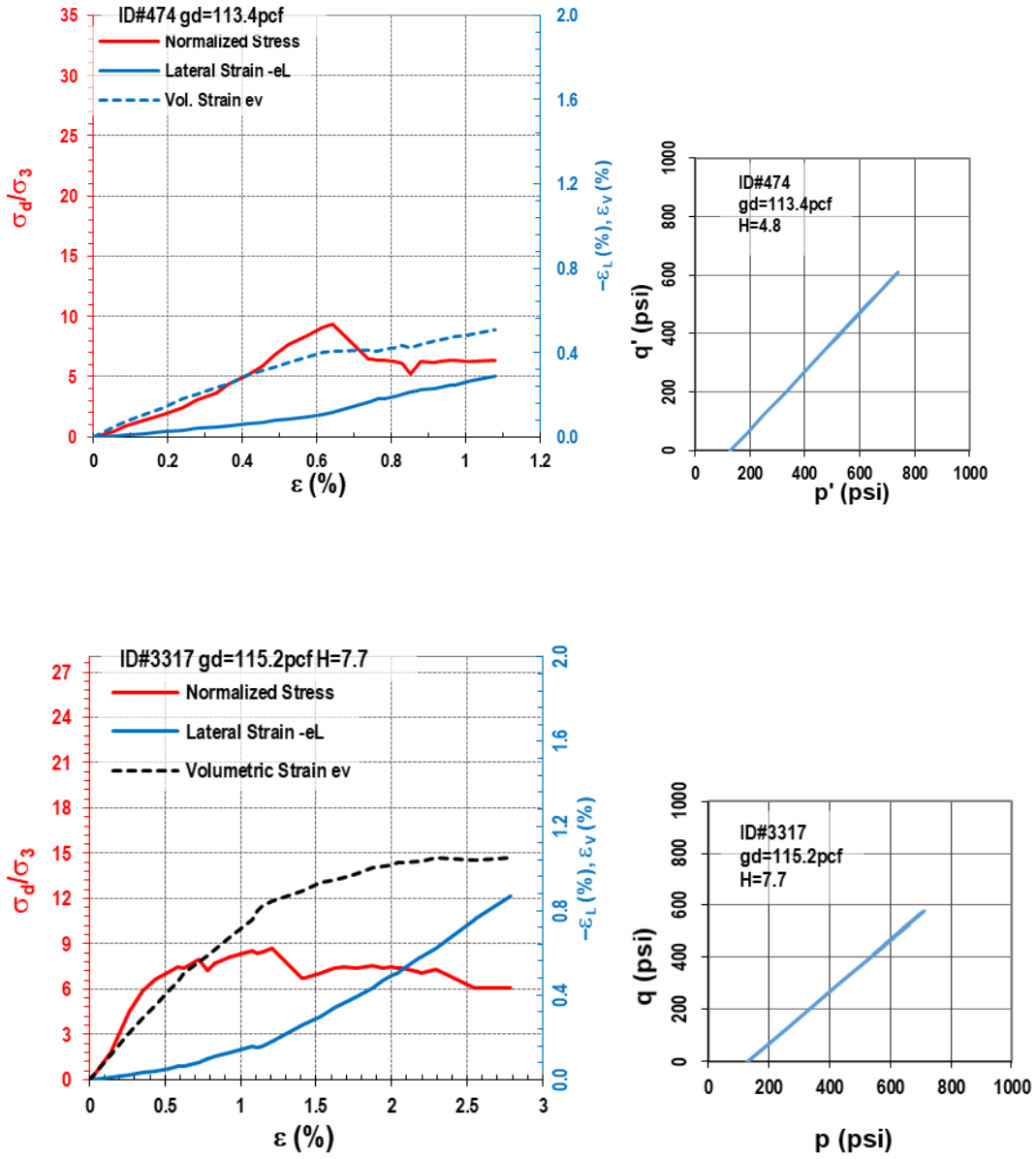

Figure E-3. Test results at σ_3 = 130 psi

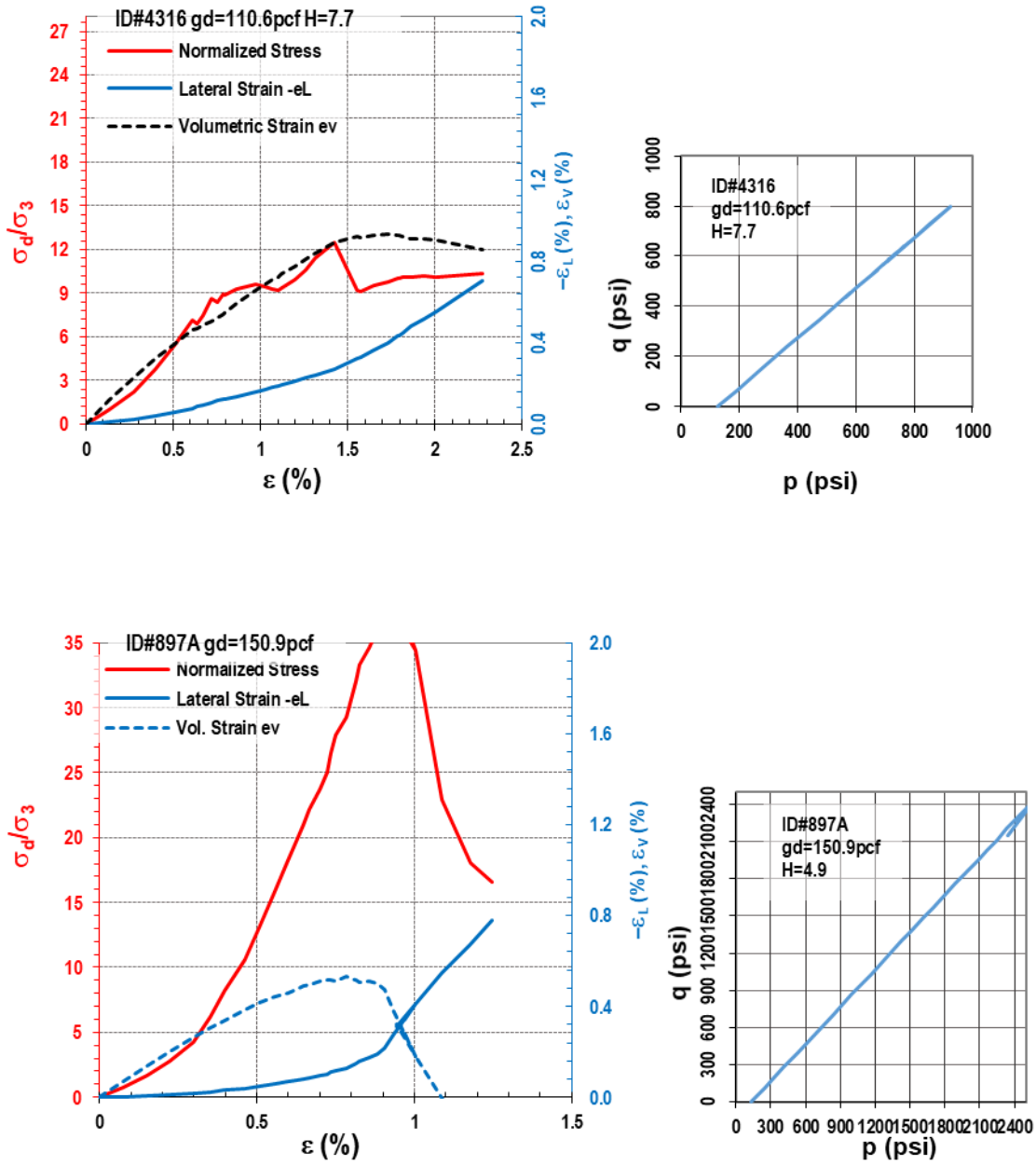

Figure E-3. Continued.

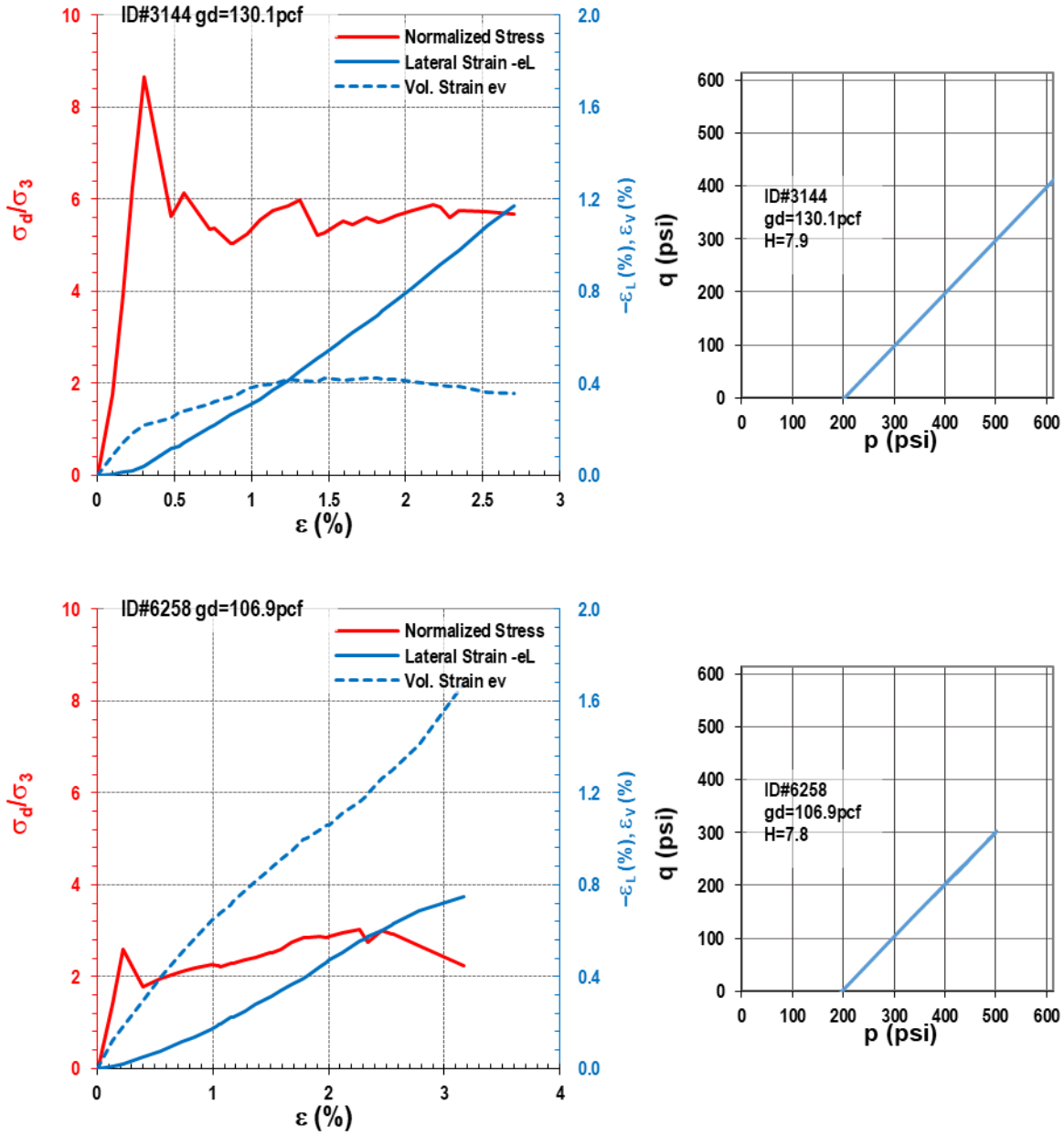

Figure E-4. Test results at σ_3 = 200 psi

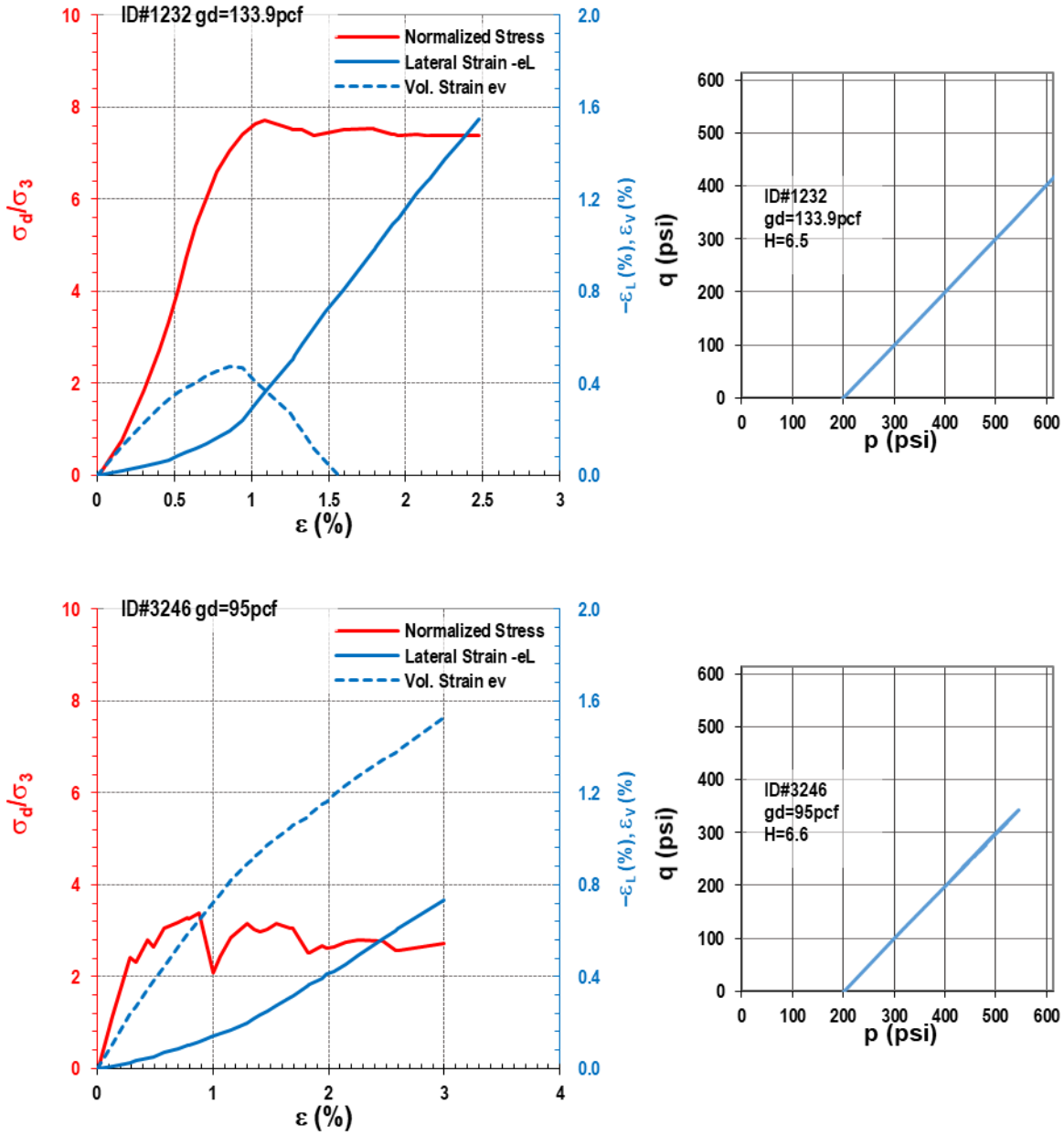

Figure E-4. Continued

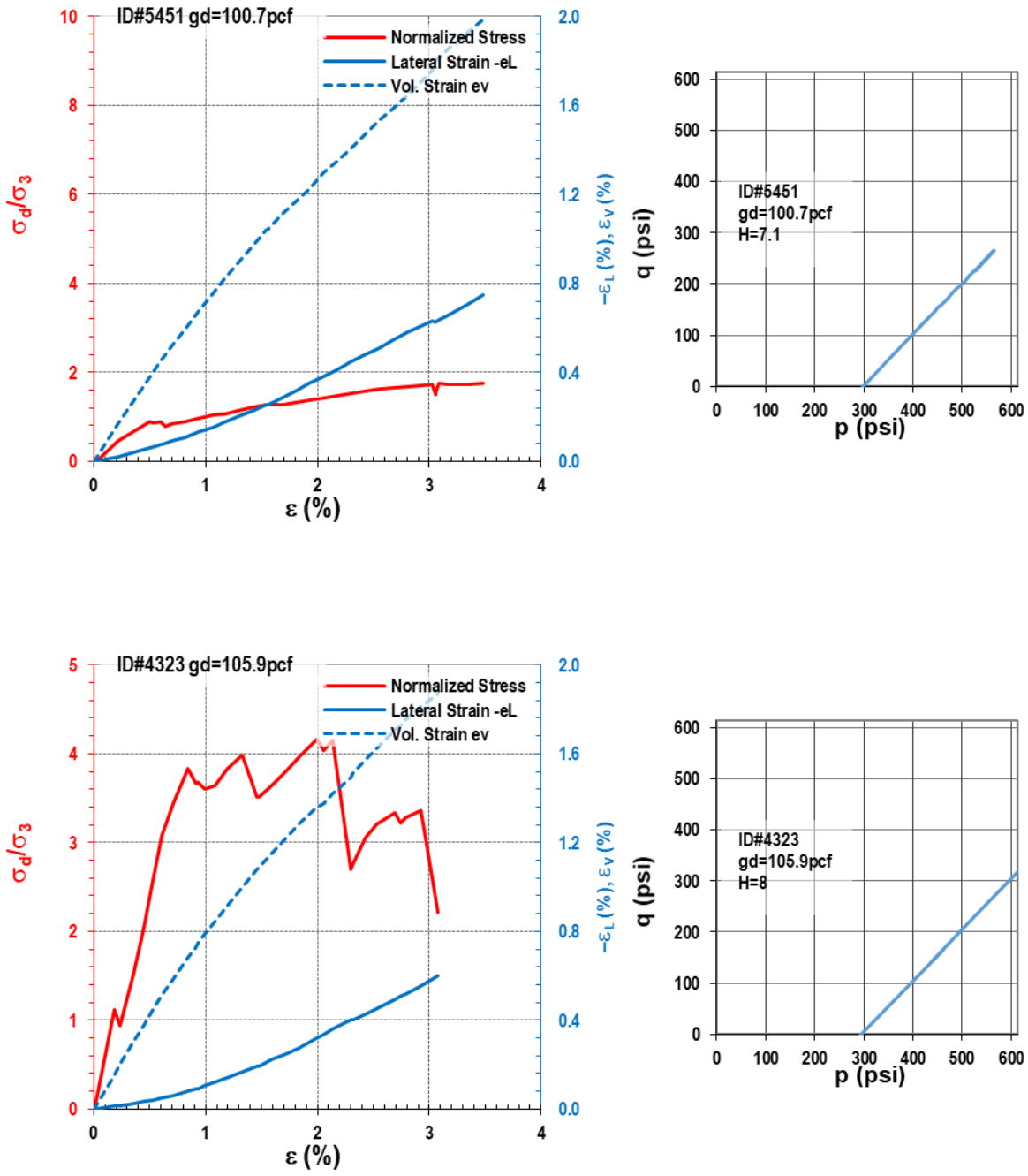

Figure E-5. Test results at σ_3 = 300 psi

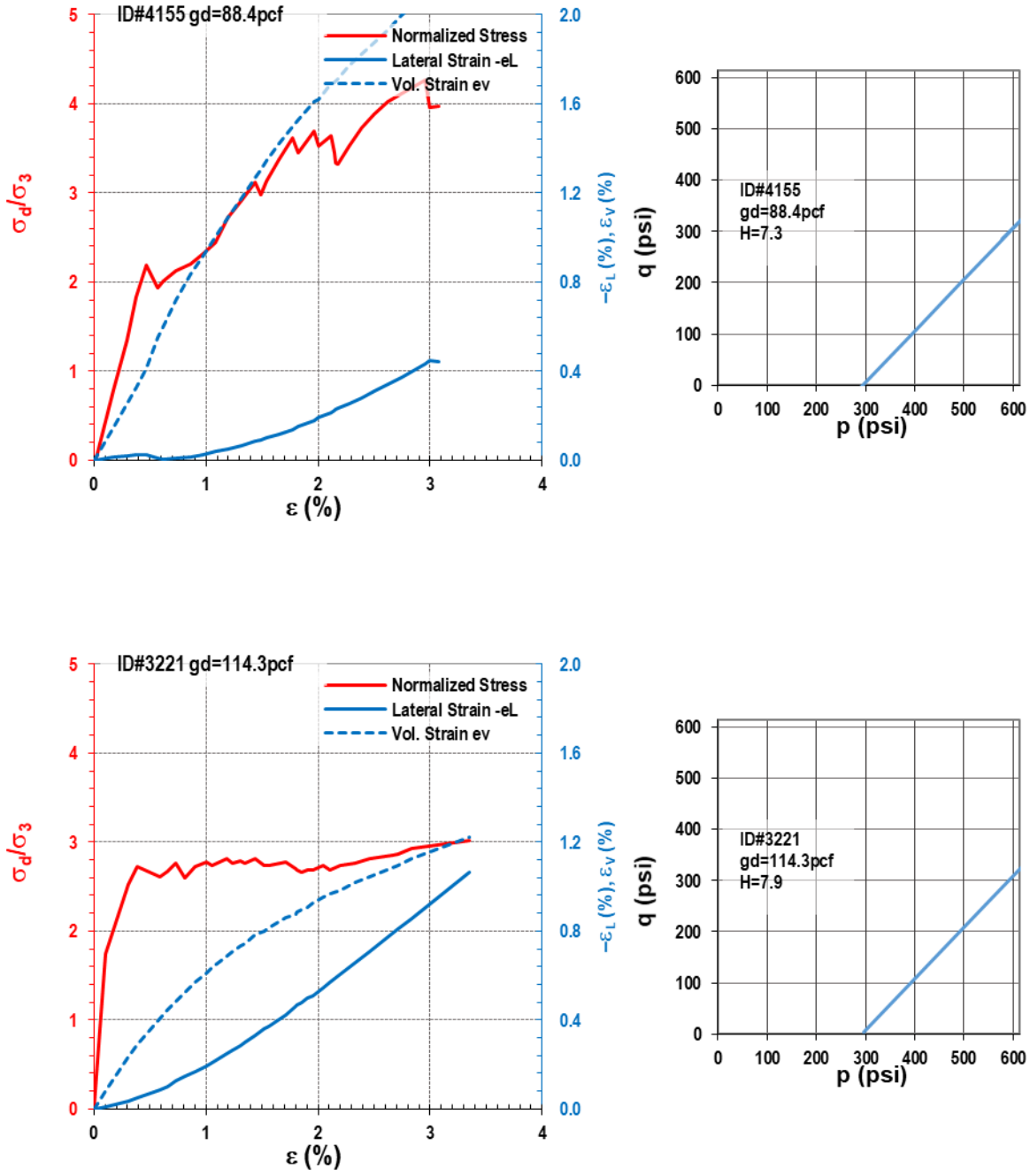

Figure E-5. Continued

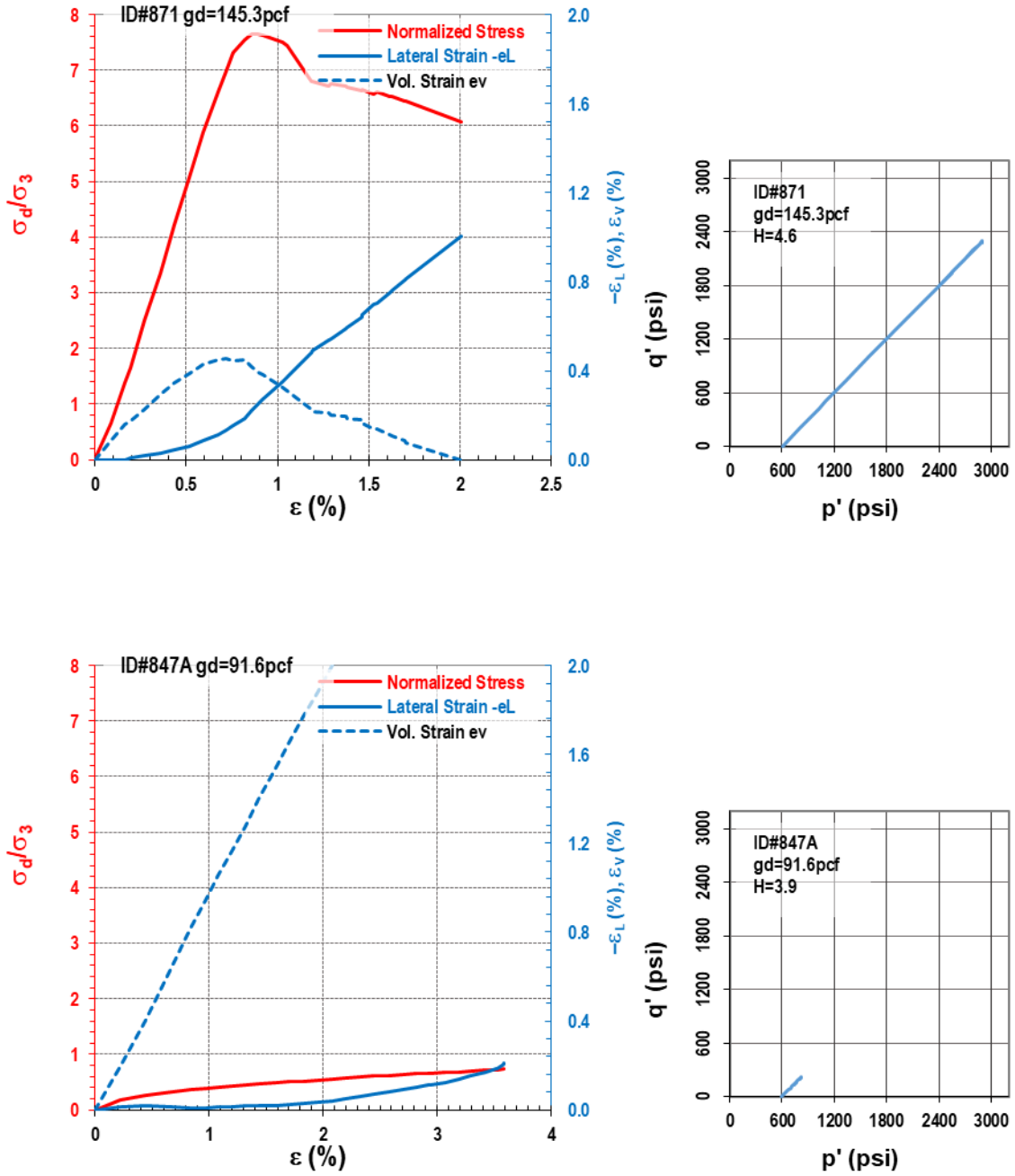

Figure E-6. Test results at σ_3 = 600 psi

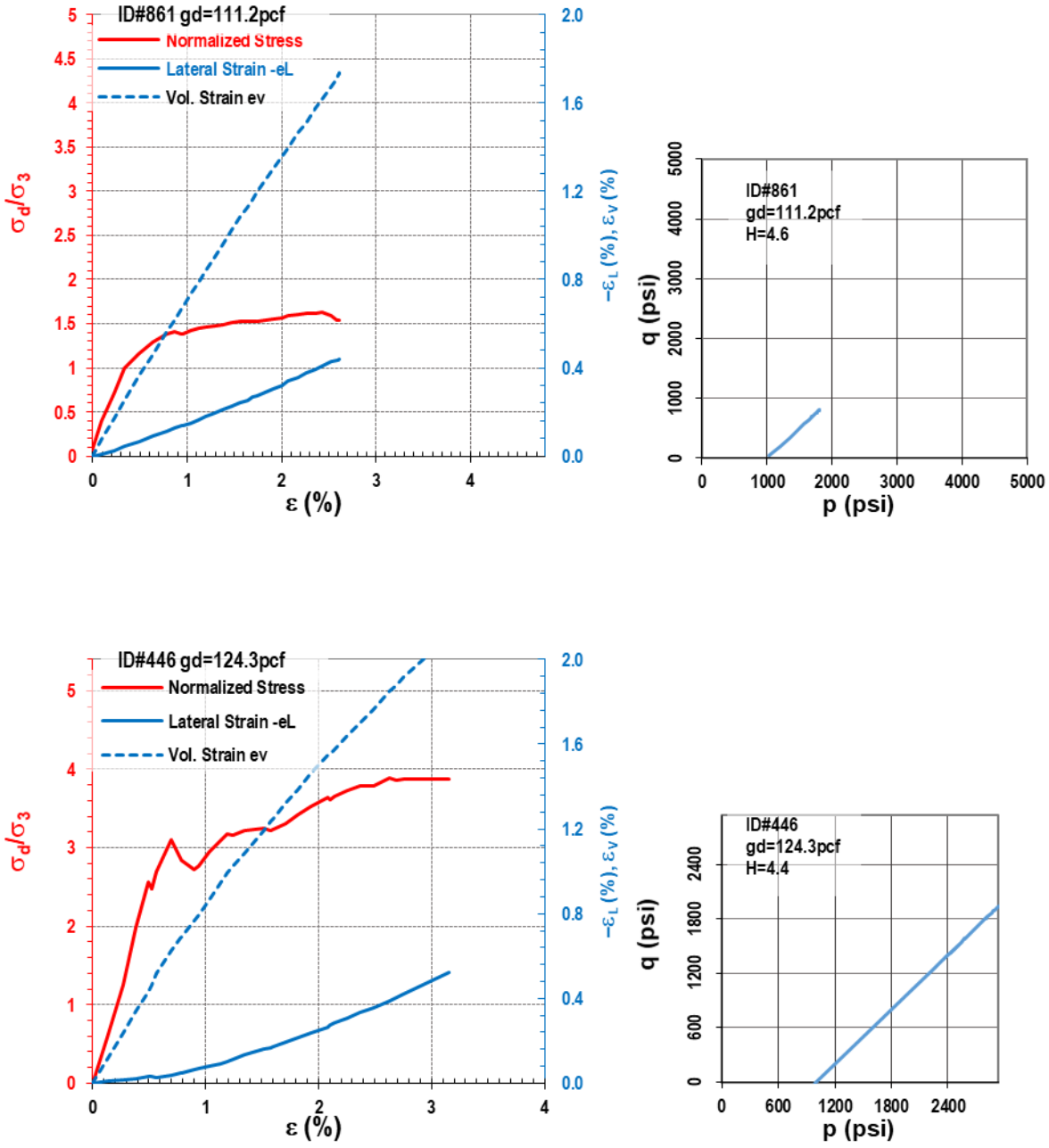

Figure E-7. Test results at σ_3 = 1000 psi

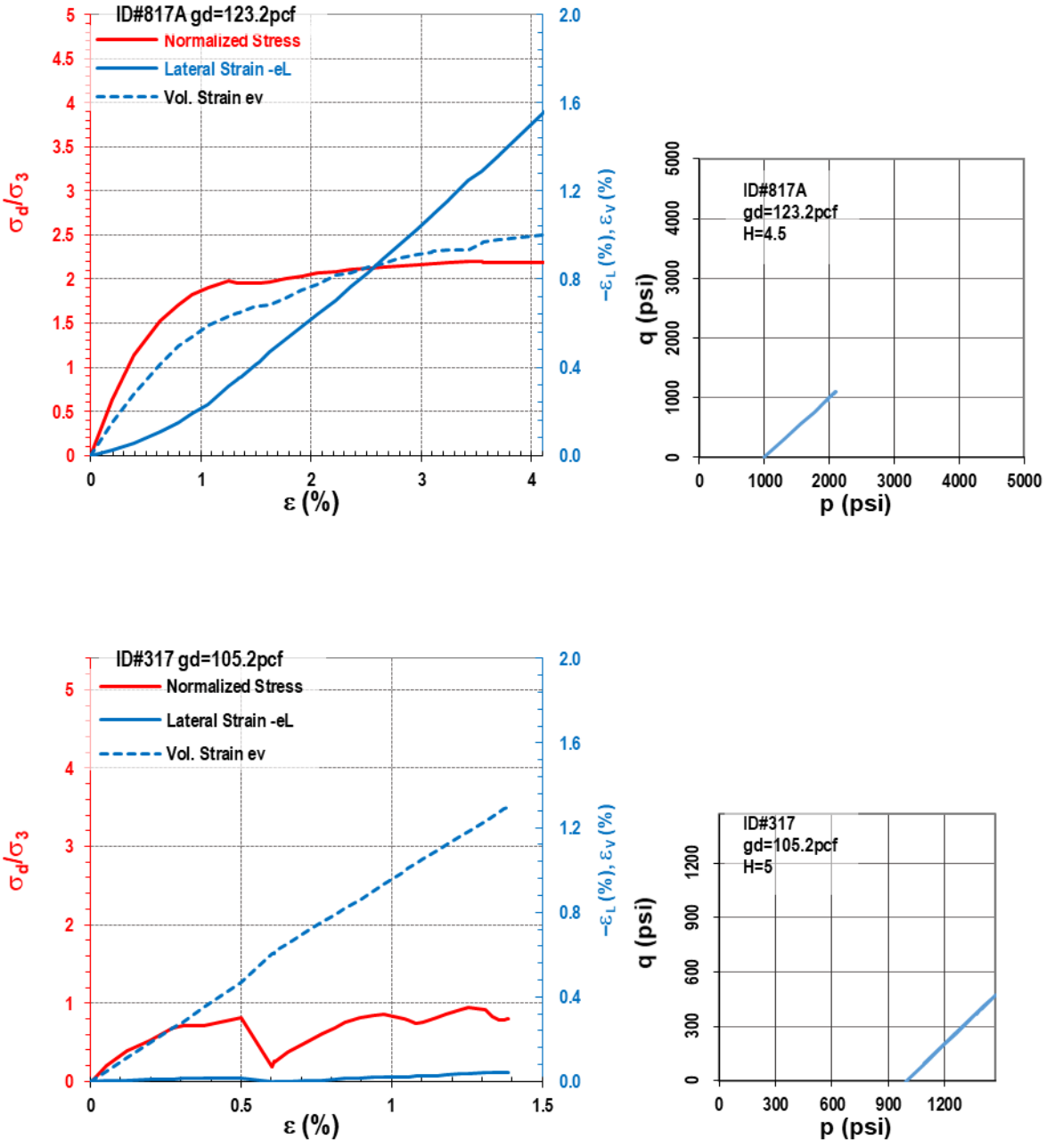

Figure E-7. Continued

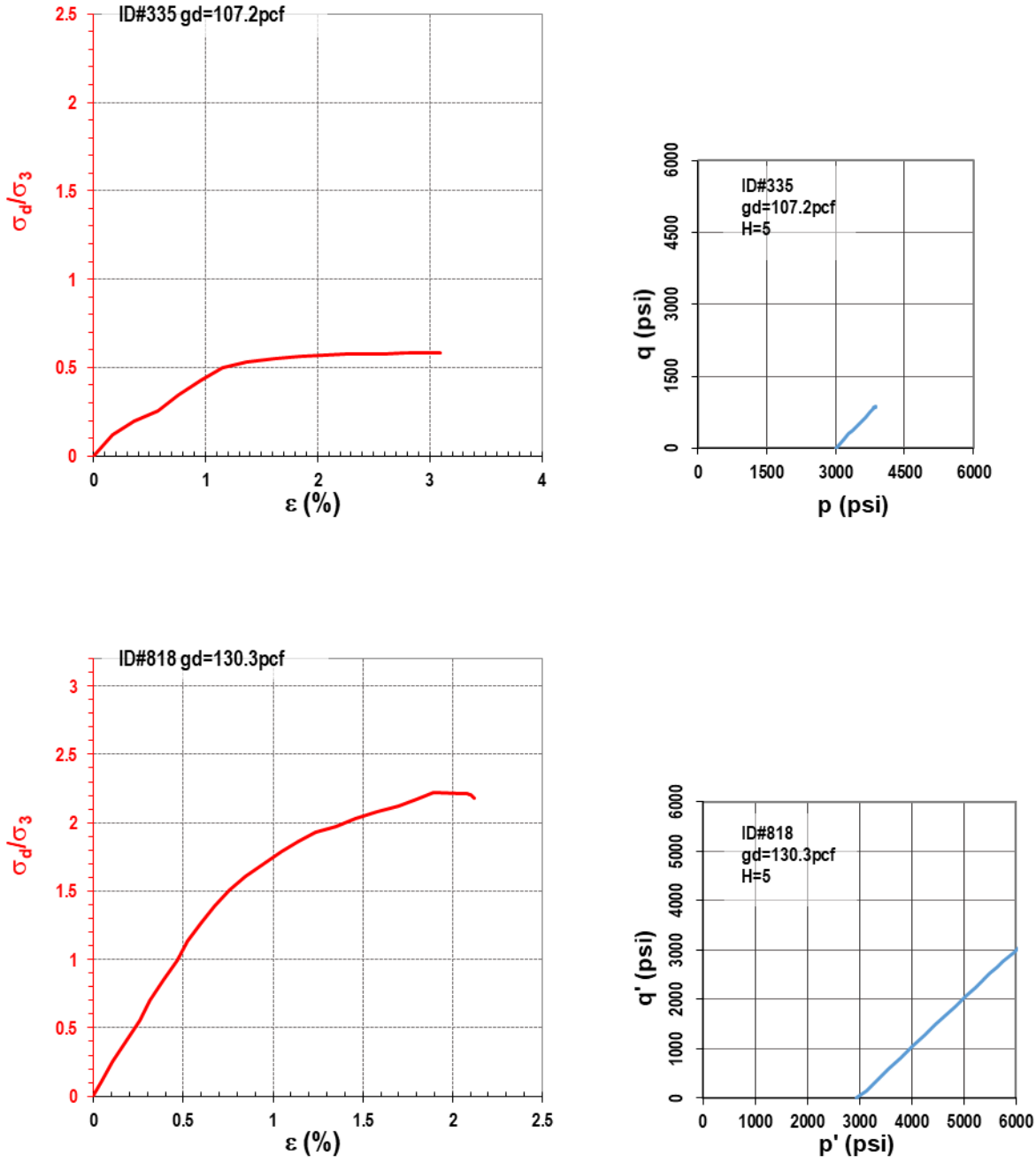

Figure E-8. Test results at σ_3 = 3000 psi

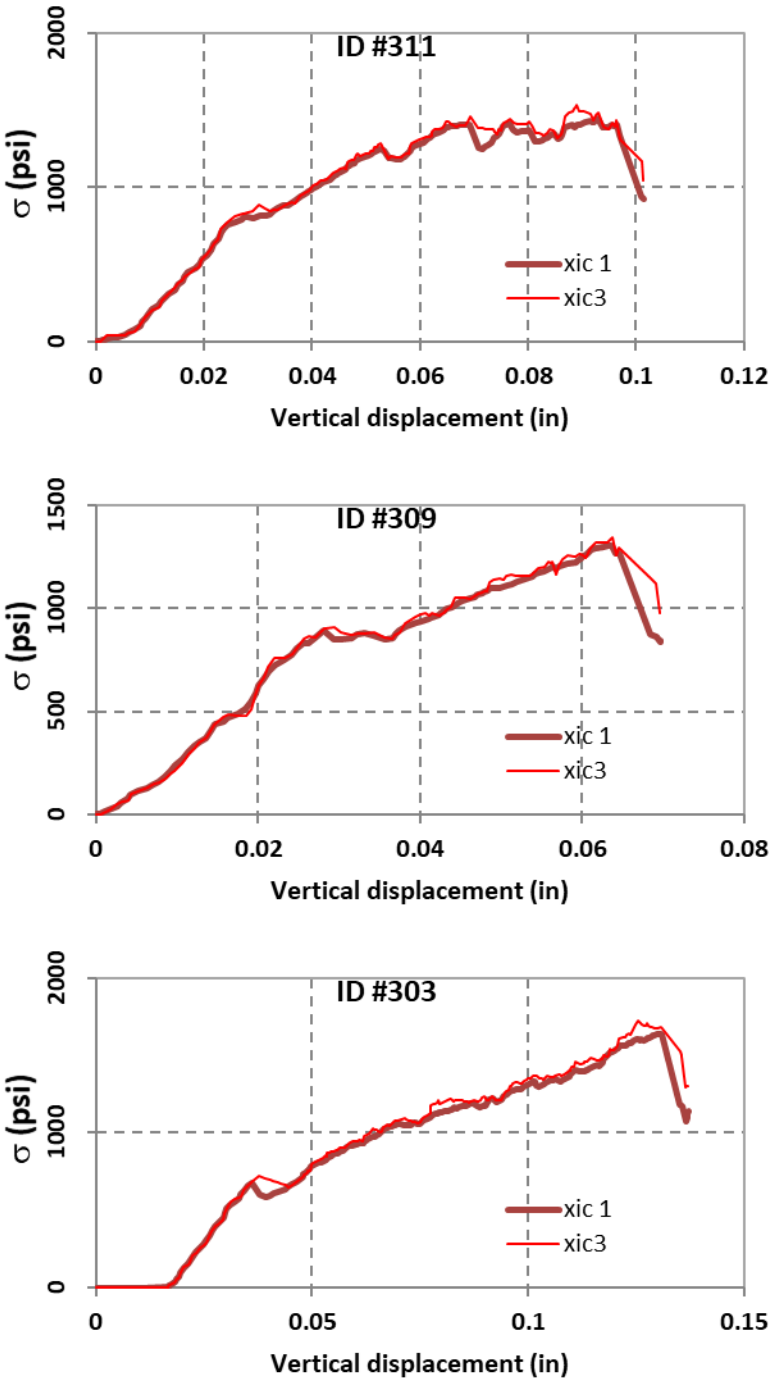

Figure E-9. Specimens crushed during isotropic loading

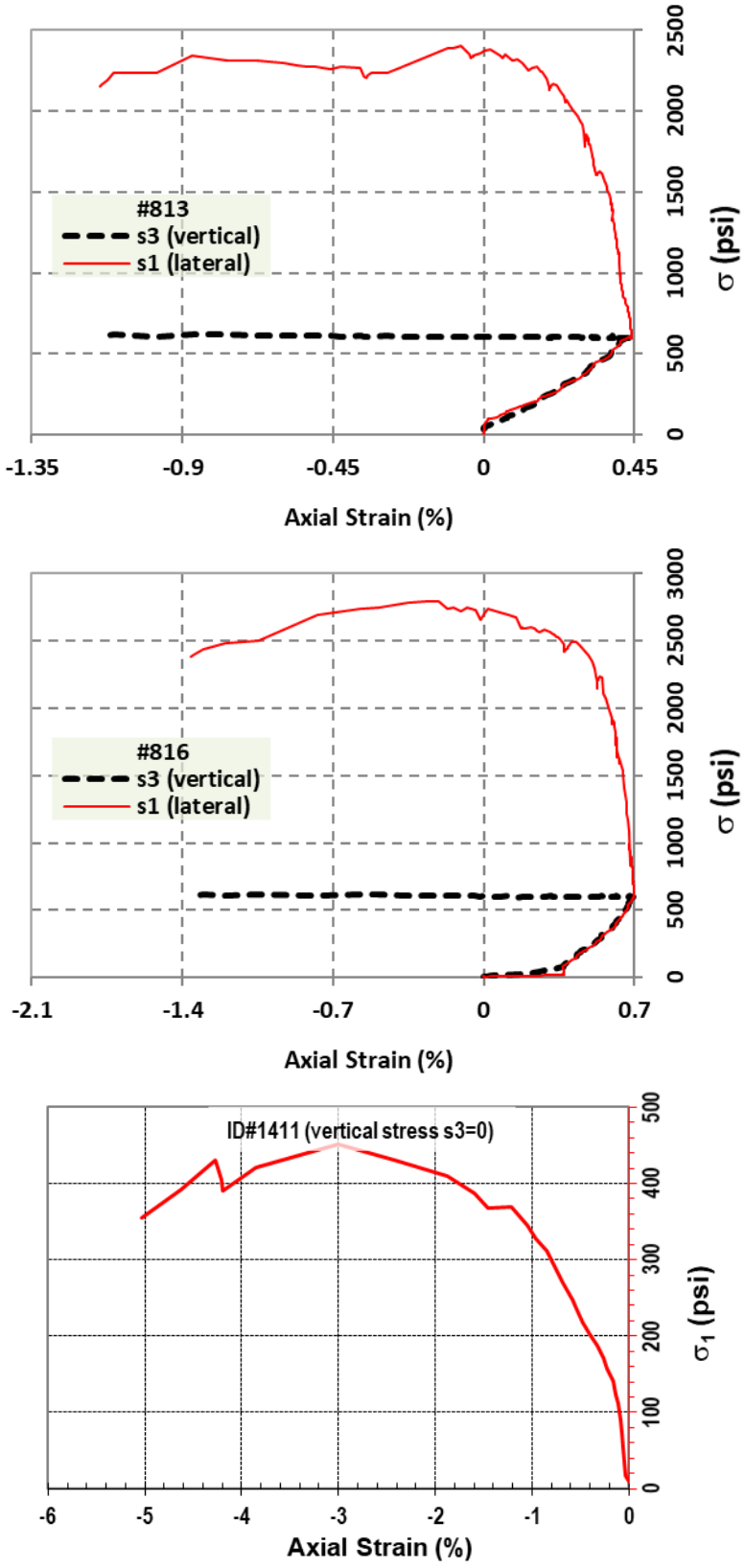

Figure E-10. Extension triaxial tests

APPENDIX F
RECOMMENDED PROCEDURE TO ESTABLISH STRENGTH ENVELOPE OF A DESIGN PROJECT

From the study results, it is indicated that from 0.7 BST to q_u to a triaxial result at σ_3 = 0.345 MPa (50 psi) confining pressure, the strength envelope is approximately linear, with slope angle of α in Lambe's p-q diagram. From σ_3 = 0.345 MPa (50 psi) to 4.1 MPa (600 psi), the sloping strength envelope portion can be simplified to a linear line, with slope angle of β in p-q diagram. 0 to 4.1MPa (600 psi) confining pressure range covers the possible pressures underneath a shallow foundation.

Therefore, the proposed procedure for a production project is:

1. Obtain a minimum of 10 q_u and 10 BST samples, calculate the mean values for q_u and BST.
2. Estimate the equivalent direct tension strength, q_t, based on 0.7*BST.
3. Obtain dry unit weight, γ_{dti}, of each rock specimen. γ_{dti} is the ratio between dry weight and cylindrical volume of the specimen:

$$\gamma_{dti} = \frac{Oven\ Dry\ Weight}{0.25\pi D^2 L_i} \quad \text{(F-1)}$$

where D is the rock core diameter

L_i is the specimen length

4. Obtain weighted average γ_{dts} from strength-test specimens (i.e., q_u, BST, as well as triaxial test specimens)

$$\gamma_{dts} = \Sigma(\gamma_{dti} L_i) / \Sigma L_i \quad \text{(F-2)}$$

i represents the strength-test-specimen #i

5. In addition, obtain dry unit measurements of non-tested material in core runs. Obtain dry unit weighted average for the whole rock layer γ_{dtw}.

$$\gamma_{dtw} = \Sigma(\gamma_{dti} L_i) / \Sigma L_i \quad \text{(F-3)}$$

i represents either the strength-test-specimen or the non-strength-test-specimen

For the rubbles in the recovered rocks, where they do not retain the cylindrical shape, there are two options:

i) Either calculate the dry unit weight of the rubbles, using rock core diameter (i.e., inner diameter of the core barrel), and the length of the rubbles placed in the core box.

ii) Or ignore this rubble portion, and count it as un-coreable material. Thus, the REC needs to be revised to a lower value, not counting the rubble.

6. Use Equations 32 & 33, use the average unit weight γ_{dtw} to reduce the q_u and BST values:

$$q_{tw} \approx q_t * e^{0.03(\gamma_{dtw}-\gamma_{dts})} \quad \text{(F-4)}$$
$$q_{uw} \approx q_u * e^{0.04(\gamma_{dtw}-\gamma_{dts})} \quad \text{(F-5)}$$

7. Calculate c (or a) – intercept, Eq. F-5

$$c = 0.5\sqrt{q_{uw}q_{tw}} \quad \text{(F-6)}$$
$$c = a / \cos\varphi \text{ or } a = c\cos\varphi \quad \text{(F-7)}$$

8. Calculate φ (or α) – initial slope, Eq. F-7

$$\sin\varphi = \frac{q_{uw}-q_{tw}}{q_{uw}+q_{tw}} \quad \text{(in p-q diagram: } \tan\alpha = \frac{q_{uw}-q_{tw}}{q_{uw}+q_{tw}}\text{)} \quad \text{(F-8)}$$

9. Calculate p_p – onset of structure rearrangement, Eq. (F-8).

$$p_p \text{ (psi)} = \frac{50+a}{1-\tan\alpha} = \frac{50+c\cos\varphi}{1-\sin\varphi} \quad \text{(F-9)}$$

Thus, after step 9, we would have the 1st portion of the bilinear curve in Figure F-1:

$$q = a + p\tan\alpha \quad \text{(F-10)}$$

10. Obtain an additional 4 to 8 samples for triaxial testing to estimate ω, the samples would cover the range of dry unit weights in the q_u and BST samples above. All of them would be tested under the same σ_3 at 600 psi. The results will be scatter. Let say, the results are in Figure F-2.

11. Then we use the γ_{dtw} from step 3 to get σ_d/σ_3, for example γ_{dtw} =103 and σ_d/σ_3 = 0.8 in Figure F-3.

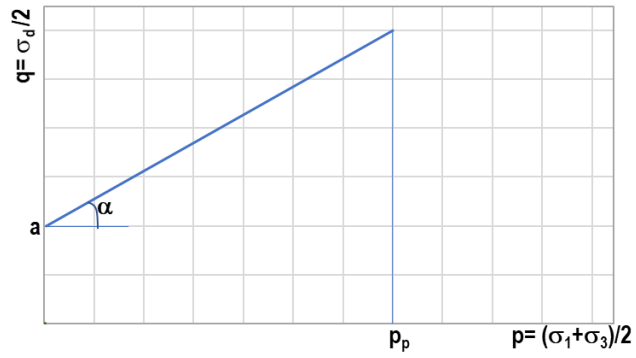

Figure F-1. First portion of bilinear curve

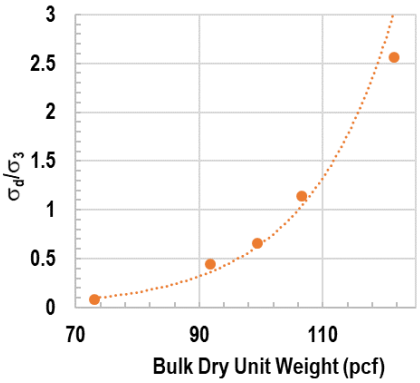

Figure F-2. Example of test triaxial results at 600-psi

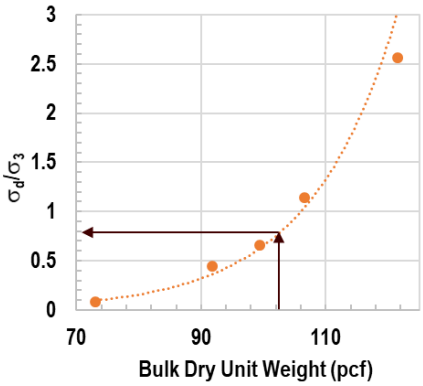

Figure F-3. Estimate representative triaxial results for the rock layer.

12. Thus, $\sigma_d = 600 * 0.8 = 480$ psi, and $q_{600} = \sigma_d / 2 = 240$, $p_{600} = q_{600} + \sigma_3 = 8400$

Plot this dot into Figure F-1, we'll have the β slope in p-q diagram:

$$\tan\beta = \frac{q_{600} - q_p}{p_{600} - p_p}$$

then $\sin\omega = \tan\beta$

13. Adjust all parameters based on %REC. Since each core run is the same 5-ft, the weighted average of REC would be the same as average. Therefore, it is recommended that REC = average (REC_i) from all core runs.

$$q_m = q * REC \quad \text{(F-11)}$$

$$a_m = REC*a \quad \text{(F-12)}$$

$$tan\alpha_m = REC*\tan\alpha \quad \text{(F-13)}$$

$$tan\beta_m = REC*\tan\beta \quad \text{(F-14)}$$

$$p_{pm} = p_p \quad \text{(F-15)}$$

Note: Another alternative was initially proposed, by reducing REC into γ_{dtw}, and do not do Eqs. F-9 to F-13, thus all q_u, q_t, etc. will be adjusted down just by γ_{dtw}. However, multiplying REC into γ_{dtw} would equal to the weighted-average of rock and air, for example REC = 50%, then we have γ_{dtw} = 51.5 pcf (less than water), thus it would be illogical (for example Figure F-3 would not be usable). In reality, the uncoreable material could have γ_{dt} of says 70 to 90 pcf (unknown).

Table F-1. Example data

All γ_{dt}	γ_{dt} for strength specimens	q_u (psi)	BST (psi)	σ_d/σ_3
105.1	105.1	133.7		
136.3	136.3	641.0		
90.1	90.1	228.3		
61.6	61.6	47.8		
91.2	91.2	97.3		
123.8	123.8	366.6		
95.9	95.9	180.2		
128.4	128.4	562.2		
141.6	141.6	496.7		
117.2	117.2	658.7		
108.2	108.2		61.2	
88.3	88.3		24.3	
104.3	104.3		44.8	
98.7	98.7		56.8	
129.6	129.6		107.0	
141.8	141.8		265.5	
137.1	137.1		148.1	
138.2	138.2		93.0	

Table F-1. Continued.

All γ_{dt}	γ_{dt} for strength specimens	q_u (psi)	BST (psi)	σ_d/σ_3
110.5	110.5		72.1	
107.3	107.3		73.9	
91.8	91.8			0.45
99.4	99.4			0.66
106.6	106.6			1.14
121.6	121.6			2.56
73.1	73.1			0.08
79.5				
87.7				
79.0				
81.5				
94.2				
69.7				
104.6				
106.0				
83.0				
91.6				
109.7				
97.0				
90.2				
111.9				
108.9				
102.8				
82.6				

14. Mean values from a minimum of 10 q_u and 10 BST lab tests: q_u = 341.3 psi, BST= 94.7 psi

15. Equivalent q_t = 0.7 * 94.7 = 66.3 psi

16. Mean value from 25 strength tests (10 q_u , 10 BST and 5 triaxial tests): γ_{dts} =109.9 pcf

17. Mean value from all 42 specimens (25 strength tests, and 17 no strength tests): γ_{dtw} =103 pcf

18. Dry-unit-weight-adjusted strength values for q_{uw} & q_{tw}:

$q_{uw} = 341.3 * e^{0.04(103-109.9)} = 258.9$

$q_{tw} = 66.3 * e^{0.03(103-109.9)} = 53.9$

19. $c = 0.5\sqrt{q_{uw}q_{tw}} = 59.1$ psi

20. $\sin\varphi = \tan\alpha = \frac{q_{uw}-q_{tw}}{q_{uw}+q_{tw}} = 0.6555 \Rightarrow \varphi = 41$

21. a = c*cos φ = 44.6

22. $p_p = \frac{50+a}{1-\sin\varphi}$ = 274.6 and $q_p = p_p - 50$ = 224.6 (or q_p = 44.6 + 0.6555*274.6 = 224.6)
thus, we have the 1st portion of the bilinear envelope in Figure F-4: q=44.6 + 0.6555 p

23. From triaxial tests, all performed at same σ_3 = 600-psi in Figure F-5. γ_{dtw} =103 pcf => σ_d / σ_3 = 0.8. σ_d = 600 * 0.8 = 480 psi, and $q_{600} = \sigma_d / 2$ = 240, $p_{600} = q_{600} + \sigma_3$ = 840. Add this coordinate (840,240) to the envelope chart, and we have a complete envelope for intact rock, as shown in Figure F-6.

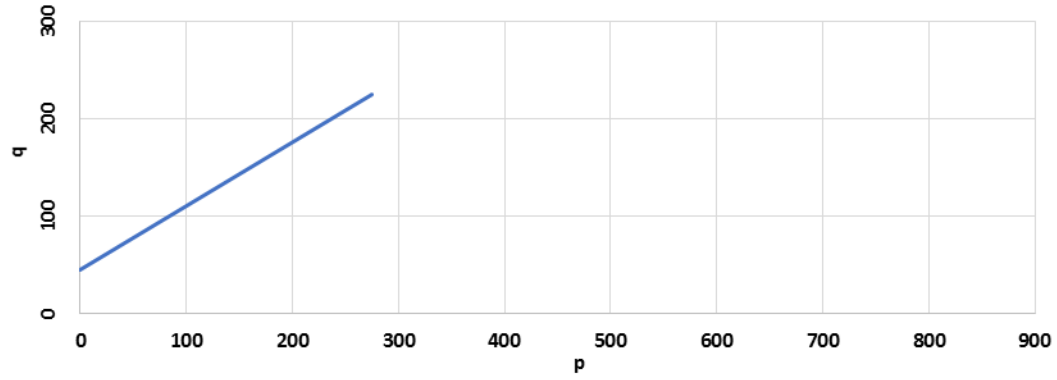

Figure F-4. First part of the bilinear envelope

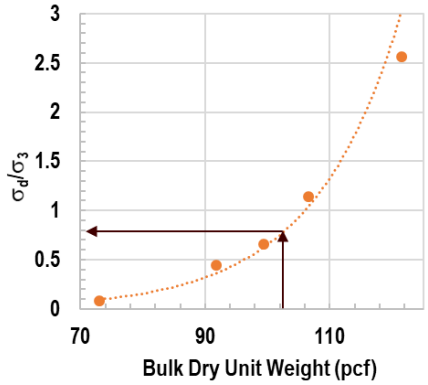

Figure F-5. Obtaining σ_d/σ_3 corresponding to γ_{dtw}

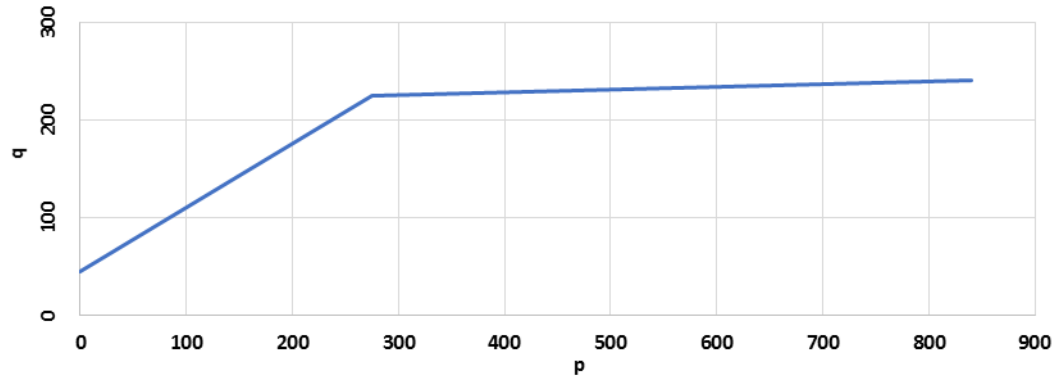

Figure F-6. Completion of bilinear envelope for intact rock

24. From Figure F-6, the 2nd slope in p-q diagram can be calculated:

$\tan\beta = \frac{240-224.6}{840-274.6} = 0.0272$

$\beta = 1.56$ and $\sin\omega = \tan\beta$, thus $\omega = 1.56$

Figure F-6 presents the mean value for strength envelope of intact rock. A more conservative envelope for intact rock can be obtained by reducing all the q_u, q_t, and γ_{dt} by the standard deviation of the bias.

25. For rock mass, the mean value for REC for all core runs is 60%:

$$a_m = 60\%*a = 26.8 \quad \text{(F-16)}$$

$$\tan\alpha_m = 60\%*\tan\alpha = 60\%*0.6555 = 0.3933 \quad \text{(F-17)}$$

$$\tan\beta_m = 60\%*\tan\beta = 60\% * 0.0272 = 0.0163 \quad \text{(F-18)}$$

$$p_{pm} = p_p = 274.6 \quad \text{(F-19)}$$

So, the rock mass envelope is the bilinear curve below, which is presented in Figure F-7:

If $p < 274.6$ psi: $q = 26.8 + 0.3933\ p$

If $p \geq 274.6$ psi: $q = 26.8 + 0.3933*274.6 + 0.0163\ p$

$= 134.8 + 0.0163\ p$

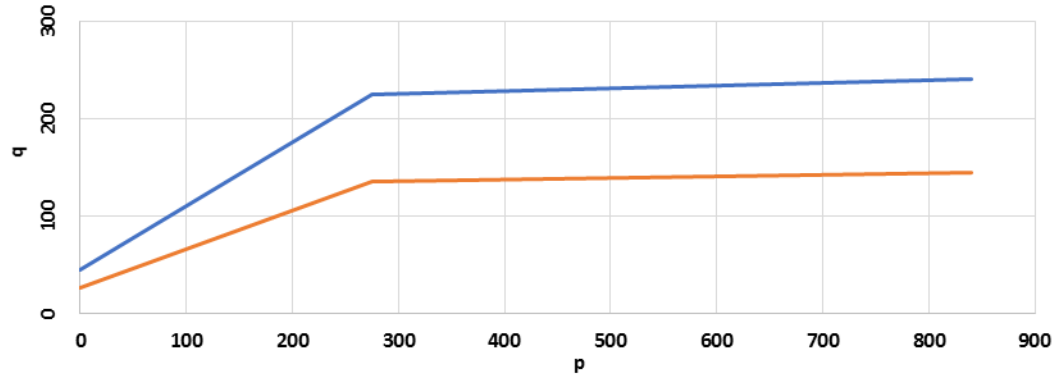

Figure F-7. Envelopes for intact rock and rock mass

LIST OF REFERENCES

AASHTO. (2017). "*AASHTO LRFD Bridge Design Specification*". American Association of State Highway and Transportation Officials, Washington, D.C.

AASHTO Standard T-100. (2015). "*Standard Specifications for Transportation Materials and Methods of Sampling and Testing, and AASHTO Provisional Standards*", American Association of State Highway and Transportation Officials, Washington, D.C.

ACI 318-14. (2014). "*Building Code Requirements for Structural Concrete and Commentary*", American Concrete Institute, Farmington Hills, MI.

Arioglu N., Girgin Z., Arioglu E. (2006). "*Evaluation of Ratio between Splitting Tensile Strength and Compressive Strength for Concrete up to 120 MPa and its Application in Strength Criterion*". ACI Materials Journal, Vol 103, pp. 18-24

Arthur, J.D., Fischler, C., Kromhout, C., Clayton, J.M., Kelley, G.M., Lee, R.A., O'Sullivan, M., Green, R.C., and Werner, C.L. (2008). "*Hydrogeologic framework of the southwest Florida water management district*", Bulletin 68, Florida Geological Survey, Tallahassee, FL.

ASTM Standard D854 (2014). "*Standard Test Methods for Specific Gravity of Soil Solids by Water Pycnometer",* ASTM International, West Conshohocken, PA.

ASTM Standard D3967 (2016). "*Standard Test Method for Splitting Tensile Strength of Intact Rock Core Specimens",* ASTM International, West Conshohocken, PA.

ASTM Standard D6473 (2015). "*Standard Test Method for Specific Gravity and Absorption of Rock for Erosion Control",* ASTM International, West Conshohocken, PA.

ASTM Standard D7012 (2014). "*Standard Test Methods for Compressive Strength and Elastic Moduli of Intact Rock Core Specimens under Varying States of Stress and Temperatures",* ASTM International, West Conshohocken, PA.

Boggs Jr., S. (2006). "*Principles of Sedimentology and Stratigraphy*", Pearson Prentice Hall Publishing.

Briaud J-L., Smith B., Rhee K-Y., Lacy H., Nicks J. (2009). "The Washington Monument Case History", in: *International Journal of Geoengineering Case Histories*, Vol 1-3, pp.170-188

Brown D., Turner J.P., and Castelli, R.J. 2010). "*Drilled Shafts: Construction Procedures and LRFD Design Methods*", FHWA NHI-10-016 Report.

Bullock, P. (2004). "*In situ Rock Modulus Apparatus*", Florida Department of Transportation Project BC-354 TWO 13 Final Report. Gainesville, FL.

Carter, J. P. and Kulhawy, F. H. (1988). "*Analysis and Design of Foundations Socketed into Rock*". Report No. EL-5918. Empire State Electric Engineering Research Corporation and Electric Power Research Institute, New York, 158.

Chang C., Zobacka M.D., Khaksar A. (2006). "Empirical Relations between Rock Strength and Physical Properties in Sedimentary Rocks" in: *Journal of Petroleum Science and Engineering*, Vol 51(3), pp. 223-237.

Chappell, J.M. (2009). "Sea Level Change, Quaternary" in: *Encyclopedia of Paleoclimatology and Ancient Environments*. (Ed. Vivien Gornitz), pp. 893-898.

Deer, D.U., and Miller, R.P. (1966). "*Engineering Classification and Index Properties for Intact Rock*", Technical Report No. AFWL-TR-65-116, Air Force Weapons Laboratory, Kirtland Air Force Base, Albuquerque, NM.

Eagar, T.W. and Musso, C. (2001). " Why did the world trade center collapse? Science, engineering, and speculation", in: The Journal of The Minerals, Vol 53, pp. 8-11.

Elliott G. M. and Brown E. T. (1985). "Yield of a soft, high porosity rock", in: *Geotechnique*, Vol 35, pp. 413-423.

Fereidooni, D. and Khajevand, R. (2018). "Determining the Geotechnical Characteristics of Some Sedimentary Rocks from Iran with an Emphasis on the Correlations between Physical, Index, and Mechanical Properties" in: *Geotechnical Testing Journal*, Vol 41(3), pp. 555-573.

Florida Department of Transportation (FDOT) (2015). "*Florida Test Method for Carbonates and Organic Matter in Base Materials*", State Materials Office, Florida.

Florida Department of Transportation (FDOT) (2018). "*Soils and Foundations Handbook*", State Materials Office, Florida.

Goodman, R.E. (1989). "*Introduction to Rock Mechanics*", John Wiley & Sons Publishing.

Gowd, T.N., Rummel, F. (1977). "Effect of fluid injection on the fracture behavior of porous rock" in *International Journal of Rock Mechanics and Mining Sciences & Geomechanics Abstracts*, Vol 14, pp. 203-208.

Hannant, D. J.; Buckley, K. J.; and Croft, J. (1973). "The Effect of Aggregate Size on the Use of the Cylinder Splitting Test as a Measure of Tensile Strength" in *Materials and Structures*, Vol 6, No. 31, pp. 15-21.

Hester, T.C. and Schmoker, J.W. (1985). "*Porosity, grain-density, and inferred aragonite-content data from the Miami Limestone, Miami area and lower Florida Keys*", Open-File Report 85-21, U.S. Geological Survey, Reston, VA.

Hoek, E. and Brown, E. T. (1980). "Empirical strength criterion for rock masses", in *Journal of the Geotechnical Engineering Division*, Vol 106-9, pp. 1013-1035.

Hoek, E. and Brown, E. T. (1988). “The Hoek-Brown Failure Criterion - a 1988 Update.” in “*Proceedings of the 15th Canadian Rock Mechanics Symposium*”, editor Curran, J. H., Toronto, Civil Engineering Department, University of Toronto, pp 31–38.

Hoek, E. and Brown, E. T. (2018). “The Hoek-Brown failure criterion and GSI – 2018 edition”, in: *Journal of Rock Mechanics and Geotechnical Engineering,* in press, accepted manuscript. doi.org/10.1016/j.jrmge.2018.08.001

Hoek, E., Carranza-Torres, C., and Corkum, B. (2002), “Hoek-Brown failure criterion – 2002 Edition” in *Proceedings of the NARMS-TAC Conference*, Toronto, Vol 1, pp. 267-273

Hoek, E. and Franklin, J.A. (1968). “Simple triaxial cell for field or laboratory testing of rock”, in: *Transactions of the Institution of Mining and Metallurgy 77, Section A*, pp. 22-26

Jaeger, J.C. and Cook N.G. (1969). “*Fundamentals of Rock Mechanics*”, The Chaucer Press, Ltd.

Johnston I. (1985). “Strength of Intact Geomechanical Materials”, in: *ASCE Journal of Geotechnical Engineering 111*, pp. 730-749.

Jumikis, A.R (1983). “*Rock Mechanics*”, Gulf Publishing Company.

Kimmerling, R. (2002). “*Shallow Foundations*", Geotechnical Engineering Circular No. 6., Federal Highway Administration, Washington D.C.

Lafuente, B., Downs, R.T., Yang, H., and Stone, N. (2015). “The power of databases: the RRUFF project” in: *Highlights in Mineralogical Crystallography*, Armbruster, T. and Danisi R.M., editors, Berlin, Germany, pp 1-30

Lambe, T.W. and Whitman, R.V. (1969). “*Soil Mechanics*”, John Wiley & Sons Publishing, New York.

McVay M.C, Chung J., Nguyen, T., Thiyyakkandi, S., Lyu, W., Schwartz, J., Huang, L., Le, V. (2017), “*Evaluation of Static Resistance of Deep Foundation*”. Florida Department of Transportation, Final Report for BDV31-977-05. Gainesville, FL.

McVay M.C, Townsend F., Williams R. (1992), “Design of Socketed Drilled Shafts in Limestone” in: *ASCE Journal of Geotechnical Engineering 118*, pp.1626-1637.

Missimer, T.M. and Scott T.M. (2001). “Geology and Hydrogeology of Lee County, Florida - Special Publication No. 49”, Florida Geological Survey.

Mogi K. (1966). “Pressure dependence of rock strength and transition from brittle to ductile flow”, in *Bulletin of Earthquake Research Institution,* Vol 44, pp. 215-232.

Paikowsky, S.G., Canniff M.C., Lesny K., Kisse A., Amatya S., Muganga R. (2010). “*LRFD Design and Construction of Shallow Foundations for Highway Bridge Structures*", NCHRP Report 651. Transportation Research Board, Washington D.C.

Perras M.A. and Diederichs, M.S. (2014). “A Review of the Tensile Strength of Rock: Concepts and Testing” in *Geotechnical and Geological Engineering Journal*, Vol 32, pp. 525-546

Rogers M. (2016). “*Real time construction monitoring for drilled shafts socketed into Florida limestone*” – Ph.D. Dissertation, University of Florida, Gainesville, FL.

Scott, T.M. (2001). “*Text to Accompany the Geologic Map of Florida*", Open File Report 80, Florida Geological Survey, Tallahassee, FL.

Scott, T. M., Campbell, K. M., Rupert, F. R., Arthur, J. D., Missimer, T. M., Lloyd, J. M., Yon, J. W., and Duncan, J. G. (2001). “*Geologic Map of the State of Florida*", Map Series 146, Florida Geological Survey & Florida Department of Environmental Protection, Tallahassee, FL.

Schwartz, A.E. (1964). “Failure of rock in the triaxial shear test”, in: *“Proceedings of the 6th U.S Symposium on Rock Mechanics”*, American Rock Mechanics Association. Rolla, MI; pp. 109-51

Sowers, G. (1996). “*Building on Sinkholes: Design and Construction of Foundations in Karst Terrain”,* ISBN: 0784401764, American Society of Civil Engineers.

Truzman, M (2016). “Use of Geological Strength Index to Characterize the Miami Limestone for Shallow Foundation Design”, in: “*Proceeding of the 50th U.S. Rock Mechanics/Geomechanics Symposium”*, American Rock Mechanics Association.

Wong, T., David, C., Zhu W. (1997). “The transition from brittle faulting to cataclastic flow in porous sandstones: Mechanical deformation”, in: *Journal of Geophysical Research*, Vol 102-B2, pp: 3009-3025.

BIOGRAPHICAL SKETCH

Thai Nguyen obtained his bachelor's degree from Vietnam in 1996 and his master's degree from University of Florida in 2001. He had been working in Vietnam for five years (1996 – 1999, and 2001-2003) as a lecturer at National University of Civil Engineering, and since then has been working in United States for three geotechnical consultants (Langan Engineering and Environmental Services Consulting, Amec Foster Wheeler, and H2R Corp., which used to be Williams Earth Sciences, and part of Gannett Fleming). He is considering several options upon achieving his Ph.D. degree, either continuing his employment with H2R Corp., or getting a position involving with research studies with Department of Transportation, or becoming a lecturer or professor of practice when the opportunities arrive. However, his long-term goal is into the very far future upon "retirement", he would like to enjoy life in Vietnam while hopefully teaching one or two geotechnical classes. Believe it or not, in his perspective, life in Vietnam is much more joyful than most anywhere else on earth.